arXiv:2207.03451v3 [quant-ph] 13 Feb 2023

Unitary Partitioning and the Contextual Subspace Variational Quantum Eigensolver

Alexis Ralli,[1,*] Tim Weaving,[1,†] Andrew Tranter,[2,3,‡] William M. Kirby,[2,§] Peter J. Love,[4,5,¶] and Peter V. Coveney[1,6,**]

[1] *Centre for Computational Science, Department of Chemistry, University College London, London, WC1H 0AJ, United Kingdom*
[2] *Department of Physics and Astronomy, Tufts University, Medford, Massachusetts 02155, USA*
[3] *Cambridge Quantum Computing, 9a Bridge Street Cambridge, CB2 1UB, United Kingdom*
[4] *Department of Physics and Astronomy, Tufts University, Medford, MA 02155, USA*
[5] *Computational Science Initiative, Brookhaven National Laboratory, Upton, New York 11973, USA*
[6] *Informatics Institute, University of Amsterdam, Amsterdam, 1098 XH, Netherlands*

(Dated: February 14, 2023)

The contextual subspace variational quantum eigensolver (CS-VQE) is a hybrid quantum-classical algorithm that approximates the ground-state energy of a given qubit Hamiltonian. It achieves this by separating the Hamiltonian into contextual and noncontextual parts. The ground-state energy is approximated by classically solving the noncontextual problem, followed by solving the contextual problem using VQE, constrained by the noncontextual solution. In general, computation of the contextual correction needs fewer qubits and measurements compared with solving the full Hamiltonian via traditional VQE. We simulate CS-VQE on different tapered molecular Hamiltonians and apply the unitary partitioning measurement reduction strategy to further reduce the number of measurements required to obtain the contextual correction. Our results indicate that CS-VQE combined with measurement reduction is a promising approach to allow feasible eigenvalue computations on noisy intermediate-scale quantum devices. We also provide a modification to the CS-VQE algorithm; the CS-VQE algorithm previously could cause an exponential increase in Hamiltonian terms, but with this modification now at worst will scale quadratically.

I. INTRODUCTION

One of the fundamental goals of quantum chemistry is to solve the time-independent non-relativistic Schrödinger equation. The eigenvalues and eigenvectors obtained allow different molecular properties to be studied from first principles. Standard methods project the problem onto a Fock space (η electrons distributed in M orbitals) and solve. Under this approximation, the problem scales exponentially with system size, where the number of Slater determinants (configurations) scales as $\binom{M}{\eta}$ making the problem classically intractable [1]. Quantum computers can efficiently represent the full configuration interaction (FCI) Hilbert space and offer a potential way to efficiently solve such molecular problems [2, 3]. This use case is often the canonical example of where the first quantum computers will be advantageous over conventional computers [4, 5].

In the fault-tolerant regime, quantum phase estimation (QPE) [6] provides a practical way to perform quantum chemistry simulations in polynomial time [2]. However, current noisy intermediate-scale quantum (NISQ) devices cannot implement this algorithm due to the deep quantum circuits and long coherence times required [7, 8].

The constraints on present-day devices have given rise to a family of quantum-classical algorithms that leverage as much classical processing as possible to reduce the quantum resources required to solve the problem at hand. Common examples of NISQ algorithms are the variational quantum eigensolver (VQE) [9], quantum approximate optimization algorithm (QAOA) [10] and variational quantum linear solver (VQLS) [11]. A good example is the recently proposed entanglement forging method [12], where the electronic structure problem for H_2O was reduced from a 10-qubit problem to multiple 5 qubit problems that were each studied using conventional VQE and classically combined. Recently another novel approach known as the quantum-classical hybrid quantum Monte Carlo (QC-QMC) method was used to unbias the sign problem in the projector Monte Carlo (PMC) method, which implements imaginary time evolution [13]. At a high level, the accuracy of a constrained PMC calculation is determined by the quality of trial wave functions. Quantum computers offer a way to efficiently store highly entangled trial wave functions and measure certain overlaps, which would require exponential resources classically. Huggins *et al.* performed QC-QMC simulations of different chemical systems on Google's Sycamore processor and obtained results competitive with state-of-the-art classical methods [13].

The contextual-subspace VQE algorithm is another hybrid quantum-classical approach [14]. It gives an approximate simulation method, where the quantum resources required can be varied for a trade off in accuracy. This

* alexis.ralli.18@ucl.ac.uk
† timothy.weaving.20@ucl.ac.uk
‡ tufts@atranter.net
§ william.kirby@tufts.edu
¶ peter.love@tufts.edu
** p.v.coveney@ucl.ac.uk

allows problems to be studied where the full Hamiltonian would normally be too large to investigate on current NISQ hardware. This was shown in the original CS-VQE paper, where chemical accuracy for various molecular systems was reached using significantly fewer qubits compared with the number required for VQE on the full system [14]. As CS-VQE reduces the number of qubits required for simulation, the number of terms in a Hamiltonian requiring separate measurements is also reduced.

A natural question that arises from this is whether measurement reduction schemes can be utilized to reduce the overall measurement cost of these already reduced CS-VQE Hamiltonians [15–28]. The goal of this work was to investigate the possible reductions given by the unitary partitioning strategy [15, 29, 30] and whether chemical accuracy on larger molecules can be reached on currently available NISQ hardware.

This paper is structured as follows. Section II summarizes the CS-VQE algorithm. Here we provide a modification to the unitary partitioning step of the CS-VQE algorithm the CS-VQE algorithm previously could cause the number of terms in a Hamiltonian to exponentially increase, but with this modification now will at worst cause a quadratic increase. Section III is split into a description of the method in Section III A and two main parts, Sections III B and III C. Section III B examines a model problem to exemplify each step of the CS-VQE algorithm. Section III C gives the numerical results of applying unitary partitioning measurement reduction to a test bed of different molecular structure Hamiltonians, where the contextual subspace approximation has been employed.

II. BACKGROUND

To keep our discussion self-contained and establish notation, we summarize the necessary background theory of the contextual-subspace VQE algorithm in this section.

A. Contextuality

The foundation of quantum contextuality is the Bell-Kochen-Specker (BKS) theorem [31]. In lay terms, every measurement provides a classical probability distribution (via the spectral theorem) and a joint distribution can be built as a product over all possible measurements [32]. The BKS theorem proves that it is impossible to reproduce the probabilities of every possible measurement outcome for a quantum system as marginals of this joint probability distribution [33]. This is related to how quantum mechanics does not allow models that are locally causal in a classical sense [34]. Contextuality is a generalization of nonlocality [34, 35]. This means that quantum measurement cannot be understood as simply revealing a pre-existing value of some underlying hidden variable [36, 37]. Bell's theorem also reaches a similar conclusion against hidden variables [38], but in a different way.

A good example of this phenomenon is the "Peres-Mermin square" [37, 39], where no state preparation is involved and only observables are considered. We include an example in Appendix A and remark on the relation to VQE. Colloquially, for a noncontextual problem it is possible to assign deterministic outcomes to observables simultaneously without contradiction; however, for a contextual problem this is not possible [14].

The following subsections set out the contextual subspace VQE algorithm and we provide an alternate way to construct $U_{\mathcal{W}}$ (defined below) compared to the original work [14]. This modification addresses the exponential scaling part of the method. Further background on the full CS-VQE algorithm is given in the Supplemental Material [40].

B. Contextual subspace VQE

Consider a Hamiltonian expressed as:

$$\begin{aligned} H_{\text{full}} &= \sum_a c_a P_a = \sum_a c_a \Big(\bigotimes_{j=0}^{n-1} \sigma_j^{(a)} \Big) \\ &= \sum_a c_a \big(\sigma_0^{(a)} \otimes \sigma_1^{(a)} \otimes ... \otimes \sigma_{n-1}^{(a)} \big), \end{aligned} \tag{1}$$

where c_a are real coefficients. Each Pauli operator P_a is made up of an n-fold tensor product of single qubit Pauli matrices $\sigma_j \in \{\mathcal{I}, X, Y, Z\}$, where j indexes the qubit the operator acts on. The CS-VQE algorithm is based on separating such a Hamiltonian into a contextual and noncontextual part [14]:

$$H_{\text{full}} = H_{\text{con}} + H_{\text{noncon}}. \tag{2}$$

As it is possible to assign definite values to all terms in H_{noncon} without contradiction, a classical hidden variable model (or quasiquantized model) can be used to represent this system [41].

In [42], such a model is constructed along with a classical algorithm to solve it. This was based on the work of Spekkens [43, 44]. Solving this model yields a noncontextual ground-state.

Once that solution is obtained, the remaining contextual part of the problem is solved. Solutions to H_{con} must be consistent with the noncontextual ground-state, which defines a subspace of allowed states [14]. By projecting the problem into this subspace the overall energy is given by:

$$
\begin{aligned}
E(\vec{\theta};\vec{q},\vec{r}\,) =& E_{\text{noncon}}(\vec{q},\vec{r}\,) + E_{\text{con}}(\vec{\theta};\vec{q},\vec{r}\,) \\
=& E_{\text{noncon}}(\vec{q},\vec{r}\,) + \\
& \frac{\langle\psi_{\text{con}}(\vec{\theta})|\ Q_{\mathcal{W}}^{\dagger}U_{\mathcal{W}}^{\dagger}H_{\text{con}}U_{\mathcal{W}}Q_{\mathcal{W}}\ |\psi_{\text{con}}(\vec{\theta})\rangle}{\langle\psi_{\text{con}}(\vec{\theta})|\, Q_{\mathcal{W}}^{\dagger}Q_{\mathcal{W}}\ |\psi_{\text{con}}(\vec{\theta})\rangle} \\
=& \frac{\langle\psi_{\text{con}}(\vec{\theta})|\ Q_{\mathcal{W}}^{\dagger}\ U_{\mathcal{W}}^{\dagger}H_{\text{full}}U_{\mathcal{W}}\ Q_{\mathcal{W}}\ |\psi_{\text{con}}(\vec{\theta})\rangle}{\langle\psi_{\text{con}}(\vec{\theta})|\, Q_{\mathcal{W}}^{\dagger}Q_{\mathcal{W}}\ |\psi_{\text{con}}(\vec{\theta})\rangle}.
\end{aligned}
\tag{3}
$$

We have written $U_{\mathcal{W}}$ rather than $U_{\mathcal{W}}(\vec{q},\vec{r})$ to simplify our notation.

The vector $(\vec{q},\vec{r})$ should be thought of as parameters that define a particular noncontextual state: normally, this will be a parameterization for the noncontextual ground-state [14, 42]. This vector has a size of at most $2n+1$ for a Hamiltonian defined on n qubits [42]. From $(\vec{q},\vec{r})$, we define a set of stabilizers $\mathcal{W}$ which stabilize that particular noncontextual state [14]. The unitary $U_{\mathcal{W}}$ maps each of these stabilizers to a distinct single-qubit Pauli matrix; details of this are covered in II E. By enforcing the eigenvalue of these single-qubit Pauli operators we define a subspace of allowed quantum states that are consistent with the noncontextual state. To constrain the problem to this subspace, we use the projector $Q_{\mathcal{W}}$. Note that this is not a unitary operation, hence the renormalization in equation 3. By projecting our contextual Hamiltonian into this subspace $H_{\text{con}} \mapsto H_{\text{con}}^{\mathcal{W}} = Q_{\mathcal{W}}^{\dagger}U_{\mathcal{W}}^{\dagger}H_{\text{con}}U_{\mathcal{W}}Q_{\mathcal{W}}$, we ensure that solutions to $H_{\text{con}}^{\mathcal{W}}$ remain in the subspace consistent with the noncontextual solution [14]. In other words, this operation means that solutions to $H_{\text{con}}^{\mathcal{W}}$ will remain consistent with the noncontextual solution. Section II E goes into detail on this.

The contextual trial or ansatz state is prepared as $|\psi_{\text{con}}(\vec{\theta})\rangle = U_{\mathcal{W}}^{\dagger}V(\vec{\theta})\,|0\rangle^{\otimes n}$, where $V(\vec{\theta})$ is the parameterized operator that prepares it. The projector $Q_{\mathcal{W}}$, in equation 3, then projects this state into the subspace of possible states consistent with the noncontextual ground-state. Again this depends on which stabilizer eigenvalues are fixed. Note that as $Q_{\mathcal{W}}$ is not a unitary operation the state must be renormalized. Further analysis of the contextual subspace VQE projection ansatz is provided in [45]. In section II C we discuss how to solve the noncontextual problem.

C. Noncontextual Hamiltonian

For a given noncontextual Hamiltonian, we define $\mathcal{S}^{H_{\text{noncon}}}$ to be the set of P_i present in H_{noncon}. This set can be expanded as two subsets denoted as $\mathcal{Z}$ and $\mathcal{T}$, representing the set of fully commuting operators and its complement respectively [14, 42]. The set $\mathcal{T}$ can be expanded into N cliques, where operators within a clique must all commute with each other and operators between cliques must pairwise anticommute. This is because commutation forms an equivalence relation on $\mathcal{T}$ if and only if $\mathcal{S}^{H_{\text{noncon}}}$ is noncontextual [14, 42].

A hidden variable model for such a system can be built, where the set of observables $\mathcal{R}$ that define the phase-space points of the hidden variable model is [14, 42, 46]:

$$
\begin{aligned}
\mathcal{R} &\equiv \{P_0^{(j)} | j = 0, 1, \ldots, N-1\} \cup \{G_0, G_1, G_2, ...\} \\
&\equiv \{P_0^{(j)} | j = 0, 1, \ldots, N-1\} \cup \mathcal{G}.
\end{aligned}
\tag{4}
$$

The set $\mathcal{G}$ represents an independent set of Pauli operators that generates the set of commuting observables $\mathcal{Z}$. Each $P_0^{(j)}$ corresponds to a chosen Pauli operator in the j-th clique of $\mathcal{T}$: by convention we say that this is the first operator in the set, but this can be any operator in the jth clique.

With respect to the phase-space model given in [42], a valid noncontextual state is defined by the parameters $(\vec{q},\vec{r})$, which set the expectation value of the operators in $\mathcal{R}$ (Equation 4). Each operator in $\mathcal{G}$ is assigned the value $\langle G_i\rangle = q_i = \pm 1$. The operators in $\mathcal{T}$ are assigned the values $\langle P_0^{(j)}\rangle = r_j$, where $\vec{r}$ is a unit vector ($|\vec{r}| = 1$) [14, 42]. The number of elements in $\vec{q}$ and $\vec{r}$ are $|\mathcal{G}|$ and N respectively. For n qubits the size of $|\mathcal{R}|$ is bounded by $2n+1$, which bounds the size of $(\vec{q},\vec{r})$ [42, 46].

The observables for the N anticommuting $P_0^{(j)}$ operators in $\mathcal{R}$ can be combined into the observable [42]:

$$
A(\vec{r}) = \sum_{j=0}^{N-1} r_j P_0^{(j)}. \tag{5}
$$

We denote the set of Pauli operators making up this operator as $\mathcal{A} \equiv \{P_0^{(j)} | j = 0, 1 \ldots, N-1\}$.

The expectation value of $A(\vec{r})$ is assigned by the hidden variable model to always be $+1$, due to:

$$
\langle A(\vec{r})\rangle = \sum_{j=0}^{N-1} r_j \langle P_0^{(j)}\rangle = \sum_{j=0}^{N-1} r_j r_j = \sum_{j=0}^{N-1} |r_j|^2 = +1, \tag{6}
$$

using $\langle P_0^{(j)}\rangle = r_j$ and $|\vec{r}| = 1$.

The expectation value for H_{noncon} can be induced, by setting the expectation values of operators in $\mathcal{R}$ (Equation 4), as this set generates $\mathcal{S}^{H_{\text{noncon}}}$ [14, 42]. To find the ground-state of H_{noncon}, we perform a brute force search over this space. For each possible ± 1 combination of expectation values for each G_j ($2^{|\mathcal{G}|}$ possibilities), the energy is minimized with respect to the unit vector $\vec{r}$ - that sets the expectation values $\langle P_0^{(j)}\rangle = r_j$. The Supplemental Material provides further algorithmic details [40]. The vector $(\vec{q},\vec{r})$ that was found to give the lowest energy defines the noncontextual ground-state. Each noncontextual state $(\vec{q},\vec{r})$, corresponds to subspaces of quantum states, which we will describe in subsection II D.

D. Contextual subspace

In [15] and [29] it was shown that an operator constructed as a normalized linear combination of pairwise anticommuting Pauli operators, such as $A(\vec{r})$ (Equation 5), is equivalent to a single Pauli operator up to a unitary rotation R. We can therefore write $A(\vec{r}) \mapsto P_0^{(k)} = RA(\vec{r})R^\dagger$ for a selected $P_0^{(k)} \in \mathcal{A}$. We write the set $\mathcal{R}_{\vec{r}}$ (Equation 4) under this transformation:

$$\mathcal{R}_{\vec{r}} \equiv \{A(\vec{r})\} \cup \mathcal{G} \quad \mapsto \mathcal{R}^{'} \equiv \underbrace{\{P_0^{(k)}\}}_{P_0^{(k)}=RA(\vec{r})R^\dagger} \cup \mathcal{G}. \tag{7}$$

It will be shown later that the unitary R is constructed from the operators in $\mathcal{A}$. This means that the terms in $\mathcal{G}$ are unaffected by this transformation, as operators in $\mathcal{G}$ and so must universally commute so must commute with R.

A given noncontextual state $(\vec{q}, \vec{r})$ is equivalent to the joint expectation value assignment of $\langle G_i \rangle = q_i = \pm 1$ and $\langle A(\vec{r}) \rangle = +1$. This defines a set of stabilizers:

$$\mathcal{W}_{all} \equiv \{q_0 G_0, q_1 G_1, ..., q_{|\mathcal{G}|-1} G_{|\mathcal{G}|-1}, A(\vec{r})\}, \tag{8}$$

which by definition must stabilize that noncontextual state $(\vec{q}, \vec{r})$ or more precisely, the subspace of quantum states corresponding to it [1]. Note that $A(\vec{r})$ is not a conventional stabilizer, but is unitarily equivalent to a single qubit operator $P_0^{(k)}$ [15, 29].

We can consider this problem under the unitary transform defined in Equation 7. The stabilizers in $\mathcal{W}_{all}$ become:

$$\mathcal{W}_{all}^{'} \equiv \{q_0 G_0, q_1 G_1, ..., q_{|\mathcal{G}|-1} G_{|\mathcal{G}|-1}, \xi\, P_0^{(k)}\}, \tag{9}$$

which defines a regular set of stabilizers for the noncontextual state $(\vec{q}, \vec{r})$, which defines a subspace of quantum states. Here $\xi = \pm 1$, is determined by $RA(\vec{r})R^\dagger = \xi P_0^{(k)}$ and can always be chosen to be $+1$, which we do throughout this paper.

Altogether, when certain noncontextual stabilizers are fixed (by the noncontextual state) they specify a subspace of allowed quantum states that will be consistent with that noncontextual state and thus define the constraints for the contextual part of the problem. We refer to this subspace as the contextual subspace [14].

E. Mapping a contextual subspace to a stabilizer subspace

In CS-VQE, the expectation value of the full Hamiltonian is obtained according to Equation 3. First, the noncontextual problem is solved yielding the noncontextual state $(\vec{q}, \vec{r})$ - normally the ground-state $(\vec{q}_0, \vec{r}_0)$. The Supplemental Material shows how $(\vec{q}_0, \vec{r}_0)$ can be obtained via a brute force approach [40]. Next the contextual Hamiltonian is projected into the subspace of allowed quantum states consistent with the defined noncontextual state. This constraint is imposed via: $H_{\text{full}} \mapsto H_{\text{full}}^{\mathcal{W}} = Q_{\mathcal{W}}^\dagger U_{\mathcal{W}}^\dagger H_{\text{full}} U_{\mathcal{W}} Q_{\mathcal{W}}$, where the expectation value is then found on a quantum device.

The unitary operation $U_{\mathcal{W}}$ is defined by the set of contextual stabilizers $\mathcal{W} \subseteq \mathcal{W}_{all}$ (equation 8), whose eigenvalue we fix according to the noncontextual state. If $A(\vec{r}) \in \mathcal{W}$, meaning that $\langle A(\vec{r}) \rangle$ is fixed to be $+1$, then the steps summarized in Equation 7 must first be performed to reduce $A(\vec{r})$ to a single Pauli operator. Clifford operators $V_i(P)$ are then used to map each $P \in \mathcal{W}$ to a single-qubit Z operator. Each V_i is made up of at most two $\frac{\pi}{2}$ Clifford rotations, generated by Pauli operators, per element in $\mathcal{W}$. In [14] it was shown that at most there will be $2n$ of these rotations, where n is the number of qubits the problem is defined on [47]. We can write this operator as:

$$U_{\mathcal{W}}^\dagger(\vec{q}, \vec{r}) = \begin{cases} \prod_{P_i \in \mathcal{W} \subseteq \mathcal{W}_{all}} V_i(P_i) & \text{if } A(\vec{r}) \notin \mathcal{W} \\ \left(\prod_{P_i \in \mathcal{W} \subseteq \mathcal{W}_{all}} V_i(P_i) \right) R & \text{if } A(\vec{r}) \in \mathcal{W}. \end{cases} \tag{10}$$

Applying $U_{\mathcal{W}}^\dagger \mathcal{W} U_{\mathcal{W}} = \mathcal{W}^Z$ results in a set of single-qubit Z Pauli operators. An implementation note is that each operator $V_i(P_i)$ in $U_{\mathcal{W}}$ depends on the others. This can be seen by expanding $U_{\mathcal{W}}^\dagger \mathcal{W} U_{\mathcal{W}}$. Therefore each V_i operator is dependent on the stabilizers in $\mathcal{W}$ and the order in which they occur. We recursively define each V_i as follows:

1. Set $\mathcal{W} = R\mathcal{W}R^\dagger$ if and only if $A(\vec{r}) \in \mathcal{W}$.
2. Find the unitary V_0 mapping the first Pauli operator $P_0 \in \mathcal{W}$ to a single qubit Pauli operator.
3. Apply this operator to each operator in the set: $V_0 \mathcal{W} V_0^\dagger = \mathcal{W}^{(0)}$.
4. Find the unitary V_1 mapping $V_0 P_1 V_0^\dagger \in \mathcal{W}^{(0)}$ to a single-qubit Z Pauli operator.
5. Apply this operator to all operators in the set: $V_1 \mathcal{W}^{(0)} V_1^\dagger = \mathcal{W}^{(1)}$
6. Repeat this procedure from step (3) until all the operators are mapped to single qubit Z Pauli operators: $\mathcal{W} \mapsto \mathcal{W}^Z$.

Finally, the eigenvalue of each single-qubit Z Pauli stabilizer in $\mathcal{W}^Z$ is defined by the vector $\vec{q}$ of the noncontextual ground-state $(\vec{q}, \vec{r})$, note that $\langle A(\vec{r}) \rangle$ is fixed to $+1$ and thus $\vec{r}$ is not important here. $U_{\mathcal{W}}$ can flip the sign of these assignments, but it is efficient to classical determine by tracking how $U_{\mathcal{W}}$ affects the sign of the operators in $\mathcal{W}$.

[1] Note that a stabilizer for a state leaves it unchanged. For example, if O stabilizes $|\psi\rangle$ then $O|\psi\rangle = |\psi\rangle$

To project the Hamiltonian into the subspace consistent with the noncontextual state, we first perform the following rotation $H_{\text{full}} \mapsto H^{'}_{\text{full}} = U^{\dagger}_{\mathcal{W}} H_{\text{full}} U_{\mathcal{W}}$. As this is a unitary transform, the resultant operator has the same spectrum as before. We then restrict the rotated Hamiltonian to the correct subspace by enforcing the eigenvalue of the operators in $\mathcal{W}^Z$, where the outcomes are defined by the noncontextual state. As each operator in $\mathcal{W}^Z$ only acts nontrivially on a unique qubit, each stabilizer fixes the state of that qubit to be either $|0\rangle$ or $|1\rangle$. We write this state as:

$$|\psi_{\text{fixed}}\rangle = \bigotimes_{P_v \in \mathcal{W}^Z} |i\rangle_v \begin{cases} i=0 & \text{if } \langle P_v \rangle = +1 \\ i=1 & \text{if } \langle P_v \rangle = -1, \end{cases} \tag{11}$$

where v indexes the qubit a given single-qubit stabilizer acts on and $\langle P_v \rangle$ is defined by the noncontextual state. We can write the projector onto this state as:

$$Q_{\mathcal{W}} = |\psi_{\text{fixed}}\rangle \langle \psi_{\text{fixed}}| \otimes \mathcal{I}_{(n-|\mathcal{W}^Z|)} \tag{12}$$

where $\mathcal{I}_{(n-|\mathcal{W}^Z|)}$ is the identity operator acting on the $(n-|\mathcal{W}^Z|)$ qubits not fixed by the single-qubit P_v stabilizers. The action on a general state $|\phi\rangle$ is:

$$Q_{\mathcal{W}} |\phi\rangle = |\psi_{\text{fixed}}\rangle \langle \psi_{\text{fixed}}| \phi\rangle \otimes |\phi\rangle_{(n-|\mathcal{W}^Z|)} \tag{13}$$

where $Q_{\mathcal{W}}$ has only fixed the state of qubits v and thus each stabilizer P_v removes 1 qubit from the problem. As the states of these qubits are fixed, the expectation values of the single-qubit Pauli matrices indexed on qubits v are known. Thus the Pauli operators in the rotated Hamiltonian $H_{\text{full}} \mapsto H^{'}_{\text{full}} = U^{\dagger}_{\mathcal{W}} H_{\text{full}} U_{\mathcal{W}}$ acting on these qubits can be updated accordingly and the Pauli matrices on qubits v can be dropped. Any term in the rotated Hamiltonian that anticommutes with a fixed generator P_v is forced to have an expectation value of zero and can be completely removed from the problem Hamiltonian. The resultant Hamiltonian acts on $|\mathcal{W}^Z|$ fewer qubits. We denote this operation as $H_{\text{full}} \mapsto H^{\mathcal{W}}_{\text{full}} = Q^{\dagger}_{\mathcal{W}} U^{\dagger}_{\mathcal{W}} H_{\text{full}} U_{\mathcal{W}} Q_{\mathcal{W}}$. The noncontextual approximation will be stored in the identity term of the problem and therefore does not need to be tracked separately.

The choice of which stabilizer eigenvalues to fix (i.e. what is included in $\mathcal{W}$) and which to allow to vary remains an open question of the CS-VQE algorithm. The number of possible stabilizer combinations will be $\sum_{i=1}^{|\mathcal{W}_{all}|} \binom{|\mathcal{W}_{all}|}{i} = 2^{|\mathcal{W}_{all}|} - 1$. Rather than searching over all $2^{|\mathcal{W}_{all}|} - 1$ combinations of stabilizers to fix, in this paper we use the heuristic given in [14]. This begins at the full noncontextual approximation, where $\mathcal{W}$ contains all possible stabilizers. We then add a qubit to the quantum correction, by removing an operator from $\mathcal{W}$ and greedily choosing each pair that gives the lowest ground-state energy estimate [14]. Alternative strategies on how to do this remain an open question of CS-VQE. A possible way to approach this problem is to look at the priority of different terms in H_{con} [48]. Note that the quality of the approximation is sensitive to which stabilizers are included in $\mathcal{W}$. When fewer stabilizers are considered (included in $\mathcal{W}$), the resultant rotated Hamiltonians will act on more qubits and approximate the true ground-state energy better.

In [14], Kirby *et al.* construct R as a sequence of rotations (exponentiated Pauli operators) defined by $A(\vec{r})$ as in the unitary partitioning method [15, 29]. We denote this operation R_S. The Supplemental Material gives the full definition of this operator [40]. If R_S is considered as just an arbitrary sequence of exponentiated Pauli operator rotations, then the transformation $H_{\text{full}} \mapsto H^{R_S}_{\text{full}} = R_S H_{\text{full}} R_S^{\dagger}$ results in an operator whose terms have increased by a factor of $\mathcal{O}(2^N)$, where N is the number of cliques defined from $\mathcal{T}$ [14]. This presents a possible roadblock for the CS-VQE algorithm, as classically precomputing $U^{\dagger}_{\mathcal{W}} H_{\text{full}} U_{\mathcal{W}}$ could cause the number of terms to exponentially increase. We give a further analysis of this in the Supplemental Material [40]. Additional structure between R_S and H_{full} can make the base of the exponent slightly lower; however, the scaling still remains exponential in the number of qubits n, where $|\mathcal{A}| \leq 2n+1$ [42]. The only case in which there is not an exponential increase in terms is for the trivial instance that R_S commutes with H_{full}. In the next section, we provide an alternative construction of R via a linear combination of unitaries (LCU) that results in only a quadratic increase in the number of terms of the Hamiltonian when transformed. This avoids the need to apply the unitary partitioning operator R (via a sequence of rotations) coherently in the quantum circuit after the ansatz circuit, which was proposed in [14].

F. Linear combination of unitaries construction of R

In the unitary partitioning method [15, 29], it was shown that R could also be built as a linear combination of Pauli operators[15, 30]. We provide the full construction in the Supplemental Material [40]. We denote the operator as R_{LCU}. Rotating a general Hamiltonian H_{full} by this operation R_{LCU} results in:

$$\begin{aligned} R_{LCU} H_{\text{full}} R^{\dagger}_{LCU} = & \sum_{i}^{|H_{\text{full}}|} (\mu_i) P_i + \\ & \sum_{j}^{|\mathcal{A}|-1} \sum_{\substack{i \\ \forall \{P_j P_k, P_i\}=0}}^{|H_{\text{full}}|} \mu_{ij} P_j P_k P_i + \\ & \sum_{j}^{|\mathcal{A}|-1} \sum_{i}^{|H_{\text{full}}|} \sum_{\substack{l>j \\ \forall \{P_i, P_j P_l\}=0}}^{|\mathcal{A}|-1} \mu_{ijl} P_i P_j P_l. \end{aligned} \tag{14}$$

The Pauli operators P_j, P_k and P_l are operators in $\mathcal{A}$, further details are covered in the Supplemental Material [40]. Overall, this unitary transformation causes the number of terms in the Hamiltonian to scale as $\mathcal{O}\big(\,|H_{\text{full}}|\cdot|\mathcal{A}|^2\,\big)$. This scaling is quadratic in the size of $\mathcal{A}$ and as $|\mathcal{A}| \leq 2n+1$ [42], the number of terms in the rotated system will at worst scale quadratically with the number of qubits n. In a different context, this scaling result was also obtained for involutory linear combinations of entanglers [49]. Overall, unlike the sequence of rotations approach, this non-Clifford operation doesn't cause the number of terms in a Hamiltonian to increase exponentially.

The transformation given in Equation 14 $H_{\text{full}} \mapsto H_{\text{full}}^{LCU} = R_{LCU}^{\dagger} H_{\text{full}} R_{LCU}$ is performed classically in CS-VQE. This is efficient to do because it just involves Pauli operator multiplication, which can be done symbolically or via a symplectic approach [50]. This operation could be applied within the quantum circuit. However, in contrast to the deterministic sequence of rotations approach, this implementation would be probabilistic as it requires post selection on an ancillary register [15, 30, 51, 52]. Amplitude amplification techniques could improve this, but would require further coherent resources [53–56]. Performing this transformation in a classical pre-processing step therefore reduces the coherent resources required and at worst increases the number of terms needing measuring quadratically with respect to the number of qubits.

G. CS-VQE implementation

In [14], $U_{\mathcal{W}}(\vec{q},\vec{r})$ was fixed to include all the stabilizers of the noncontextual ground-state $\mathcal{W} \equiv \mathcal{W}_{all}$ (Equation 8), rather than possible subsets $\mathcal{W} \subseteq \mathcal{W}_{all}$. The whole Hamiltonian was mapped according to $H_{\text{full}} \mapsto H_{\text{full}}^{'} = U_{\mathcal{W}_{all}}^{\dagger} H_{\text{full}} U_{\mathcal{W}_{all}}$. In general, $A(\vec{r}) \in \mathcal{W}$ and $U_{\mathcal{W}_{all}}$ will therefore normally include the unitary partitioning operator R. The problem with this approach is that the unitary R is not a Clifford operation and the transformation can cause the number of terms in the Hamiltonian to increase. This increase is exponential if R_S is used and quadratic if R_{LCU} is employed. As this step can generate more terms, R should only be included in $U_{\mathcal{W}}$ if the eigenvalue of $A(\vec{r})$ is fixed to $+1$, otherwise it is a redundant operation as the spectrum of the operator rotated by R is unchanged. We therefore modify the CS-VQE algorithm to construct $U_{\mathcal{W}}$ from the CS-VQE noncontextual generator eigenvalues that are fixed. This means that $\mathcal{W} \subseteq \mathcal{W}_{all}$ and ensures that the number of terms can only increase if the eigenvalue of $A(\vec{r})$ is fixed.

III. NUMERICAL RESULTS

We describe the method in Section III A and then split our results into the two remaining sections. First, we explore a toy problem, showing the steps of the CS-VQE algorithm. We show how classically applying R without fixing the eigenvalue of $A(\vec{r})$ to $+1$ can unnecessarily increase the number of terms in a Hamiltonian without changing its spectrum. Finally, in Section III C we apply measurement reduction combined with CS-VQE to a set of electronic structure Hamiltonians and show that this can significantly reduce the number of terms requiring separate measurement. The raw data for these results are supplied in the Supplemental Material [40].

A. Method

We investigated the same electronic structure Hamiltonians considered in the original CS-VQE paper [14]. All molecules considered had a multiplicity of 1 and thus a singlet ground-state. The same qubit tapering was performed to remove the $\mathbb{Z}_2$ symmetries [57]. For each tapered Hamiltonian, we generate a set of reduced Hamiltonians $\{Q_{\mathcal{W}}^{\dagger} U_{\mathcal{W}}^{\dagger} H_{\text{full}} U_{\mathcal{W}} Q_{\mathcal{W}}\}$ where the size of $\mathcal{W}$ varies from 1 to $|\mathcal{W}_{all}|$, representing differing noncontextual approximations, as summarized in Section II G. To generate the different CS-VQE Hamiltonians, we modify the original CS-VQE source code used in [14, 58]. The code was modified to implement the unitary partitioning step of CS-VQE if and only if the eigenvalue of $A(\vec{r})$ was fixed. This ensured that the number of terms in the rotated Hamiltonian did not increase unnecessarily, as described in Section II G.

For each electronic structure Hamiltonian generated in this way, we then apply the unitary partitioning measurement reduction scheme to further reduce the number of terms requiring separate measurement [15, 29, 30]. Partitioning into anticommuting sets was performed using NETWORKX [59]. A graph of the qubit Hamiltonian is built, where nodes represent Pauli operators and edges are between nodes that commute. A graph coloring can be used to find the anticommuting cliques of the graph. This searches for the minimum number of colors required to color the graph, where no neighbors of a node can have the same color as the node itself. The "largest first" coloring strategy in NETWORKX was used in all cases [59, 60].

We calculate the ground-state energy of each Hamiltonian in this paper by directly evaluating the lowest eigenvalues. This was achieved by diagonalizing them on a conventional computer.

B. Toy example

We consider the qubit Hamiltonian:

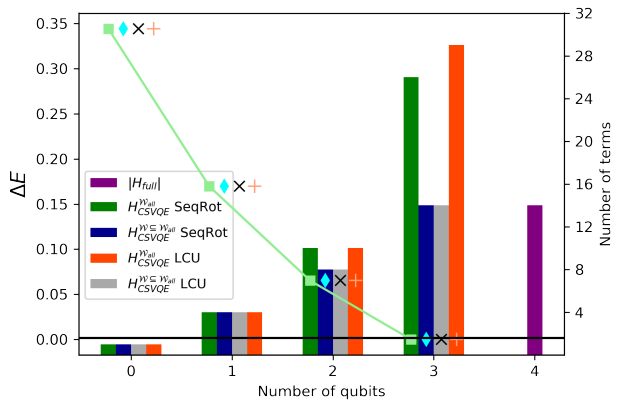


FIG. 1: ground-state energy and the number of terms of different contextual subspace projected Hamiltonians generated in CS-VQE. Each Hamiltonian has been transformed as $Q^\dagger_{\mathcal{W}}U^\dagger_{\mathcal{W}}HU_{\mathcal{W}}Q_{\mathcal{W}}$, apart from the 4 qubit case, which is the full H. The scatter plot is associated with the left-hand y-axis and gives the energy error as: $\Delta E = |E_{approx} - E_{true}|$. The bar chart gives the number of terms in each Hamiltonian and is associated with the right-hand y-axis. From left to right the following generators are fixed: $\{YIYI, IXYI, IIIZ, \mathcal{A}(\vec{r}_0)\}$, $\{IXYI, IIIZ, \mathcal{A}(\vec{r}_0)\}$, $\{IXYI, IIIZ\}$, $\{IIIZ\}$ and $\{\}$. The $\mathcal{W} = \{\}$ case represents standard full VQE over the full problem. The 0 qubit case presents the scenario where the problem is fully noncontextual and no quantum correction is made. The full details as to how each Hamiltonian is built is provided in the Supplemental Material [40]. The horizontal black line indicates an absolute error of 1.6×10^{-3}. SeqRot, sequence of rotations

Molecule	Basis	Number of gates for R_S
BeH_2	(STO-3G)	[90, 72]
Mg	(STO-3G)	[189, 162]
$H_3{}^+$	(3-21G)	[209, 176]
O_2	(STO-3G)	[184, 160]
OH^-	(STO-3G)	[104, 80]
CH_4	(STO-3G)	[325, 286]
Be	(STO-3G)	[14, 8]
NH_3	(STO-3G)	[299, 260]
H_2S	(STO-3G)	[120, 96]
H_2	(3-21G)	[66, 48]
HF	(3-21G)	[735, 672]
F_2	(STO-3G)	[133, 112]
HCl	(STO-3G)	[36, 24]
HeH^+	(3-21G)	[88, 64]
MgH_2	(STO-3G)	[403, 364]
CO	(STO-3G)	[325, 286]
LiH	(STO-3G)	[36, 24]
N_2	(STO-3G)	[207, 180]
NaH	(STO-3G)	[493, 442]
H_2O	(STO-3G)	[120, 96]
$H_3{}^+$	(STO-3G)	[3, 0]
LiOH	(STO-3G)	[378, 336]
LiH	(3-21G)	[459, 408]
H_2	(6-31G)	[66, 48]
$NH_4{}^+$	(STO-3G)	[325, 286]
HF	(STO-3G)	[36, 24]

TABLE I: Gate requirements to implement R as a sequence of rotations in the unitary partitioning measurement reduction step. The square tuple gives the upper bound on the number of single qubit and CNOT gates required - $[single, CNOT]$. These resource requirements are based on the largest anticommuting clique of each Hamiltonian, as these have the largest circuit requirements for R_S.

$$\begin{aligned} H = {} & 0.6\,IIYI + 0.7\,XYXI + 0.7\,XZXI + 0.6\,XZZI + \\ & 0.1\,YXYI + 0.7\,ZZZI + 0.5\,IIIZ + 0.1\,XXXI + \\ & 0.5\,XXYI + 0.2\,XXZI + 0.2\,YXXI + 0.2\,YYZI + \\ & 0.1\,YZXI + 0.1\,ZYYI, \end{aligned} \tag{15}$$

and use it to exemplify the steps of the CS-VQE algorithm. The results are reported to three decimal places and full numerical details can be found in the Supplemental Material [40].

Following the CS-VQE procedure [14], we first split the Hamiltonian into its contextual and noncontextual parts (Equation 2):

$$\begin{aligned} H_{\text{noncon}} = {} & 0.5\,\underbrace{IIIZ}_{\mathcal{Z}} + \\ & 0.7\,XZXI + 0.7\,ZZZI + \\ & 0.1\,YXYI + 0.6\,IIYI + \\ & \underbrace{0.7\,XYXI + 0.6\,XZZI}_{\mathcal{T}} \end{aligned} \tag{16a}$$

$$\begin{aligned} H_{\text{con}} = {} & 0.1\,XXXI + 0.5\,XXYI + 0.2\,XXZI + \\ & 0.2\,YXXI + 0.2\,YYZI + 0.1\,YZXI + \\ & 0.1\,ZYYI. \end{aligned} \tag{16b}$$

Each row after the first in Equation 16a, is a clique of $\mathcal{T}$. From here, we define the set $\mathcal{R}$ (Equation 4):

$$\mathcal{R} = \underbrace{\{YIYI, IXYI, IIIZ\}}_{\mathcal{G}} \cup \underbrace{\{XZXI, YXYI, XYXI\}}_{\{P_0^{(j)} | j=0,1,..,N-1\}}. \tag{17}$$

Note how different combinations of the operators in Equation 17 allow all the operators in H_{noncon} (Equation 16a) to be inferred under the Jordan product, defined as: $P_a \circ P_b = \frac{\{P_a, P_b\}}{2}$. Basically, the Jordan product is equal to the regular matrix product if the operators commute, and equal to zero if the operators anticommute. Next the noncontextual problem was solved.

The expectation value for H_{noncon} can be induced, by setting the expectation values of operators in $\mathcal{R}$ (Equation 17), as the Pauli operators in H_{noncon} are generated by $\mathcal{R}$ under the Jordan product. The expectation value of

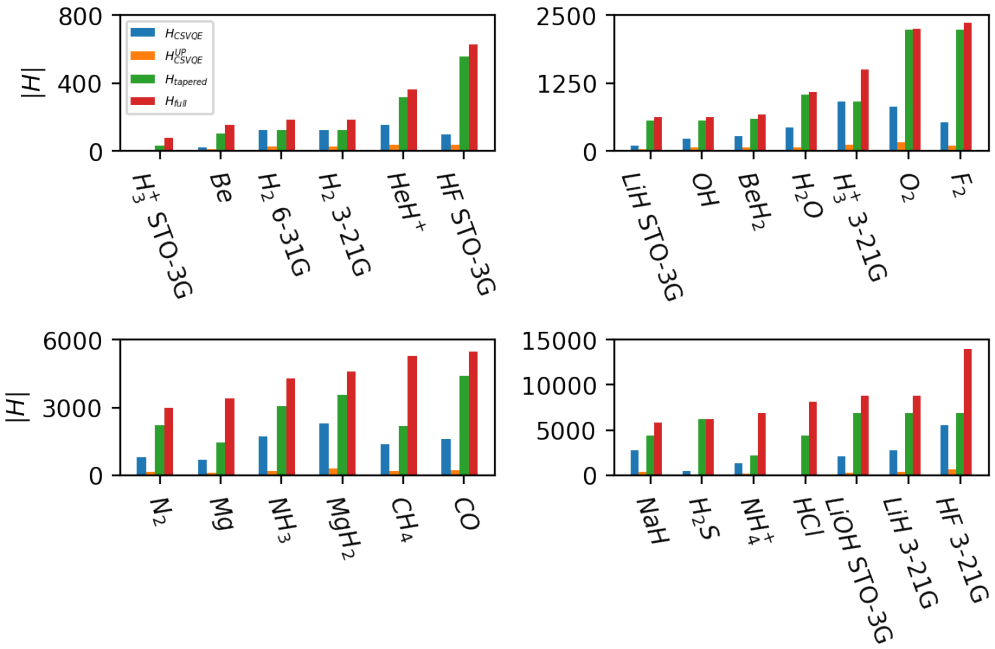


FIG. 2: Number of Pauli operators requiring separate measurement to determine the ground-state energy of a particular molecular Hamiltonian to within chemical accuracy. For each molecule the full Hamiltonian, tapered Hamiltonian, CS-VQE and CS-VQE with unitary partitioning measurement reduction applied are given. Full numerical numerical details of each are provided in the Supplemental Material [40]. The size of the Hamiltonian for LiH (3-21G singlet) with measurement reduction applied is different for the sequence of rotations and LCU unitary partitioning methods. This is an artifact of the graph color heuristic finding different anticommuting cliques in the CS-VQE Hamiltonian.

each operator in H_{noncon} can therefore be inferred without contradiction. To find the ground-state of H_{noncon}, we checked all possible ± 1 expectation values for each G_j ($2^3 = 8$ possibilities). For each possible ± 1 combination, the energy was minimized with respect to the unit vector $\vec{r}$, which sets the expectation value for each $\langle P_0^{(j)} \rangle = r_j$. The vector $(\vec{q}, \vec{r})$ that was found to give the lowest energy defines the noncontextual ground-state. In this case the ground-state is:

$$(\underbrace{-1,+1,-1}_{\vec{q}_0},\underbrace{+0.253,-0.658,-0.709}_{\vec{r}_0}). \tag{18}$$

This noncontextual state defines the operator $\mathcal{A}(\vec{r}_0)$:

$$A(\vec{r}_0) = 0.253\,YXYI - 0.658\,XYXI - 0.709\,XZXI. \tag{19}$$

From this we can write $\mathcal{R}_{\vec{r}}$ (Equation 7)

$$\mathcal{R}_{\vec{r}} \equiv \{A(\vec{r}_0)\} \cup \{YIYI, IXYI, IIIZ\} \tag{20}$$

To map $A(\vec{r}_0)$ to a single Pauli operator we use unitary partitioning [15, 29, 30]. The required unitary can be constructed as either a sequence of rotations [15],

$$R_S = e^{-1i\cdot 0.788\cdot ZYZI} \cdot e^{+1i\cdot 1.204\cdot ZZZI}, \tag{21}$$

or linear combination of unitaries [15],

$$R_{LCU} = 0.792\,IIII + 0.416i\,ZZZI - 0.448i\,ZYZI. \tag{22}$$

These operators perform the following reduction: $R_S A(\vec{r}_0) R_S^\dagger = R_{LCU} A(\vec{r}_0) R_{LCU}^\dagger = YXYI$.

If the eigenvalue of $A(\vec{r}_0)$ is fixed, then we should consider $\mathcal{R}_{\vec{r}}$ (Equation 20) under the unitary transform R_{LCU} or R_S (Equation 7):

$$\begin{aligned}\mathcal{R}' &= R_{S/LCU} A(\vec{r}) R_{S/LCU}^\dagger \cup \{YIYI, IXYI, IIIZ\} \\ &= \{YXYI\} \cup \{YIYI, IXYI, IIIZ\}.\end{aligned} \tag{23}$$

Equations 18, 20 and 23 define the noncontextual stabilizers:

$$\begin{aligned}\mathcal{W}_{all} &\equiv \{+1\,A(\vec{r}_0)\ , -1\,YIYI, +1\,IXYI, -1\,IIIZ\}, \\ \mathcal{W}'_{all} &\equiv \{+1\,YXYI, -1\,YIYI, +1\,IXYI, -1\,IIIZ\}.\end{aligned} \tag{24}$$

Next, we define different $U_{\mathcal{W}}$ (Equation 10), depending on which stabilizers $\mathcal{W}$ we wish to fix. For this

problem we found the optimal ordering of which stabilizers to fix to be $\{-1\,YIYI, +1\,IXYI, +1\,\mathcal{A}(\vec{r}_0), -1\,IIIZ\}$ followed by $\{+1\,IXYI, -1\,IIIZ, +1\,\mathcal{A}(\vec{r}_0)\}$ followed by $\{+1\,IXYI, -1\,IIIZ\}$ followed by $\{-1\,IIIZ\}$. This was achieved by a brute force search over all $\sum_{i=1}^{|\mathcal{W}_{all}|}\binom{|\mathcal{W}_{all}|}{i} = 2^4 - 1 = 15$ possibilities for $\mathcal{W}$.

The members of the resulting set of four different $\mathcal{W}$ each represent different noncontextual approximations. These give four different $U_{\mathcal{W}}$ built according to Equation 10. The full definition of each operator is given in the Supplemental Material [40].

Taking a specific example, for $\mathcal{W} = \{+IXYI, -IIIZ, +\mathcal{A}(\vec{r}_0)\}$ we define $U_{\mathcal{W}}^{\dagger}$ (Equation 10). This operator transforms $\mathcal{W}$ as $\mathcal{W}^Z = U_{\mathcal{W}}^{\dagger}\mathcal{W}U_{\mathcal{W}} = \{+IZII, -IIIZ, +IIZI\}$. The eigenvalues of the operators in $\mathcal{W}^Z$ are fixed by the noncontextual state to be $\langle IZII\rangle = +1$, $\langle IIZI\rangle = +1$, $\langle IIIZ\rangle = -1$. This defines the projector:

$$\begin{aligned} Q_{\mathcal{W}} &= \Big(\underbrace{|0\rangle\langle 0| + |1\rangle\langle 1|}_{\mathcal{I}_{(n-|\mathcal{W}^Z|)}}\Big) \otimes \underbrace{|0\rangle\langle 0| \otimes |0\rangle\langle 0| \otimes |1\rangle\langle 1|}_{|\psi_{\text{fixed}}\rangle} \\ &= I \otimes |001\rangle\langle 001| \,. \end{aligned} \tag{25}$$

The reduced Hamiltonian is therefore

$$\begin{aligned} H \mapsto H_{\mathcal{W}}^{LCU} &= Q_{\mathcal{W}}^{\dagger} U_{\mathcal{W}}^{\dagger\,(LCU)} H_{\text{full}} U_{\mathcal{W}}^{(LCU)} Q_{\mathcal{W}} \\ &= -1.827\, I - 0.414\, X - 0.292\, Z + 0.648\, Y. \end{aligned} \tag{26}$$

The Supplemental Material gives further details about this operation and provides the specifics for the other projected Hamiltonians [40].

Overall four Hamiltonians are generated, representing different levels of approximation, that act on 0, 1, 2 and 3 qubits respectively. The 4 qubit case represents the standard VQE on the full Hamiltonian. Figure 1 summarizes the error ΔE of each of these compared with the true ground-state energy (scatter plot). The number of terms in each Hamiltonian is given by the bar chart. The green and orange results have $\mathcal{W} \equiv \mathcal{W}_{all}$ for all cases and represent the old CS-VQE implementation. For these results, in the 3 and 4 qubit Hamiltonians have an increased number of terms due to $R_{S/LCU}$ being implemented, even though the eigenvalue of $\mathcal{A}(\vec{r}_0)$ is not being fixed to +1. On the other hand, the gray and blue results in Figure 1 build $U_{\mathcal{W}}$ according to Equation 10, where $\mathcal{W} \subseteq \mathcal{W}_{all}$. This approach ensures that $R_{S/LCU}$ is only applied when necessary.

C. Measurement reduction

Figures 2 and 3 summarize the results of applying the unitary partitioning measurement reduction strategy to a set of electronic structure Hamiltonians We report the number of terms and number of qubits in each Hamiltonian required to achieve chemical accuracy compared with the original problem. The Supplemental Material gives further information about each result, where the different levels of noncontextual approximation are shown [40]. As previously discussed in [14], even though CS-VQE in general is an approximate method, chemical accuracy can still be achieved using significantly fewer qubits. Applying unitary partitioning on-top of the reduced CS-VQE Hamiltonians required to achieve chemical accuracy can further reduce the number of terms by roughly an order of magnitude. This is consistent with the previous results in [30].

To actually obtain a measurement reduction, one needs to show that the number of measurement required to measure the energy of a molecular system, to a certain precision ϵ, is reduced. Currently, Figure 2 only shows that we have reduced the number of Pauli terms being measured. We have not commented on the variance. In the Supplemental Material [40], we prove that simultaneous measurement of normalized anticommuting cliques can never do worse than performing no measurement reduction and will more often than not give an improvement. The proof given is state independent. There are other measurement strategies based on grouping techniques, such as splitting a Hamiltonian into commuting or qubit-wise commuting cliques [16, 17, 21, 24, 25]. The measurement reduction obtained from these methods is more complicated, as the covariance of operators within a clique must be carefully accounted for [24, 61]. This is one of the reasons we do not analyze the performance of these strategies in this paper. Many other measurement methods have also been proposed [18–20, 22, 23, 25–28, 62, 63] and their effect on the number of measurements would be interesting to investigate.

In Table I, we report the upper bound on the gate count required to implement measurement reduction as a sequence of rotations. The LCU method would require ancilla qubits and analysis of the circuit depth is more complicated. Further analysis can be found in [30]. The number of extra coherent resources required to implement unitary partitioning measurement reduction is proportional to the size of each anticommuting clique a Hamiltonian is split into [15, 30]. The sequence of rotations circuit depth scales as $\mathcal{O}\big(N_s(|C|-1)\big)$ single qubit and $\mathcal{O}\big(N_s(|C|-1)\big)$ CNOT gates, where N_s is the number of system qubits and $|C|$ is the size of the anticommuting clique being measured. Table I reports the gate count upper bound for the largest anticommuting clique of a given CS-VQE Hamiltonian. We do not consider possible circuit simplifications, such as gate cancellations. To decrease the depth of quantum circuit required for practical application, we suggest finding nonoptimal clique covers; for example, if anticommuting cliques are fixed to a size of 2, the resources required to perform R_S are experimentally realistic for current and near-term devices, as only $\mathcal{O}(N_s)$ single qubit and $\mathcal{O}(N_s)$ CNOT gates are required [30].

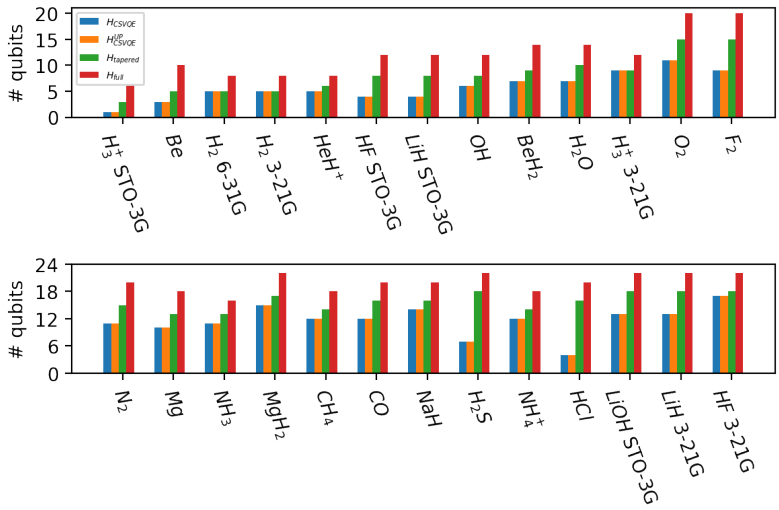


FIG. 3: Number of qubits required to simulate different electronic structure Hamiltonians in order to achieve chemical accuracy. For each molecule the full Hamiltonian, tapered Hamiltonian, CS-VQE and CS-VQE with unitary partitioning measurement reduction applied are given. Numerical details for each result are provided in the Supplemental Material.

The heuristic used to determine the operators in H_{noncon} selected terms in the full Hamiltonian greedily by coefficient magnitude, while keeping the set noncontextual [42]. The Hamiltonians studied here had weights dominated by diagonal Pauli operators, as the Hartree-Fock approximation accounts for most of the energy. This heavily constrains the operators allowed in $\mathcal{A}$. For the electronic structure Hamiltonians considered in this paper, we found in all cases that $|\mathcal{A}| = 2$. In general, we do expect more commuting terms in H_{noncon} than anticommuting terms. This is because there are more possible commuting Pauli operators defined on n qubits compared with anticommuting operators (2^n vs $2n+1$). $\mathcal{G}$ will therefore in general be the larger contributor to the superset $\mathcal{R}$ (Equation 4).

In Figure 2, the CS-VQE bars have not been split into two for the case when R is constructed as R_{LCU} or R_S. This is due to $|\mathcal{A}|$ being 2 in all cases, which is the special case when these operators (R_{LCU} and R_S) end up being identical. In this instance R has the form $R = \alpha I + i\beta P$ and thus the number of terms will only increase for every term in the Hamiltonian that P anticommutes with. However, in general $|\mathcal{A}|$ will be greater than 2 and the effect of R can dramatically affect the number of terms in the resultant rotated Hamiltonian. We observe this in Fig. 1 of the toy example, where the 2 and 3 qubit CS-VQE Hamiltonians have had $U_{\mathcal{W}_{all}}$ applied to them even though the eigenvalue of $A(\vec{r})$ is not fixed. In that example, for the 3 qubit approximation the sequence-of-rotations rotated Hamiltonian (green) actually has fewer terms than the LCU rotated operator (orange). This result is an artifact of the small problem size. In the Supplemental Material we show that the scaling will favor the LCU implementation, where the number of terms in a Hamiltonian can only increase quadratically, not exponentially, when performing the unitary partitioning rotation as a LCU rather than a sequence of rotations [40].

In the Supplemental Material, we show the convergence of CS-VQE at different noncontextual approximations. The results illustrate that CS-VQE can converge to below chemical accuracy well before the case when no noncontextual approximation is made (full VQE). Results beyond convergence are included to show the different possible levels of approximation. In practice knowledge of the true ground-state energy is not known *a priori* and so using chemical precision to motivate the noncontextual approximation will not be possible. In this setting, a way to approach quantum advantage is to note that CS-VQE is a variational method. The quantum resources required can be expanded until the energy obtained by CS-VQE is lower than that coming from the best possible classical method. At this point, either the algorithm can be terminated or further contextual corrections can be added until the energy converges, at which point the algorithm should be stopped.

IV. CONCLUSION

The work presented here shows that combining the unitary partitioning measurement reduction strategy with the CS-VQE algorithm can further reduce the number of terms in the projected Hamiltonian requiring separate measurement by roughly an order of magnitude for a given molecular Hamiltonian. The number of qubits needed to achieve chemical accuracy in most cases was also dramatically decreased, for example the H_2S (STO-3G singlet) problem was reduced to 7 qubits from 22.

We also improve two parts of the CS-VQE algorithm. First, we avoid having to apply the unitary partitioning operator R after the ansatz which averts the potential exponential increase in the number of Pauli operators of the CS-VQE Hamiltonian caused by classically computing the non-Clifford rotation of the full Hamiltonian when R defined as a sequence of rotations [14, 15]. We show that applying this operation as a linear combination of unitaries [15]: $H_{\text{full}} \mapsto H_{\text{full}}^{LCU'} = R_{LCU}^{\dagger} H_{\text{full}} R_{LCU}$, results in the number terms at worst increasing quadratically with the number of qubits. This result makes classically precomputing this transformation tractable and R no longer needs to be performed coherently after the ansatz. Secondly, we define the unitary $U_{\mathcal{W}}$, which maps each stabilizer in $\mathcal{W}_{all}$ (equation 9) to a distinct single-qubit Pauli matrix, according to which stabilizer eigenvalues are fixed by the noncontextual state. This ensures that the non-Clifford rotation required by CS-VQE is only applied when necessary and also reduces the number of redundant Clifford operations that are classically performed.

There are still several open questions for the CS-VQE algorithm. We summarize a few here. (1) What is the best optimization strategy to use when minimizing the energy over $(\vec{q}, \vec{r})$ in the classical noncontextual problem? (2) What heuristic is best to construct the largest $|H_{\text{noncon}}|$? (3) How can we efficiently determine which noncontextual stabilizers to fix while maintaining low errors? In this paper, the size of each electronic structure problem allowed us to classically compute the ground-state energies at each step, but if this is not possible then VQE calculations would be required. However, as each run requires fewer qubits and decreases the number of terms requiring separate measurement this approach may overall still be less costly than performing VQE over the whole problem, especially when combined with further measurement reduction strategies. (4) What are the most important terms to include in H_{con} or equivalently in H_{noncon}? Currently, it is not known whether $|H_{\text{noncon}}|$ should be maximized or whether selecting high priority terms [48] from the whole Hamiltonian results in a better approximation for a given problem. We leave these questions to future work.

We have written an open-source CS-VQE code that includes all the updated methodology discussed in this paper. We welcome readers to make use of this, which is freely available on GitHub [64].

ACKNOWLEDGMENTS

A. R. and T.W. acknowledge support from the Unitary Fund and the Engineering and Physical Sciences Research Council (Grants No. EP/L015242/1 and No. EP/S021582/1 respectively). T.W. also acknowledges support from CBKSciCon Ltd., Atos, Intel and Zapata. W.M.K. and P.J.L. acknowledge support by the NSF STAQ project (Grant No. PHY-1818914). W.M.K. acknowledges support from the National Science Foundation, Grant No. DGE-1842474. P.V.C. is grateful for funding from the European Commission for VECMA (800925) and EPSRC for SEAVEA (Grant No. EP/W007711/1).

[1] A. Szabo and N. S. Ostlund, *Modern Quantum Chemistry: Introduction to Advanced Electronic Structure Theory* (Macmillan, New York, 2012).

[2] A. Aspuru-Guzik, A. D. Dutoi, P. J. Love, and M. Head-Gordon, Simulated quantum computation of molecular energies, Science **309**, 1704 (2005).

[3] R. Babbush, C. Gidney, D. W. Berry, N. Wiebe, J. McClean, A. Paler, A. Fowler, and H. Neven, Encoding electronic spectra in quantum circuits with linear t complexity, Physical Review X **8**, 041015 (2018).

[4] V. E. Elfving, B. W. Broer, M. Webber, J. Gavartin, M. D. Halls, K. P. Lorton, and A. Bochevarov, How will quantum computers provide an industrially relevant computational advantage in quantum chemistry?, arXiv preprint arXiv:2009.12472 (2020).

[5] A. J. McCaskey, Z. P. Parks, J. Jakowski, S. V. Moore, T. D. Morris, T. S. Humble, and R. C. Pooser, Quantum chemistry as a benchmark for near-term quantum computers, npj Quantum Information **5**, 99 (2019).

[6] A. Y. Kitaev, Quantum measurements and the abelian stabilizer problem, arXiv preprint quant-ph/9511026 (1995).

[7] P. J. O'Malley, R. Babbush, I. D. Kivlichan, J. Romero, J. R. McClean, R. Barends, J. Kelly, P. Roushan, A. Tranter, N. Ding, *et al.*, Scalable quantum simulation of molecular energies, Physical Review X **6**, 031007 (2016).

[8] H. Mohammadbagherpoor, Y.-H. Oh, A. Singh, X. Yu, and A. J. Rindos, Experimental challenges of implementing quantum phase estimation algorithms on IBM quantum computer, arXiv preprint arXiv:1903.07605 (2019).

[9] A. Peruzzo, J. McClean, P. Shadbolt, M.-H. Yung, X.-Q. Zhou, P. J. Love, A. Aspuru-Guzik, and J. L. O'brien, A variational eigenvalue solver on a photonic quantum processor, Nature communications **5**, 4213 (2014).

[10] E. Farhi, J. Goldstone, and S. Gutmann, A quantum approximate optimization algorithm, arXiv preprint arXiv:1411.4028 (2014).

[11] C. Bravo-Prieto, R. LaRose, M. Cerezo, Y. Subasi, L. Cincio, and P. J. Coles, Variational quantum linear solver, arXiv preprint arXiv:1909.05820 (2019).

[12] A. Eddins, M. Motta, T. P. Gujarati, S. Bravyi, A. Mezzacapo, C. Hadfield, and S. Sheldon, Doubling the size of quantum simulators by entanglement forging, PRX Quantum **3**, 010309 (2022).

[13] W. J. Huggins, B. A. O'Gorman, N. C. Rubin, D. R. Reichman, R. Babbush, and J. Lee, Unbiasing fermionic quantum monte carlo with a quantum computer, Nature

603, 416 (2022).
[14] W. M. Kirby, A. Tranter, and P. J. Love, Contextual subspace variational quantum eigensolver, Quantum **5**, 456 (2021).
[15] A. Zhao, A. Tranter, W. M. Kirby, S. F. Ung, A. Miyake, and P. J. Love, Measurement reduction in variational quantum algorithms, Physical Review A **101**, 062322 (2020).
[16] A. Kandala, A. Mezzacapo, K. Temme, M. Takita, M. Brink, J. M. Chow, and J. M. Gambetta, Hardware-efficient variational quantum eigensolver for small molecules and quantum magnets, Nature **549**, 242 (2017).
[17] V. Verteletskyi, T.-C. Yen, and A. F. Izmaylov, Measurement optimization in the variational quantum eigensolver using a minimum clique cover, The Journal of Chemical Physics **152**, 124114 (2020).
[18] A. F. Izmaylov, T.-C. Yen, and I. G. Ryabinkin, Revising the measurement process in the variational quantum eigensolver: is it possible to reduce the number of separately measured operators?, Chemical Science **10**, 3746 (2019).
[19] J. Cotler and F. Wilczek, Quantum overlapping tomography, Physical Review Letters **124**, 100401 (2020).
[20] X. Bonet-Monroig, R. Babbush, and T. E. O'Brien, Nearly optimal measurement scheduling for partial tomography of quantum states, Physical Review X **10**, 031064 (2020).
[21] P. Gokhale and F. T. Chong, $o(n^3)$ measurement cost for variational quantum eigensolver on molecular Hamiltonians, arXiv preprint arXiv:1908.11857 (2019).
[22] A. Jena, S. Genin, and M. Mosca, Pauli partitioning with respect to gate sets, arXiv preprint arXiv:1907.07859 (2019).
[23] W. J. Huggins, J. R. McClean, N. C. Rubin, Z. Jiang, N. Wiebe, K. B. Whaley, and R. Babbush, Efficient and noise resilient measurements for quantum chemistry on near-term quantum computers, npj Quantum Information **7**, 23 (2021).
[24] P. Gokhale, O. Angiuli, Y. Ding, K. Gui, T. Tomesh, M. Suchara, M. Martonosi, and F. T. Chong, Minimizing state preparations in variational quantum eigensolver by partitioning into commuting families, arXiv preprint arXiv:1907.13623 (2019).
[25] O. Crawford, B. van Straaten, D. Wang, T. Parks, E. Campbell, and S. Brierley, Efficient quantum measurement of pauli operators in the presence of finite sampling error, Quantum **5**, 385 (2021).
[26] H.-Y. Huang, R. Kueng, and J. Preskill, Predicting many properties of a quantum system from very few measurements, Nature Physics **16**, 1050 (2020).
[27] C. Hadfield, S. Bravyi, R. Raymond, and A. Mezzacapo, Measurements of quantum hamiltonians with locally-biased classical shadows, Communications in Mathematical Physics **391**, 951 (2022).
[28] H.-Y. Huang, R. Kueng, and J. Preskill, Efficient estimation of pauli observables by derandomization, Physical Review Letters **127**, 030503 (2021).
[29] A. F. Izmaylov, T.-C. Yen, R. A. Lang, and V. Verteletskyi, Unitary partitioning approach to the measurement problem in the variational quantum eigensolver method, Journal of Chemical Theory and Computation **16**, 190 (2020).
[30] A. Ralli, P. J. Love, A. Tranter, and P. V. Coveney, Implementation of measurement reduction for the variational quantum eigensolver, Physical Review Research **3**, 033195 (2021).
[31] S. Kochen and E. P. Specker, The problem of hidden variables in quantum mechanics, in *The logico-algebraic approach to quantum mechanics* (Springer, New York, 1975) pp. 293–328.
[32] C. Budroni, Contextuality, memory cost and non-classicality for sequential measurements, Philosophical Transactions of the Royal Society A **377**, 20190141 (2019).
[33] C. Budroni, A. Cabello, O. Gühne, M. Kleinmann, and J.-Å. Larsson, Kochen-specker contextuality, Reviews of Modern Physics **94**, 045007 (2022).
[34] N. de Silva, Graph-theoretic strengths of contextuality, Physical Review A **95**, 032108 (2017).
[35] A. Cabello, Converting contextuality into nonlocality, Physical Review Letters **127**, 070401 (2021).
[36] M. Howard, J. Wallman, V. Veitch, and J. Emerson, Contextuality supplies the 'magic'for quantum computation, Nature **510**, 351 (2014).
[37] N. D. Mermin, Simple unified form for the major no-hidden-variables theorems, Physical review letters **65**, 3373 (1990).
[38] J. S. Bell, On the Einstein Podolsky Rosen paradox, Physics Physique Fizika **1**, 195 (1964).
[39] A. Peres, Incompatible results of quantum measurements, Physics Letters A **151**, 107 (1990).
[40] See Supplemental Material at `http://link.aps.org/supplemental/10.1103/PhysRevResearch.5.013095` for further information on the CS-VQE algorithm, the scaling analysis of the unitary partitioning rotation used in CS-VQE, the analysis of the variance of the ground-state energy obtained when using unitary partitioning for measurement reduction and the numerical details of the physical problems presented in this paper.
[41] R. W. Spekkens, Quasi-quantization: Classical statistical theories with an epistemic restriction, in *Quantum Theory: Informational Foundations and Foils*, edited by G. Chiribella and R. W. Spekkens (Springer, Dordrecht, 2016) pp. 83–135.
[42] W. M. Kirby and P. J. Love, Classical simulation of noncontextual pauli hamiltonians, Physical Review A **102**, 032418 (2020).
[43] R. W. Spekkens, Evidence for the epistemic view of quantum states: A toy theory, Physical Review A **75**, 032110 (2007).
[44] R. W. Spekkens, Quasi-quantization: classical statistical theories with an epistemic restriction, in *Quantum Theory: Informational Foundations and Foils* (Springer, 2016) pp. 83–135.
[45] T. Weaving, A. Ralli, W. M. Kirby, A. Tranter, P. J. Love, and P. V. Coveney, A stabilizer framework for the contextual subspace variational quantum eigensolver and the noncontextual projection ansatz, Journal of Chemical Theory and Computation , 1 (2023), https://doi.org/10.1021/acs.jctc.2c00910.
[46] R. Raussendorf, J. Bermejo-Vega, E. Tyhurst, C. Okay, and M. Zurel, Phase-space-simulation method for quantum computation with magic states on qubits, Physical Review A **101**, 012350 (2020).
[47] M. A. Nielsen and I. L. Chuang, Quantum computation and quantum information: 10th anniversary edition (Cambridge University Press, Cambridge, 2011) pp. 454–

459.
[48] D. Poulin, M. B. Hastings, D. Wecker, N. Wiebe, A. C. Doberty, and M. Troyer, The trotter step size required for accurate quantum simulation of quantum chemistry, Quantum Info. Comput. **15**, 361–384 (2015).
[49] R. A. Lang, I. G. Ryabinkin, and A. F. Izmaylov, Unitary transformation of the electronic hamiltonian with an exact quadratic truncation of the Baker-Campbell-Hausdorff expansion, Journal of Chemical Theory and Computation **17**, 66 (2021), pMID: 33295175, https://doi.org/10.1021/acs.jctc.0c00170.
[50] J. Dehaene and B. De Moor, Clifford group, stabilizer states, and linear and quadratic operations over gf (2), Physical Review A **68**, 042318 (2003).
[51] A. M. Childs and N. Wiebe, Hamiltonian simulation using linear combinations of unitary operations, Quantum Info. Comput. **12**, 901 (2012).
[52] G. H. Low and I. L. Chuang, Hamiltonian Simulation by Qubitization, Quantum **3**, 163 (2019).
[53] D. W. Berry, A. M. Childs, R. Cleve, R. Kothari, and R. D. Somma, Exponential improvement in precision for simulating sparse hamiltonians, in *Proceedings of the 46th Annual ACM Symposium on Theory of Computing* (Association for Computing Machinery, 2014) pp. 283–292.
[54] L. K. Grover, Quantum mechanics helps in searching for a needle in a haystack, Physical Review Letters **79**, 325 (1997).
[55] G. G. Guerreschi, Repeat-until-success circuits with fixed-point oblivious amplitude amplification, Physical Review A **99**, 022306 (2019).
[56] M. Boyer, G. Brassard, P. Hoyer, and A. Tapp, Tight bounds on quantum searching, Fortschritte der Physik: Progress of Physics **46**, 493 (1998).
[57] S. Bravyi, J. M. Gambetta, A. Mezzacapo, and K. Temme, Tapering off qubits to simulate fermionic hamiltonians, arXiv preprint arXiv:1701.08213 (2017).
[58] W. M. Kirby, ContextualSubspaceVQE, `https://github.com/wmkirby1/ContextualSubspaceVQE` (2021).
[59] A. A. Hagberg, D. A. Schult, and P. J. Swart, Exploring network structure, dynamics, and function using networkx, in *Proceedings of the 7th Python in Science Conference*, edited by G. Varoquaux, T. Vaught, and J. Millman (Pasadena, CA USA, 2008) pp. 11 – 15.
[60] D. J. Welsh and M. B. Powell, An upper bound for the chromatic number of a graph and its application to timetabling problems, The Computer Journal **10**, 85 (1967).
[61] J. R. McClean, J. Romero, R. Babbush, and A. Aspuru-Guzik, The theory of variational hybrid quantum-classical algorithms, New Journal of Physics **18**, 023023 (2016).
[62] N. C. Rubin, R. Babbush, and J. McClean, Application of fermionic marginal constraints to hybrid quantum algorithms, New Journal of Physics **20**, 053020 (2018).
[63] J. F. Gonthier, M. D. Radin, C. Buda, E. J. Doskocil, C. M. Abuan, and J. Romero, Measurements as a roadblock to near-term practical quantum advantage in chemistry: resource analysis, Physical Review Research **4**, 033154 (2022).
[64] A. Ralli and T. J. Weaving, symmer, `https://github.com/UCL-CCS/symmer` (2022).

IZ	ZI	ZZ	r_0
XI	IX	XX	r_1
XZ	ZX	YY	r_2
c_0	c_1	c_2	

TABLE II: Example Peres-Mermin square of nine possible observables for a physical system, where each measurement can be assigned a ± 1 value.

Appendix A: "Peres-Mermin Square"

The "Peres-Mermin square" [37, 39] involves the construction of nine measurements arranged in a square. In this appendix we follow the construction given in [33]. Each measurement has only two possible outcomes (dichotomic) $+1$ and -1. In a realistic interpretation, performing each measurement on an object reveals whether the property is present $(+1)$ or absent (-1), yielding nine properties.

We take three measurements along a column or row to form a "context" - a set of measurements whose values can be jointly measured i.e. the observables commute and thus share a common eigenbasis. Table II gives an example.

In a classical (noncontextual) model for this system, the nine measurements $\{IZ, ZI, ZZ, XI, IX, XX, XZ, ZX, YY\}$ can be assigned a definite value independent of the context the measurement is obtained in. For example if all measurements are assigned $+1$ in Table II, then $c_0 = c_1 = c_2 = r_0 = r_1 = r_2 = +1$ and six positive products are obtained. If a single entry in Table II is changed it will affect two products (a row and column product). We consider the following Equation in this setting:

$$\begin{aligned}\langle PM\rangle \equiv &\langle IZ\cdot ZI\cdot ZZ\rangle + \langle XI\cdot IX\cdot XX\rangle + \\ &\langle XZ\cdot ZX\cdot YY\rangle + \langle IZ\cdot XI\cdot XZ\rangle + \\ &\langle ZI\cdot IX\cdot ZX\rangle - \langle ZZ\cdot XX\cdot YY\rangle \\ =&r_0 + r_1 + r_2 + c_0 + c_1 - c_2.\end{aligned} \tag{A1}$$

We find that classically we get an inequality $\langle PM\rangle \leq 4$. We reiterate that this is the setting of eight $+1$ assignments and a single -1 assignment. This inequality is saturated when the -1 value is assigned to one of the observables in the last column of Table II.

The significance of this inequality is that it can be violated by quantum systems. Thinking of this in a quantum setting, the operators in rows and columns of Table II commute. If we multiply along the rows and columns we get $+II$ apart from the last column where $c_2 = -II$ (see Table III). This is the case regardless of what quantum state is considered . Using the expectation values of the product of these operators in Equation A1, we find $\langle PM\rangle = 6$, violating the classical bound.

Classically Equation A1 is bounded as $\langle PM\rangle \leq 4$ due to the assumption that the nine observables of the object can be assigned a value consistently. Violation of this bound implies that either the value assignment must depend on which context (row or column) the observable appears in or there is no value assignment. This phenomenon is known as quantum contextuality [33].

In VQE, a Hamiltonian is defined by a linear combination of Pauli operators. The expectation value is obtained by measuring each Pauli operator in a separate experiment and combining the results. Different groups of commuting operators form contexts. In general there will be incompatible contexts where it is impossible to consistently assign joint outcomes. In other words, different inference relations will lead to contradictions. Outcomes assigned to individual measurements are therefore context-dependent and the problem is contextual. If not, then the problem is noncontextual and a noncontextual (classical) hidden variable model can be used to solve such systems.

IZ	ZI	ZZ	$\langle +II\rangle = +1$
XI	IX	XX	$\langle +II\rangle = +1$
XZ	ZX	YY	$\langle +II\rangle = +1$
$\langle +II\rangle = +1$	$\langle +II\rangle = +1$	$\langle -II\rangle = -1$	

TABLE III: Example Peres-Mermin square of nine Hermitian operators, all with ± 1 eigenvalues - representing observables.

arXiv:2207.03451v3 [quant-ph] 13 Feb 2023

Supplemental Material
Unitary Partitioning and the Contextual Subspace Variational Quantum Eigensolver

Alexis Ralli,[1,*] Tim Weaving,[1,†] Andrew Tranter,[2,3,‡] William M. Kirby,[2,§] Peter J. Love,[2,4,¶] and Peter V. Coveney[1,5,**]

[1] *Centre for Computational Science, Department of Chemistry, University College London, WC1H 0AJ, United Kingdom*
[2] *Department of Physics and Astronomy, Tufts University, Medford, MA 02155, USA*
[3] *Cambridge Quantum Computing, 9a Bridge Street Cambridge, CB2 1UB, United Kingdom*
[4] *Computational Science Initiative, Brookhaven National Laboratory, Upton, NY 11973, USA*
[5] *Informatics Institute, University of Amsterdam, Amsterdam, 1098 XH, Netherlands*

(Dated: February 14, 2023)

CONTENTS

I. Contextual-Subspace VQE overview 1
A. Noncontextual Part 1
1. Testing for contexuality 1
2. Obtaining Noncontexual Hamiltonian 2
3. Noncontextual hidden variable model 2
4. Solving the Noncontexual Hamiltonian 5
B. Mapping to contextual subspace 6
1. Unitary partitioning via a sequence of rotations 6
2. Unitary partitioning via a linear combination of unitaries 12
3. Mapping Pauli operators to single-qubit Pauli Z operators 16

II. Unitary Partitioning Measurement Reduction 18

III. Numerical details of the toy example 21

IV. Graphical Results for CS-VQE simulation of each Molecular Hamiltonian 24

V. Tabulated Results of simulation 27

I. CONTEXTUAL-SUBSPACE VQE OVERVIEW

In the following subsections we summarise all the details required to implement the CS-VQE algorithm, where a problem Hamiltonian is split into a contextual and noncontextual part [**?**]:

$$H_{\text{full}} = H_{\text{con}} + H_{\text{noncon}}. \tag{S.1}$$

A. Noncontextual Part

1. *Testing for contexuality*

Let $\mathcal{S}^{H_{\text{full}}}$ be the set of Pauli operators, in the full system Hamiltonian, requiring measurement in a VQE experiment. It was shown in [**?** **?**], that a set of four Pauli operators $\{A, B, C, D\}$ is strongly contextual if A commutes with both B and C, but B anticommutes with C. If this condition is not present, then the set is noncontextual.

Given an arbitrary set of Pauli operators $\mathcal{P}$, this gives an algorithm to check for contextuality [**?**]. A pseudo algorithm is given in algorithm 1. First an $\mathcal{O}(|\mathcal{P}|^2)$ routine is used to remove completely commuting operators $\mathcal{Z}$, leaving the remaining set $\mathcal{T}$. Then a procedure taking $\mathcal{O}(|\mathcal{T}|^3)$ steps is used to determine whether $\mathcal{P}$ is contextual. This check for contextuality is implemented in OpenFermion [**?**].

* alexis.ralli.18@ucl.ac.uk
† timothy.weaving.20@ucl.ac.uk
‡ tufts@atranter.net
§ william.kirby@tufts.edu
¶ peter.love@tufts.edu
** p.v.coveney@ucl.ac.uk

Algorithm 1 Test for strong contextuality in a given set of Pauli operators [**?**]

Input: $\mathcal{P} = \{P_0, P_1, P_2, ...\}$ ▷ Input $\mathcal{P}$ is a set of Pauli operators.
Output: *contextual* $(True/False)$ ▷ Whether the set $\mathcal{P}$ is strongly contextual.

$\mathcal{Z} \leftarrow \{\}$
$\mathcal{T} \leftarrow \{\}$
$contextual \leftarrow False$

for $i = 0$ to $|\mathcal{P}| - 1$ **do**
  if $[P_i, P_j] = 0\ \forall j \neq i$ where $j = 0$ to $|\mathcal{P}| - 1$ **then**
    $\mathcal{Z} \leftarrow \mathcal{Z} \cup \{P_i\}$
  else
    $\mathcal{T} \leftarrow \mathcal{T} \cup \{P_i\}$
  end if
end for

for $i = 0$ to $|\mathcal{T}| - 3$ **do**
  for $j = i + 1$ to $|\mathcal{T}| - 2$ **do**
    for $k = j + 1$ to $|\mathcal{T}| - 1$ **do**

      if $[P_i, P_j] = 0$, $[P_i, P_k] = 0$ and $\{P_j, P_k\} = 0$ **then**
        $contextual \leftarrow True$
        return *contextual*
      else
        continue
      end if

    end for
  end for
end for
return *contextual*

2. Obtaining Noncontexual Hamiltonian

To begin CS-VQE, we first need to define the contextual and noncontextual parts. The task of finding the largest noncontextual subset of Pauli operators in $\mathcal{S}^{H_{\text{full}}}$ is a generalization of the disjoint cliques problem [**?** **?**], which is NP-complete. However, different heuristics can be used to approximately solve this problem.

To date, VQE experiments have mainly focused on chemistry Hamiltonians, where Hartree-Fock accounts for most of the energy. Such Hamiltonians contain Pauli operators that l_1 norms are dominated by diagonal terms - Pauli operators made up of tensor products of single qubit I and Pauli Z matrices. To find a noncontextual set in such a scenario, a greedy heuristic selecting high weight terms from the full Hamiltonian first can be used, while checking the set remains noncontextual using algorithm 1. This gives a noncontextual set containing mainly diagonal terms, with some additional operators [**?**]. Alternative procedures to find the largest noncontextual subsets remain an open question for the CS-VQE algorithm.

3. Noncontextual hidden variable model

Once the noncontextual Hamiltonian H_{noncon} is determined, we can define the set $\mathcal{S}^{H_{\text{noncon}}}$ to be the Pauli operators in H_{noncon}. We split $\mathcal{S}^{H_{\text{noncon}}}$ into two subsets $\mathcal{Z}$ and $\mathcal{T}$ - representing the set of universally commuting Pauli operators $\mathcal{Z}$ and their complement respectively [**?** **?**]:

$$\mathcal{S}^{H_{\text{noncon}}} = \mathcal{Z} \cup \mathcal{T} = \left\{ \bigcup_{\substack{i=0 \\ \forall P_i \in \mathcal{Z}}}^{|\mathcal{Z}|-1} P_i \right\} \cup \left\{ \bigcup_{\substack{i=0 \\ \forall P_i \in \mathcal{T}}}^{|\mathcal{T}|-1} P_i \right\}. \tag{S.2}$$

Slight modifications to Algorithm 1 achieve this - where $\mathcal{P}$ would be set to be $\mathcal{S}^{H_{\text{noncon}}}$ and both $\mathcal{Z}, \mathcal{T}$ should be returned.

The operators in $\mathcal{Z}$ are noncontextual, as by definition they are universally commuting and represent symmetries of H_{noncon}. For the overall super-set $\mathcal{S}^{H_{\text{noncon}}}$ to be noncontextual, the remaining operators in $\mathcal{T}$ must be made up of N disjoint cliques C_j [**?**], where operators within a clique must all commute with each other and operators between cliques pairwise anticommute. This is because commutation forms an equivalence relation on $\mathcal{T}$ if and only if $\mathcal{S}^{H_{\text{noncon}}}$ is noncontextual [**?** **?** **?**]. We can write $\mathcal{T}$ as:

$$\mathcal{T} = \bigcup_{\substack{i=0 \\ \forall P_i \in \mathcal{T}}}^{|\mathcal{T}|-1} P_i = \bigcup_{j=0}^{N-1} C_j = \bigcup_{j=0}^{N-1} \Big(\bigcup_{\substack{k=0 \\ \text{where} \\ [P_k, P_l]=0 \\ \forall P_k, P_l \in C_j}}^{|C_j|-1} P_k^{(j)} \Big). \tag{S.3}$$

We re-define each clique C_j using the identity operation defined by the first operator of the jth clique, $P_0^{(j)} P_0^{(j)} = \mathcal{I}$, which represents of the first operator in each of the N cliques. We write the jth clique as [**?**]:

$$C_j = \bigcup_{\forall P_k \in C_j} P_k^{(j)} = \bigcup_{\forall P_k \in C_j} P_k^{(j)} P_0^{(j)} P_0^{(j)} = \bigcup_{\forall P_k \in C_j} \Big(P_k^{(j)} P_0^{(j)} \Big) P_0^{(j)} = \bigcup_{k=0}^{|C_j|-1} A_k^{(j)} P_0^{(j)} \tag{S.4}$$

The new operators $A_k^{(j)} = P_k^{(j)} P_0^{(j)}$ are just Pauli operators up to a complex phase. The new operators $A_k^{(j)}$ must still commute with the universally commuting operators in $\mathcal{Z}$, but now must also commute with all the other terms in the $N-1$ cliques C_j [**?**]. Using this, the noncontextual set (Equation S.2) can be rewritten as:

$$\mathcal{S}^{H_{\text{noncon}}} = \left\{ \bigcup_{\substack{i=0 \\ \forall P_i \in \mathcal{Z}}}^{|\mathcal{Z}|-1} P_i \right\} \cup \left\{ \bigcup_{j=0}^{N-1} C_j \right\} \tag{S.5a}$$

$$= \underbrace{\left\{ \bigcup_{\substack{i=0 \\ \forall P_i \in \mathcal{Z}}}^{|\mathcal{Z}|-1} P_i \right\}}_{\mathcal{Z}} \cup \underbrace{\left\{ \bigcup_{j=0}^{N-1} \Big(\bigcup_{\substack{k=0 \\ \text{where} \\ [P_k, P_l]=0 \\ \forall P_k, P_l \in C_j}}^{|C_j|-1} A_k^{(j)} P_0^{(j)} \Big) \right\}}_{\mathcal{T}}. \tag{S.5b}$$

So far we have considered the noncontextual set of Pauli operators $\mathcal{S}^{H_{\text{noncon}}}$, which in general will be a dependent set. By this we mean that some operators in the set can be written as a product of other commuting operators in the set. We need to reduce this set $\mathcal{S}^{H_{\text{noncon}}}$ to an independent set of Pauli operators, where all operators in the noncontextual Hamiltonian can be inferred from the values of other operators in the set under the Jordan product.

To obtain an independent set from $\mathcal{S}^{H_{\text{noncon}}}$, we first take the completely commuting Pauli operators:

$$\begin{aligned} \mathcal{G}' &\equiv \mathcal{Z} \cup \left\{ \bigcup_{j=0}^{N-1} \{ A_k^{(j)} | k = 1, 2, \ldots, |C_j| - 1 \} \right\} \\ &\equiv \left\{ \bigcup_{\substack{i=0 \\ \forall P_i \in \mathcal{Z}}}^{|\mathcal{Z}|-1} P_i \right\} \cup \left\{ \bigcup_{j=0}^{N-1} \{ A_k^{(j)} | k = 1, 2, \ldots, |C_j| - 1 \} \right\}, \end{aligned} \tag{S.6}$$

and using the procedure in [**?**] find an independent subset $\mathcal{G}$:

$$\mathcal{G} \equiv \{ P_i | i = 0, 1, \ldots, |\mathcal{G}| - 1 \}. \tag{S.7}$$

Appendix C in [**?**] gives all steps required.

Finally, we need to consider the N pairwise anticommuting $P_0^{(j)}$ operators defined by the N anticommuting cliques. As the operators in $\mathcal{G}$ universally commute with all operators in the noncontextual Hamiltonian, each operator in the

set $\{P_0^{(j)}|j=0,1,\ldots,(N-1)\}$ must be independent of $\mathcal{G}$ under the Jordan product [**?**]. Combining these results, we get the set $\mathcal{R}$:

$$\mathcal{R} \equiv \{P_0^{(j)}|j=0,1,\ldots,N-1\} \cup \mathcal{G} \tag{S.8}$$

Inspecting the properties of $\mathcal{R}$, one can bound its size. The set $\mathcal{G}$ has size at most $n-1$, as n independent commuting Pauli operators form a complete commuting set of observables for n qubits. In other words, as $\mathcal{G}$ is a universally commuting set, if its size was n (or more) then taking $\mathcal{G}$ and one operator $P_0^{(j)}$ (the set $\mathcal{G} \cup \{P_0^{(j)}\}$) is also a fully commuting set - and would be a commuting set of size $n+1$ (or more) [**?**]. The maximum number of independent anticomuting operators on n qubits was shown in [**?**] to be $2n+1$. This actually bounds the size of $\mathcal{R}$, which occurs when the set $\mathcal{G}$ (and thus $\mathcal{Z}$) is empty [**?**].

Looking at the noncontextual set of Pauli operators Equation S.5, making up the H_{noncon}, we see that the subset $\mathcal{G}$ in $\mathcal{R}$ (Equation S.8) includes all the generators for the terms in $\mathcal{Z}$ and each Pauli $A_k^{(j)}$ operator. Any operator in $\mathcal{Z}$ and each Pauli $A_k^{(j)}$ operator can therefore be found by a finite combination of operators in $\mathcal{G}$. Each operator in $\mathcal{T}$ can also be generated by a combination of one $P_0^{(j)}$ operator and some combination of operators in $\mathcal{G}$. Again $\mathcal{R}$ (Equation S.8) contains all the operators required. To summarise, the set $\mathcal{R}$ contains all the required terms to reproduce the expectation value of any operator in $\mathcal{S}^{H_{\text{noncon}}}$ under the Jordan product.

We have shown how the Pauli operators making H_{noncon} can be simultaneously assigned definite values without contradiction. This allows the introduction of a phase-space description of the eigenspace of H_{noncon} [**?**]. Next we will introduce what this phase-space model is in the context of this work.

A joint value assignment of ± 1 to each operator in $\mathcal{R}$ represents the ontic state of the physical system. Probability distributions corresponding to valid quantum states must obey an uncertainty relation [**?** **?**]. To enforce these two conditions are sufficient. (1) The commuting generators $\mathcal{G}$ have definite values and (2) the expectation values for the $P_0^{(j)}$ terms form a unit vector [**?**]. In this frame, our noncontextual state is defined as [**?**]:

$$(\vec{q},\vec{r}) = (q_0, q_1, \ldots, q_{|\mathcal{G}|-1},\ r_0, r_1, \ldots, r_{N-1}). \tag{S.9}$$

With respect to the phase-space model [**?**], a valid noncontextual state $(\vec{q},\vec{r})$ sets the expectation value of the operators in $\mathcal{R}$, where $\langle G_i\rangle = q_i = \pm 1$ and $\langle P_0^{(j)}\rangle = r_j$ such that $\left(\sum_{j=0}^{N-1} |r_j|^2\right)^{1/2} = 1$.

It was shown in [**?**] that probabilities for outcomes G_i and $P_0^{(j)}$ should be obtained as the marginals of:

$$P(p_{j=0}, p_{j=1}, \ldots, p_{j=(N-1)}, g_0, g_1, \ldots, g_{|\mathcal{G}|-1}) = \left(\prod_{i=0}^{|\mathcal{G}|-1} \delta_{g_i,q_i}\right)\left(\prod_{j=0}^{N-1} \frac{1}{2}|p_j + r_j|\right). \tag{S.10}$$

Further analysis is given in [**?**].

In summary, a noncontextual state is fully defined by $(\vec{q},\vec{r})$ which determines all the expectation values of the operators in $\mathcal{R}$ (Equation S.8), where $\langle G_i\rangle = q_i \in \{-1,+1\}$ and $\langle P_0^{(j)}\rangle = r_j$. We summarise this as:

$$\underbrace{\{\ \underbrace{\langle P_0^{(0)}\rangle}_{r_0}, \underbrace{\langle P_0^{(1)}\rangle}_{r_1}, \ldots, \underbrace{\langle P_0^{(N-1)}\rangle}_{r_{N-1}}\ \}}_{\vec{r}} \text{ and } \underbrace{\{\ \underbrace{\langle G_0\rangle}_{q_0}, \underbrace{\langle G_1\rangle}_{q_1}, \ldots, \underbrace{\langle G_{|\mathcal{G}|-1}\rangle}_{q_{|\mathcal{G}|-1}}\ \}}_{\vec{q}}. \tag{S.11}$$

The expectation value of all the operators in $\mathcal{S}^{H_{\text{noncon}}}$ are generated from some finite combination of terms in $\mathcal{R}$ under the Jordan product. This by extension will induce the expectation value for H_{noncon}. Explicitly, let $P_i^{\mathcal{Z}} \in \mathcal{Z} \subseteq \mathcal{S}^{H_{\text{noncon}}}$ then if we let $\mathcal{J}^{\mathcal{G}}_{P_i^{\mathcal{Z}}}$ be the set of indices such that $P_i^{\mathcal{Z}} = \prod_{i\in\mathcal{J}^{\mathcal{G}}_{P_i^{\mathcal{Z}}}} G_i$; then [**?**]:

$$\langle P_i^{\mathcal{Z}}\rangle = \prod_{i\in\mathcal{J}^{\mathcal{G}}_{P_i^{\mathcal{Z}}}} \langle G_i\rangle = \prod_{i\in\mathcal{J}^{\mathcal{G}}_{P_i^{\mathcal{Z}}}} q_i. \tag{S.12}$$

In words, we combine the expectation value of some finite set of Pauli operators in the independent set $\mathcal{G}$ - given by $\mathcal{J}^{\mathcal{G}}_{P_i^{\mathcal{Z}}}$ - to reproduce the expectation value for $\langle P_i^{\mathcal{Z}}\rangle$.

Similarly, the expectation value for each $A_k^{(j)} P_0^{(j)} \in \mathcal{T} \subseteq \mathcal{S}^{H_{\text{noncon}}}$ (Equation S.5) term is given by:

$$\langle A_i^{(j),\in\mathcal{G}} P_0^{(j),\in\mathcal{T}} \rangle = \Big(\prod_{i \in \mathcal{J}^{\mathcal{G}}_{A_i^{(j)}}} \langle G_i \rangle \Big) r_j = \Big(\prod_{i \in \mathcal{J}^{\mathcal{G}}_{A_i^{(j)}}} q_i \Big) r_j, \tag{S.13}$$

where $\mathcal{J}^{\mathcal{G}}_{A_i^{(j)}}$ are the set of indices such that $\langle A_i^{(j)} \rangle = \prod_{i \in \mathcal{J}^{\mathcal{G}}_{A_i^{(j)}}} \langle G_i \rangle$ and $\langle P_0^{(j)} \rangle = r_j$ [**?**].

We can write the noncontexual Hamiltonian as:

$$H_{\text{noncon}} = \Big(\sum_{i=0}^{|\mathcal{Z}|-1} c_i P_i^{\mathcal{Z}} \Big) + \sum_{j=0}^{N-1} \Bigg[\sum_{k=0}^{|C_j|-1} a_k A_k^{(j)} P_0^{(j)} \Bigg] \tag{S.14}$$

and find the energy by:

$$\langle H_{\text{noncon}} \rangle = E_{noncon}(\vec{q}, \vec{r}) = \Big(\sum_{i=0}^{|\mathcal{Z}|-1} \beta_i \langle P_i^{\mathcal{Z}} \rangle \Big) + \sum_{j=0}^{N-1} \Bigg[\sum_{k=0}^{|C_j|-1} \beta_k \langle A_k^{(j)} P_0^{(j)} \rangle \Bigg], \tag{S.15}$$

where β_i and β_k are real coefficients and each expectation value is given by Equation S.12 and S.13 [**?**].

4. Solving the Noncontexual Hamiltonian

To find the ground state of H_{noncon}, we minimize Equation S.15 via a brute-force search as described in [**?**]. Algorithm 2 summarises the steps. This could be done in the work presented here, because $\mathcal{R}$ was small for all molecular systems considered. First a trial $\vec{q}$ is defined. This is a set of ± 1 expectation values for each G_j. An initial guess of the amplitudes r_i of the unit vector $\vec{r}$ is made and the energy (Equation S.15) is minimized over this continuous parameterization of $\vec{r}$ for a fixed trial $\vec{q}$, until the energy converges to a minimum. These steps are repeated for all the $2^{|\mathcal{G}|}$ assignments of $\vec{q}$. The $(\vec{q}, \vec{r})$ combination that gives the lowest overall energy represents the noncontextual ground state of the physical system. In the main text we denote this parameterization as $(\vec{q}_0, \vec{r}_0)$. Note for a fixed $\vec{q}$, we optimize over $\vec{r}$. This can be thought of as optimizing a function defined on a hypersphere. Currently we haven't explored the properties of this function.

It remains an open question for the CS-VQE algorithm if alternate optimization strategies are possible, for example using chemical intuition during optimization. This brute force approach of searching over all $2^{|\mathcal{G}|}$ possibilities for $\vec{q}$ may not be necessary. In the next section, we discuss how to map the contextual problem into a subspace consistent with a defined noncontextual state $(\vec{q}, \vec{r})$.

Algorithm 2 Brute force method to solve noncontexual problem

$\mathcal{Q} \leftarrow \{q_0, q_1, ..., q_{|\mathcal{G}|-1}\}^{2^{|\mathcal{G}|}}$ ▷ Set $\mathcal{Q}$ contains all possible $\vec{q}$ vectors, where $q_i \in \{+1, -1\}$.

$\vec{q}_0 \leftarrow \{\}$
$\vec{r}_0 \leftarrow \{\}$
$E^0_{\text{noncon}} \leftarrow 0$

for $\vec{q}_{\text{test}}$ in $\mathcal{Q}$ **do**
  $\vec{r}_{opt}, E^{opt}_{\text{noncon}} \leftarrow \underset{\vec{r}}{argmin}[E_{\text{noncon}}(\vec{q}_{\text{test}}, \vec{r})]$ ▷ for a given $\vec{q}_{\text{test}}$, minimize the energy (Equation S.15)with respect to $\vec{r}$.
  if $E^{opt}_{\text{noncon}} < E^0_{\text{noncon}}$ **then**
    $\vec{q}_0 \leftarrow \vec{q}_{\text{test}}$
    $\vec{r}_0 \leftarrow \vec{r}_{opt}$
    $E^0_{\text{noncon}} \leftarrow E^{opt}_{\text{noncon}}$
  else
    continue
  end if
end for

return $\vec{q}_0, \vec{r}_0, E^0_{\text{noncon}}$

B. Mapping to contextual subspace

In section **??** of the main text, the full Hamiltonian is mapped contextual subspace consistent with the noncontextual ground state by implementing $U_{\mathcal{W}}$ (Equation **??**) followed by projecting the rotated Hamiltonian with $Q_{\mathcal{W}}$. However, the definitions for the operators making up $U_{\mathcal{W}}$ were omitted. This subsection gives these details and is split into three parts. The first two parts consider how R is constructed. This is the problem of mapping a linear combination of pairwise anticommuting Pauli operators to a single Pauli operator and is known as unitary partitioning [**?** **?**]. In the context of this work, we use this to define R such that $RA(\vec{r})R^\dagger \mapsto P_0^{(k)}$. In the original formulation of CS-VQE only the sequence of rotations construction of R is used in the algorithm. We provide an alternative approach using the linear combination of unitaries construction proposed in [**?**], which results in superior scaling. We show the effect each conjugate rotation R has on the number of terms in a given qubit Hamiltonian. The last subsection gives the unitary rotations required to map a commuting set of Pauli operators to single qubit Pauli Z operators.

In each of these subsections, we use the notation that Pauli operators with multiple indices represent the multiplication of Pauli operators: $P_aP_bP_c = P_{abc}$. These terms will also be Pauli operators up to a complex phase.

1. *Unitary partitioning via a sequence of rotations*

In this subsection, we show how $A(\vec{r}) \mapsto P_0^{(k)} = R_S A(\vec{r}) R_S^\dagger$, where R_S is defined by a sequence of rotations [**?** **?**]. Given the set of anticommuting operators $A(\vec{r})$ (Equation **??**), we can define the following self-inverse operators:

$$\{\mathcal{X}_{kj} = iP_0^{(k)}P_0^{(j)} \;\; \forall P_0^{(j)} \in \mathcal{A} \text{ where } j \neq k\}, \tag{S.16}$$

where $P_0^{(k)} \in \mathcal{A}$. To simplify the notation we drop the subscript 0 (denoting the first operator in a clique) and write each $P_0^{(k)}$, $P_0^{(j)}$ as P_k and P_j respectively.

The adjoint rotation generated by one of these operator $\mathcal{X}_{kj}$ operators will be:

$$\begin{aligned} e^{(-i\frac{\theta_{kj}}{2}\mathcal{X}_{kj})}A(\vec{r})e^{(+i\frac{\theta_{kj}}{2}\mathcal{X}_{kj})} &= R_{S_{kj}}(\theta_{kj})A(\vec{r})R_{S_{kj}}^\dagger(\theta_{kj}) \\ &= \big(r_j\cos\theta_{kj} - r_k\sin\theta_{kj}\big)P_j + \big(\beta_j\sin\theta_{kj} + r_k\cos\theta_{kj}\big)P_k + \sum_{\substack{P_l\in\mathcal{A}\\ \forall l\neq k,j}}\beta_l P_l. \end{aligned} \tag{S.17}$$

The coefficient of P_j can be made to go to 0, by setting $r_j\cos\theta_{kj} = r_k\sin\theta_{kj}$. This approach removes the term with index j and increases the coefficient of P_k from $r_k \mapsto \sqrt{r_k^2 + r_j^2}$ [**?**]. This process is repeated over all indices excluding $j = k$ until only the P_k term remains. This procedure can be concisely written using the following operator [**?**]:

$$R_S = \prod_{\substack{j=0\\ \forall j\neq k}}^{|\mathcal{A}|-1} e^{(-i\frac{\theta_{kj}}{2})\mathcal{X}_{kj}} = \prod_{\substack{j=0\\ \forall j\neq k}}^{|\mathcal{A}|-1} R_{S_{kj}}(\theta_{kj}) = \prod_{\substack{j=0\\ \forall j\neq k}}^{|\mathcal{A}|-1} \Big[\cos\big(\frac{\theta_{kj}}{2}\big)\mathcal{I} - i\sin\big(\frac{\theta_{kj}}{2}\big)\mathcal{X}_{kj}\Big], \tag{S.18}$$

which is simply a sequence of rotations. The angle θ_{kj} is defined recursively at each step of the removal process, as the coefficient of P_k increases at each step and thus must be taken into account. The correct solution for θ_{kj} must be chosen given the signs of r_k and r_k [**?**]. The overall action of this sequence of rotations is:

$$R_S A(\vec{r}) R_S^\dagger = P_k. \tag{S.19}$$

Looking at Equation S.18, expanding the product of rotations results in R_S containing $\mathcal{O}(2^{|\mathcal{A}|-1})$ Pauli operators. We write this operator as:

$$R_S = \sum_{b}^{\mathcal{O}(2^{|\mathcal{A}|-1})} \delta_b P_b. \tag{S.20}$$

The adjoint rotation of R_S on a general Hamiltonian $H_q = \sum_a^{|H_q|} c_a P_a$ is:

$$\begin{aligned} R_S H_q R_S^\dagger &= \Big(\sum_b^{\mathcal{O}(2^{|\mathcal{A}|-1})} \delta_b P_b \Big) \sum_a^{|H_q|} c_a P_a \Big(\sum_c^{\mathcal{O}(2^{|\mathcal{A}|-1})} \delta_c^* P_c \Big) \\ &= \sum_b^{\mathcal{O}(2^{|\mathcal{A}|-1})} \sum_a^{|H_q|} \sum_c^{\mathcal{O}(2^{|\mathcal{A}|-1})} (\delta_b c_a \delta_c^*) P_b P_a P_c. \end{aligned} \tag{S.21}$$

We see that the number of terms increases as $\mathcal{O}(2^{|\mathcal{A}|}|H_q|)$ which was previously shown in [**?**]. What we show next is additional structure in R_S - due to the X_{kj} operators - means the base of the exponent can be slightly lower; however, it still remains exponential in $|\mathcal{A}|$.

Consider the adjoint rotation of a particular X_{kj} in R_S (Equation S.18):

$$\begin{aligned} R_{S_{kj}} &= \cos\big(\frac{\theta_{kj}}{2}\big)\mathcal{I} + \sin\big(\frac{\theta_{kj}}{2}\big) P_{kj}, \\ R_{S_{kj}}^\dagger &= \cos\big(\frac{\theta_{kj}}{2}\big)\mathcal{I} + \sin\big(\frac{\theta_{kj}}{2}\big) P_{jk}. \end{aligned} \tag{S.22}$$

Performing the adjoint rotation on H_q results in the following:

$$\begin{aligned} R_{S_{kj}} H_q R_{S_{kj}}^\dagger &= \Big[\alpha_{kj}\mathcal{I} + \beta_{kj} P_{kj}\Big] \sum_a c_a P_a \Big[\alpha_{kj}\mathcal{I} + \beta_{kj} P_{jk}\Big] \\ &= \sum_a c_a \big(\alpha_{kj} P_a + \beta_{kj} P_{kj} P_a\big) \Big[\alpha_{kj}\mathcal{I} + \beta_{kj} P_{jk}\Big] \\ &= \sum_a c_a \big(\alpha_{kj}^2 P_a + \alpha_{kj}\beta_{kj} P_a P_{jk} + \alpha_{kj}\beta_{kj} \underline{P_{kj}} P_a + \beta_{kj}^2 P_{kj} P_a P_{jk}\big) \\ &= \sum_a c_a \big(\alpha_{kj}^2 P_a + \alpha_{kj}\beta_{kj} \underline{P_a P_{jk}} - \alpha_{kj}\beta_{kj} \underline{P_{jk} P_a} + \beta_{kj}^2 P_{kj} P_a P_{jk}\big) \\ &= \sum_a c_a \big(\alpha_{kj}^2 P_a + \alpha_{kj}\beta_{kj} [P_a, P_{jk}] + \beta_{kj}^2 P_{kj} P_a P_{jk}\big) \\ &= \sum_a c_a \begin{cases} \big(\alpha_{kj}^2 P_a + \beta_{kj}^2 P_{kj} P_a P_{jk}\big), & \text{if } [P_a, P_{jk}] = 0 \\ \big(\alpha_{kj}^2 P_a + 2\alpha_{kj}\beta_{kj} P_a P_{jk} + \beta_{kj}^2 P_{kj} P_a P_{jk}\big), & \text{else } \{P_a, P_{jk}\} = 0 \end{cases} \end{aligned} \tag{S.23}$$

When $[P_a, P_{jk}] = 0$, we get:

$$\begin{aligned} \sum_a c_a \big(\alpha_{kj}^2 P_a + \beta_{kj}^2 P_{kj} \underline{P_a P_{jk}}\big) &= \sum_a c_a \big(\alpha_{kj}^2 P_a + \beta_{kj}^2 \underline{P_{kj} P_{jk}} P_a\big) \\ &= \sum_a c_a \big(\alpha_{kj}^2 P_a + \beta_{kj}^2 P_a\big) \\ &= \sum_a c_a \big(\alpha_{kj}^2 + \beta_{kj}^2\big) P_a \\ &= \sum_a c_a P_a. \end{aligned} \tag{S.24}$$

When $\{P_a, P_{jk}\} = 0$, we find:

$$\begin{aligned}\sum_a c_a\big(\alpha_{kj}^2 P_a + 2\alpha_{kj}\beta_{kj}P_aP_{jk} + \beta_{kj}^2 P_{kj}\underline{P_aP_{jk}}\big) &= \sum_a c_a\big(\alpha_{kj}^2 P_a + 2\alpha_{kj}\beta_{kj}P_aP_{jk} - \beta_{kj}^2\underline{P_{kj}P_{jk}}P_a\big)\\ &= \sum_a c_a\big(\alpha_{kj}^2 P_a + 2\alpha_{kj}\beta_{kj}P_aP_{jk} - \beta_{kj}^2 P_a\big)\\ &= \sum_a c_a\big(\alpha_{kj}^2 P_a + sin(\theta_{kj})P_aP_{jk} - \beta_{kj}^2 P_a\big)\\ &= \sum_a c_a\big((\alpha_{kj}^2 - \beta_{kj}^2)P_a + sin(\theta_{kj})P_aP_{jk}\big)\\ &= \sum_a c_a\big(cos(\theta_{kj})P_a + sin(\theta_{kj})P_aP_{jk}\big).\end{aligned} \tag{S.25}$$

Both cases use the following identities:

$$\begin{aligned}\alpha_{kj}^2 - \beta_{kj}^2 &= \cos^2\big(\frac{\theta_{kj}}{2}\big) - \sin^2\big(\frac{\theta_{kj}}{2}\big) = \cos\big(\theta_{kj}\big),\\ \alpha_{kj}^2 + \beta_{kj}^2 &= 1,\\ 2\alpha_{kj}\beta_{kj} &= 2\cos\big(\frac{\theta_{kj}}{2}\big)\sin\big(\frac{\theta_{kj}}{2}\big) = \sin\big(\theta_{kj}\big),\end{aligned} \tag{S.26}$$

where $\alpha_{kj} = \cos\big(\frac{\theta_{kj}}{2}\big)$ and $\beta_{kj} = \sin\big(\frac{\theta_{kj}}{2}\big)$. Using these results Equation S.23 reduces to:

$$\begin{aligned}R_{S_{kj}}H_qR_{S_{kj}}^\dagger &= \sum_{\substack{a\\ \forall[P_a,P_{jk}]=0}} c_aP_a + \sum_{\substack{a\\ \forall\{P_a,P_{jk}\}=0}} c_a\Big(cos(\theta_{kj})P_a + sin(\theta_{kj})P_aP_{jk}\Big)\\ &= \sum_a \eta_aP_a + \sum_{\substack{a\\ \forall\{P_a,P_{jk}\}=0}} \eta_a\big(P_{jk}P_a\big),\end{aligned} \tag{S.27}$$

where η_a represent the new real coefficients.

Consider the application of the next rotation operator R_{kl} in R_S (note k index represents the same Pauli operator P_k):

$$R_{S_{kl}}R_{S_{kj}}H_qR_{S_{kj}}^\dagger R_{S_{kl}}^\dagger = R_{S_{kl}}\Big(\sum_a \eta_aP_a\Big)R_{S_{kl}}^\dagger + \underline{R_{S_{kl}}\Big(\sum_{\substack{a\\ \forall\{P_a,P_{jk}\}=0}} \eta_a\big(P_{jk}P_a\big)\Big)R_{S_{kl}}^\dagger} \tag{S.28}$$

Focusing on the last term in Equation S.28:

$$
\begin{aligned}
R_{S_{kl}}\Bigg(\sum_{\substack{a\\ \forall\{P_a,P_{jk}\}=0}}\eta_a\big(P_{jk}P_a\big)\Bigg)R_{S_{kl}}^{\dagger} &= \Big[\gamma_{kl}\mathcal{I}+\delta_{kl}P_{kl}\Big]\sum_{\substack{a\\ \forall\{P_a,P_{jk}\}=0}}\eta_a\big(P_{jk}P_a\big)\Big[\gamma_{kl}\mathcal{I}+\delta_{kl}P_{lk}\Big]\\
&= \sum_{\substack{a\\ \forall\{P_a,P_{jk}\}=0}}\eta_a\Big(\gamma_{kl}P_{jk}P_a+\delta_{kl}P_{kl}P_{jk}P_a\Big)\Big[\gamma_{kl}\mathcal{I}+\delta_{kl}P_{lk}\Big]\\
&= \sum_{\substack{a\\ \forall\{P_a,P_{jk}\}=0}}\eta_a\Big(\gamma_{kl}^2P_{jk}P_a+\gamma_{kl}\delta_{kl}P_{jk}P_aP_{lk}+\gamma_{kl}\delta_{kl}P_{k\underline{l}}P_{\underline{j}k}P_a+\delta_{kl}^2P_{kl}P_{jk}P_aP_{lk}\Big)\\
&= \sum_{\substack{a\\ \forall\{P_a,P_{jk}\}=0}}\eta_a\Big(\gamma_{kl}^2P_{jk}P_a+\gamma_{kl}\delta_{kl}P_{jk}P_aP_{lk}-\gamma_{kl}\delta_{kl}P_{\underline{kj}}P_{lk}P_a+\delta_{kl}^2P_{kl}P_{jk}P_aP_{lk}\Big)\\
&= \sum_{\substack{a\\ \forall\{P_a,P_{jk}\}=0}}\eta_a\Big(\gamma_{kl}^2P_{jk}P_a+\gamma_{kl}\delta_{kl}P_{jk}P_aP_{lk}+\gamma_{kl}\delta_{kl}P_{jk}P_{lk}P_a+\delta_{kl}^2P_{kl}P_{jk}P_aP_{lk}\Big)\\
&= \sum_{\substack{a\\ \forall\{P_a,P_{jk}\}=0}}\eta_a\Big(\gamma_{kl}^2P_{jk}P_a+\gamma_{kl}\delta_{kl}P_{jk}\{P_a,P_{lk}\}+\delta_{kl}^2P_{kl}P_{jk}P_aP_{lk}\Big)\\
&= \sum_{\substack{a\\ \forall\{P_a,P_{jk}\}=0}}\eta_a\begin{cases}\Big(\gamma_{kl}^2P_{jk}P_a+2\gamma_{kl}\delta_{kl}P_{jk}P_aP_{lk}+\delta_{kl}^2P_{kl}P_{jk}P_aP_{lk}\Big), & \text{if } [P_a,P_{lk}]=0\\ \Big(\gamma_{kl}^2P_{jk}P_a+\delta_{kl}^2P_{kl}P_{jk}P_aP_{lk}\Big), & \text{if } \{P_a,P_{lk}\}=0\end{cases}
\end{aligned}
\tag{S.29}
$$

For the case $\{P_a, P_{lk}\} = 0$:

$$
\begin{aligned}
\sum_{\substack{a\\ \forall\{P_a,P_{jk}\}=0}}\eta_a\Big(\gamma_{kl}^2P_{jk}P_a+\delta_{kl}^2P_{kl}P_{jk}\underline{P_aP_{lk}}\Big) &= \sum_{\substack{a\\ \forall\{P_a,P_{jk}\}=0}}\eta_a\Big(\gamma_{kl}^2P_{jk}P_a-\delta_{kl}^2\underline{P_{kl}P_{jk}}P_{lk}P_a\Big)\\
&= \sum_{\substack{a\\ \forall\{P_a,P_{jk}\}=0}}\eta_a\Big(\gamma_{kl}^2P_{jk}P_a+\delta_{kl}^2P_{jk}P_{kl}P_{lk}P_a\Big)\\
&= \sum_{\substack{a\\ \forall\{P_a,P_{jk}\}=0}}\eta_a\Big(\gamma_{kl}^2P_{jk}P_a+\delta_{kl}^2P_{jk}P_a\Big)\\
&= \sum_{\substack{a\\ \forall\{P_a,P_{jk}\}=0}}\eta_a\Big(P_{jk}P_a\Big).
\end{aligned}
\tag{S.30}
$$

We observe that there is no increase in the number of terms and the weight of each Pauli operator changes.

For the case $[P_a, P_{lk}] = 0$:

$$\begin{aligned}
\sum_{\substack{a \\ \forall\{P_a,P_{jk}\}=0}} \eta_a\big(\gamma_{kl}^2 P_{jk}P_a + 2\gamma_{kl}\delta_{kl}P_{jk}P_aP_{lk} + \delta_{kl}^2 P_{kl}P_{jk}\underline{P_aP_{lk}}\big) &= \sum_{\substack{a \\ \forall\{P_a,P_{jk}\}=0}} \eta_a\big(\gamma_{kl}^2 P_{jk}P_a + 2\gamma_{kl}\delta_{kl}P_{jk}P_aP_{lk} + \delta_{kl}^2 \underline{P_{kl}P_{jk}}P_{lk}P_a\big) \\
&= \sum_{\substack{a \\ \forall\{P_a,P_{jk}\}=0}} \eta_a\big(\gamma_{kl}^2 P_{jk}P_a + 2\gamma_{kl}\delta_{kl}P_{jk}P_aP_{lk} - \delta_{kl}^2 P_{jk}P_{kl}P_{lk}P_a\big) \\
&= \sum_{\substack{a \\ \forall\{P_a,P_{jk}\}=0}} \eta_a\big(\gamma_{kl}^2 P_{jk}P_a + 2\gamma_{kl}\delta_{kl}P_{jk}P_aP_{lk} - \delta_{kl}^2 P_{jk}P_a\big) \\
&= \sum_{\substack{a \\ \forall\{P_a,P_{jk}\}=0}} \eta_a\big((\gamma_{kl}^2 - \delta_{kl}^2)P_{jk}P_a + 2\gamma_{kl}\delta_{kl}P_{jk}P_aP_{lk}\big) \\
&= \sum_{\substack{a \\ \forall\{P_a,P_{jk}\}=0}} \eta_a\big(\cos\big(\theta_{kl}\big)P_{jk}P_a + \sin\big(\theta_{kl}\big)P_{jk}P_aP_{lk}\big).
\end{aligned} \tag{S.31}$$

The number of terms in the resulting operator has increased for each case where $[P_a, P_{lk}] = 0$. The action of two rotations of R_S on the whole Hamiltonian results in:

$$\begin{aligned}
R_{S_{kl}}R_{S_{kj}}HR_{S_{kj}}^\dagger R_{S_{kl}}^\dagger =& R_{S_{kl}}\bigg(\sum_a \eta_a P_a\bigg)R_{S_{kl}}^\dagger + R_{S_{kl}}\bigg(\sum_{\substack{a \\ \forall\{P_a,P_{jk}\}=0}} \eta_a\big(P_{jk}P_a\big)\bigg)R_{S_{kl}}^\dagger \\
=& R_{S_{kl}}\bigg(\sum_a \eta_a P_a\bigg)R_{S_{kl}}^\dagger + \sum_{\substack{a \\ \forall\{P_a,P_{jk}\}=0 \\ \forall\{P_a,P_{lk}\}=0}} \eta_a P_{jk}P_a + \\
& \sum_{\substack{a \\ \forall\{P_a,P_{jk}\}=0 \\ [P_a,P_{lk}]=0}} \eta_a\big(\cos\big(\theta_{kl}\big)P_{jk}P_a + \sin\big(\theta_{kl}\big)P_{jk}P_aP_{lk}\big) \\
=& R_{S_{kl}}\bigg(\sum_a \eta_a P_a\bigg)R_{S_{kl}}^\dagger + \sum_{\substack{a \\ \forall\{P_a,P_{jk}\}=0}} \mu_a P_{jk}P_a + \sum_{\substack{a \\ \forall\{P_a,P_{jk}\}=0 \\ [P_a,P_{lk}]=0}} \mu_a P_{jk}P_aP_{lk} \\
=& \sum_a \nu_a P_a + \sum_{\substack{a \\ \forall\{P_a,P_{lk}\}=0}} \nu_a\big(P_{lk}P_a\big) + \sum_{\substack{a \\ \forall\{P_a,P_{jk}\}=0}} \mu_a P_{jk}P_a + \sum_{\substack{a \\ \forall\{P_a,P_{jk}\}=0 \\ [P_a,P_{lk}]=0}} \mu_a P_{jk}P_aP_{lk}.
\end{aligned} \tag{S.32}$$

where Greek letters are new coefficients according to the expansion. We use the results of Equations S.30 and S.31 to determine what occurs to the second term of Equation S.32. We have applied the result in Equation S.27 to the first term ($R_{S_{kl}}\bigg(\sum_i \eta_i P_i\bigg)R_{S_{kl}}^\dagger$) in Equation S.32.

From these results we can infer how the terms in H_q will scale for a general sequence of rotations of size $|R_S|$ (Equation S.18), which in general change as:

$$|H_q|\sum_{g=0}^{|R_S|}\binom{|R_S|}{g} = 2^{|R_S|}|H_q| \tag{S.33}$$

This operation increases the number of terms in H_q to $\mathcal{O}\big(2^{(|\mathcal{A}|-1)}|H_q|\ \big)$. However, the structure of the sequence of rotation operator actually requires 2^g commuting/anticommuting conditions to be met for new Pauli operators to be generated by subsequent rotations. We therefore need to consider the probability that a given Pauli operator will either commute or anticommute with another. For the case of single qubit Pauli matrices $\sigma_a, \sigma_b \in \{I, X, Y, Z\}$ by a simple counting argument $P([\sigma_a, \sigma_b] = 0) = \frac{5}{8}$ and $P(\{\sigma_a, \sigma_b\} = 0) = \frac{3}{8}$, for Pauli matrices selected uniformly at random. Generalising this to tensor products of Pauli matrices on n qubits, for a Pauli operator to anticommute with another there needs to be an odd number of anticommuting tensor factors. First consider the binomial distribution:

$$P(x) = \binom{n}{x} p^x q^{n-x}, \tag{S.34}$$

where n is the number of trials (repeated experiments), p is the probability of success - here the probability a single Pauli matrix anticommutes with another ($p = \frac{3}{8}$) - and q is the probability of failure - here the probability a single Pauli matrix commutes with another ($q = \frac{5}{8}$). Under these conditions, $P(x)$ gives the probability that two n-fold Pauli operators, selected uniformly at random, anticommute in x-many tensor factors. Therefore, the probability of two uniformly random Pauli operators anticommuting (commuting) is given as a sum over odd (even) values of $x \leq n$:

$$P\big(\{P_a, P_b\} = 0\big) = \sum_{c=1}^{\lceil n/2 \rceil} P(2c-1). \tag{S.35}$$

Now, the binomial theorem states

$$(p+q)^n = \sum_{c=0}^{n} \binom{n}{c} p^c q^{n-c} \tag{S.36}$$

for any $p, q \in \mathbb{R}$ and define the following difference:

$$(p+q)^n - (-p+q)^n = \sum_{c=0}^{n} \binom{n}{c} \underbrace{\big[1-(-1)^c\big]}_{=\begin{cases} 2, & \text{if } c \text{ odd} \\ 0, & \text{if } c \text{ even} \end{cases}} p^c q^{n-c} = 2 \sum_{c=1}^{\lceil n/2 \rceil} \binom{n}{2c-1} p^{2c-1} q^{n-(2c-1)}. \tag{S.37}$$

Overall we find the probability that two n-fold Pauli operators anticommute to be:

$$\begin{aligned} P\big(\{P_a, P_b\} = 0\big) &= \sum_{c=1}^{\lceil n/2 \rceil} P(2c-1) \\ &= \sum_{c=1}^{\lceil n/2 \rceil} \binom{n}{2c-1} \cdot \left(\frac{3}{8}\right)^{2c-1} \cdot \left(\frac{5}{8}\right)^{n-(2c-1)} \\ &= \frac{1}{2}\left[\left(\frac{3}{8} + \frac{5}{8}\right)^n - \left(-\frac{3}{8} + \frac{5}{8}\right)^n \right] \\ &= \frac{1}{2}\left[1 - \left(\frac{1}{4}\right)^n\right], \end{aligned} \tag{S.38}$$

when each operator P_a, P_b is chosen uniformly at random. The n choose $2c-1$ term in equation S.38 counts all the possible ways an odd number of single qubit pairs of Pauli tensor factors can differ on n qubits, the first fraction gives the probability that there are $2c-1$ anticommuting terms on each pair of qubits and the final fraction gives the probability that the remaining $n-(2c-1)$ qubit positions pairwise commute on each qubit. The penultimate line of equation S.38 uses the definition in S.37, with the factor of two taken into account. Through equation S.38, it can be seen that the probability of two n-fold Pauli operators anticommuting quickly converges to 0.5 as the number of qubits n increases. The motivation for S.37 arises from observing that the quantity we subtract, $(1/4)^n$, is the probability of obtaining an n-fold identity operator, which has the unique property of commuting universally. The complement $1-(1/4)^n$ therefore corresponds with the probability of selecting uniformly at random a Pauli operator with at least one non-trivial tensor factor. After discounting identity operators from consideration, the probabilities of anticommuting or commuting coincide, hence each occurs half of the time, explaining the $1/2$ factor in S.38; the probability bias towards commutation is a consequence of the identity operator commuting universally, whereas there is no such operator that can anticommute universally.

If we consider how the number of terms in H_q changes upon the sequence of rotations transformation: $H_q \mapsto R_S H_q R_S^\dagger$ where terms either commute or anticommute with a probability of 0.5, then the scaling is as follows:

$$\sum_{g=0}^{|R_S|} \frac{|H_q|}{2^g} \binom{|R_S|}{g} = \left(\frac{3}{2}\right)^{|R_S|} |H_q|. \tag{S.39}$$

Equation S.33 is modified to have a constant factor of 2^{-g}, where g represents the number of commuting or anticommuting conditions required for operators in H_q to obey in order to increase the number of terms upon a rotation of R_S. Here each condition is assumed to occur with a probability of 0.5. This operation increases the number of terms in H_q to $\mathcal{O}\big(1.5^{(|\mathcal{A}|-1)}|H_q|\ \big)$. Note $|R_S| = |\mathcal{A}| - 1$. In general, the scaling will be $\mathcal{O}\big(x^{(|\mathcal{A}|-1)}|H_q|\ \big)$ where $1 \leq x \leq 2$, depending on how each rotation in the sequence of rotations commutes with terms in H_q. The $x = 1$ case occurs if each rotation in R_S commutes with the whole Hamiltonian. Apart from this special case, the number of terms in H_q will increase exponentially with the size of $\mathcal{A}$ or equivalently with the number of qubits n (as $|\mathcal{A}| \leq 2n+1$ [**?**]) when R is defined by a sequence of rotations.

2. Unitary partitioning via a linear combination of unitaries

Here we show how $A(\vec{r}) \mapsto P_0^{(k)} = R_{LCU} A(\vec{r}) R_{LCU}^\dagger$, where R_{LCU} is defined by a linear combination of Pauli operators. We consider the set of anticommuting Pauli operators making up $A(\vec{r})$ (Equation **??**). We can re-write this Equation, with the term we are reducing to ($r_k P_0^{(k)}$) outside the sum:

$$A(\vec{r}) = r_k P_0^{(k)} + \sum_{\substack{j=0 \\ \forall j \neq k}}^{N-1} r_j P_0^{(j)}. \tag{S.40}$$

To simplify the notation we drop the subscript 0 (denoting the first operator in a clique) and write each $P_0^{(k)}$, $P_0^{(j)}$ as P_k and P_j respectively.

A re-normalization can be performed on the remaining sum yielding:

$$\begin{aligned} A(\vec{r}) &= r_k P_k + \Omega \sum_{\substack{j=0 \\ \forall j \neq k}}^{N-1} \delta_j P_j \\ &= r_k P_k + \Omega H_{\mathcal{A}\setminus\{r_k P_k\}}, \end{aligned} \tag{S.41}$$

where:

$$\sum_{\substack{j=0 \\ \forall j \neq k}}^{N-1} |\delta_j|^2 = 1, \tag{S.42a}$$

$$r_j = \Omega \delta_j, \tag{S.42b}$$

$$H_{\mathcal{A}\setminus\{r_k P_k\}} = \sum_{\substack{j=0 \\ \forall j \neq k}}^{N-1} \delta_j P_j. \tag{S.42c}$$

Using the Pythagorean trigonometric identity: $\sin^2(x) + \cos^2(x) = 1$, $A(\vec{r})$ can be re-written as:

$$\begin{aligned} A(\vec{r}) &= \cos(\phi_k) P_k + \sin(\phi_k) \sum_{\substack{j=0 \\ \forall j \neq k}}^{N-1} \delta_i P_j \\ &= \cos(\phi_k) P_k + \sin(\phi_k) H_{\mathcal{A}\setminus\{r_k P_k\}}. \end{aligned} \tag{S.43}$$

Comparing Equations S.41 and S.43, it is clear that $\cos(\phi_k) = r_k$ and $\sin(\phi_k) = \Omega$.

It was shown in [**?**] that one can consider rotations of $A(\vec{r})$ around an axis that is Hilbert-Schmidt orthogonal to both $H_{\mathcal{A}\setminus\{r_k P_k\}}$ and P_k :

$$\mathcal{X} = \frac{i}{2}\big[H_{\mathcal{A}\setminus\{r_k P_k\}}, P_k\big] = i \sum_{\substack{j=0 \\ \forall j \neq k}}^{|H_{\mathcal{A}\setminus\{r_k P_k\}}|-1} \delta_j P_j P_k. \tag{S.44}$$

$\mathcal{X}$ anticommutes with $\mathcal{A}$ and is self-inverse [**?**]:

$$\mathcal{X}^2 = \left(i \sum_{j=0}^{|H_{\mathcal{A}\setminus\{r_k P_k\}}|-1} \delta_j P_j P_k\right)\left(i \sum_{l=0}^{|H_{\mathcal{A}\setminus\{r_k P_k\}}|-1} \delta_l P_l P_k\right), \tag{S.45a}$$

$$= - \sum_{j=0}^{|H_{\mathcal{A}\setminus\{r_k P_k\}}|-1} \sum_{l=0}^{|H_{\mathcal{A}\setminus\{r_k P_k\}}|-1} \delta_j \delta_l P_j P_k P_l P_k, \tag{S.45b}$$

$$= - \sum_{k=0}^{|H_{\mathcal{A}\setminus\{r_k P_k\}}|-1} \sum_{\substack{l=0 \\ \forall l=j}}^{|H_{\mathcal{A}\setminus\{r_k P_k\}}|-1} \delta_j \delta_j P_j P_k P_j P_k - \sum_{j=0}^{|H_{\mathcal{A}\setminus\{r_k P_k\}}|-1} \sum_{\substack{l=0 \\ \forall l\neq j}}^{|H_{\mathcal{A}\setminus\{r_k P_k\}}|-1} \delta_j \delta_l P_j P_k P_l P_k, \tag{S.45c}$$

$$= + \sum_{k=0}^{|H_{\mathcal{A}\setminus\{r_k P_k\}}|-1} \delta_j^2 \underbrace{P_k P_j}_{\text{order change}} P_j P_k - \sum_{j=0}^{|H_{\mathcal{A}\setminus\{r_k P_k\}}|-1} \sum_{l>j}^{|H_{\mathcal{A}\setminus\{r_k P_k\}}|-1} \delta_j \delta_l \underbrace{\{P_j P_k, P_l P_k\}}_{=0 \text{ when } j\neq l}, \tag{S.45d}$$

$$= + \sum_{j=0}^{|H_{\mathcal{A}\setminus\{r_k P_k\}}|-1} \delta_j^2 \mathcal{I}, \tag{S.45e}$$

$$= \mathcal{I} \tag{S.45f}$$

and has the following action [**?**]:

$$\mathcal{X} A(\vec{r}) = i\big(- \sin\phi_k P_k + \cos\phi_k H_{\mathcal{A}\setminus\{r_k P_k\}}\big). \tag{S.46}$$

One can also define the rotation [**?** **?**]:

$$R_{LCU} = e^{\left(-i\frac{\alpha}{2}\mathcal{X}\right)} = \cos\big(\frac{\alpha}{2}\big)\mathcal{I} - i\sin\big(\frac{\alpha}{2}\big)\mathcal{X} \tag{S.47a}$$

$$= \cos\big(\frac{\alpha}{2}\big)\mathcal{I} - i\sin\big(\frac{\alpha}{2}\big)\left(i \sum_{\substack{j=0 \\ \forall j\neq k}}^{|H_{\mathcal{A}\setminus\{r_k P_k\}}|-1} \delta_j P_j P_k\right) \tag{S.47b}$$

$$= \cos\big(\frac{\alpha}{2}\big)\mathcal{I} + \sin\big(\frac{\alpha}{2}\big) \sum_{\substack{j=0 \\ \forall j\neq k}}^{|H_{\mathcal{A}\setminus\{r_k P_k\}}|-1} \delta_j P_{jk}, \tag{S.47c}$$

$$= \delta_{\mathcal{I}}\mathcal{I} + \sum_{\substack{j=0 \\ \forall j\neq k}}^{|H_{\mathcal{A}\setminus\{r_k P_k\}}|-1} \delta_j P_{jk}. \tag{S.47d}$$

The conjugate rotation will be:

$$R_{LCU}^{\dagger} = \cos\big(\frac{\alpha}{2}\big)\mathcal{I} + i\sin\big(\frac{\alpha}{2}\big) i \sum_{\substack{j=0 \\ \forall j\neq k}}^{|H_{\mathcal{A}\setminus\{r_k P_k\}}|-1} \delta_j P_j P_k, \tag{S.48a}$$

$$= \cos\big(\frac{\alpha}{2}\big)\mathcal{I} + \sin\big(\frac{\alpha}{2}\big) \sum_{\substack{j=0 \\ \forall j\neq k}}^{|H_{\mathcal{A}\setminus\{r_k P_k\}}|-1} \delta_j \underbrace{P_k P_j}_{\text{order change}}, \tag{S.48b}$$

$$= \delta_{\mathcal{I}}\mathcal{I} + \sum_{\substack{j=0 \\ \forall j\neq k}}^{|H_{\mathcal{A}\setminus\{r_k P_k\}}|-1} \delta_j P_{kj}. \tag{S.48c}$$

Note the different order of j and k for R_{LCU} and $R_{LCU}^\dagger$. The adjoint action of R_{LCU} on $A(\vec{r})$ is:

$$R_{LCU}A(\vec{r})R_{LCU}^\dagger = \cos\big(\phi_k - \alpha\big)P_k + \sin\big(\phi_k - \alpha\big)H_{\mathcal{A}\setminus\{r_kP_k\}}. \tag{S.49}$$

By choosing $\alpha = \phi_k$, the following transformation occurs $R_{LCU}A(\vec{r})R_{LCU}^\dagger = P_k$ [**? ?**]. This fully defines the R_{LCU} operator required by unitary partitioning. Next we need to consider the use of this operator in CS-VQE.

The adjoint action of R_{LCU} on a general Hamiltonian $H_q = \sum_i^{|H_q|} c_iP_i$ is:

$$\begin{aligned}
R_{LCU}H_qR_{LCU}^\dagger =& \left(\delta_{\mathcal{I}}\mathcal{I} + \sum_j^{|R_{LCU}|-1}\delta_jP_{jk}\right)\sum_i^{|H_q|}c_iP_i\left(\delta_{\mathcal{I}}\mathcal{I} + \sum_l^{|R_{LCU}|-1}\delta_lP_{kl}\right) && \text{(S.50a)}\\
=& \left(\delta_{\mathcal{I}}\sum_i^{|H_q|}c_iP_i + \sum_j^{|R_{LCU}|-1}\sum_i^{|H_q|}\delta_jc_iP_{jk}P_i\right)\left(\delta_{\mathcal{I}}\mathcal{I} + \sum_l^{|R_{LCU}|-1}\delta_lP_{kl}\right) && \text{(S.50b)}\\
=& \ \delta_{\mathcal{I}}^2\sum_i^{|H_q|}c_iP_i && \text{(S.50c)}\\
&+ \sum_l^{|R_{LCU}|-1}\sum_i^{|H_q|}\delta_{\mathcal{I}}c_i\delta_lP_iP_{kl} + \sum_j^{|R_{LCU}|-1}\sum_i^{|H_q|}\delta_{\mathcal{I}}\delta_jc_iP_{jk}P_i && \text{(S.50d)}\\
&+ \sum_j^{|R_{LCU}|-1}\sum_i^{|H_q|}\sum_l^{|R_{LCU}|-1}\delta_jc_i\delta_lP_{jk}P_iP_{kl} && \text{(S.50e)}
\end{aligned}$$

We can rewrite the final term (Equation S.50e) as:

$$\begin{aligned}
\sum_j^{|R_{LCU}|-1}\sum_i^{|H_q|}\sum_l^{|R_{LCU}|-1}\delta_jc_i\delta_lP_{jk}P_iP_{kl} =& \sum_j^{|R_{LCU}|-1}\sum_i^{|H_q|}\sum_{\substack{l=j\\[P_{jk},P_i]=0}}^{|R_{LCU}|-1}(c_i\delta_j\delta_j^*)P_i && \text{(S.51a)}\\
&+ \sum_j^{|R_{LCU}|-1}\sum_i^{|H_q|}\sum_{\substack{l=j\\\{P_{jk},P_i\}=0}}^{|R_{LCU}|-1}(-c_i\delta_j\delta_j^*)P_i && \text{(S.51b)}\\
&+ \sum_j^{|R_{LCU}|-1}\sum_i^{|H_q|}\sum_{l\neq j}^{|R_{LCU}|-1}(\delta_jc_i\delta_l)P_{jk}P_iP_{kl}. && \text{(S.51c)}
\end{aligned}$$

Here we have applied the identity of conjugating a Pauli operator P_u with another Pauli operator P_v resulting in two cases:

$$P_vP_uP_v = \begin{cases} P_u, & \text{if } [P_v, P_u] = 0\\ -P_u, & \text{otherwise } \{P_v, P_u\} = 0\end{cases} \tag{S.52}$$

Focusing on the last term of Equation S.51, we can simplify S.51c as j and l run over the same indices we can re-write each $l \neq j$ sum as $l > j$ and expand into two terms:

$$\sum_j^{|R_{LCU}|-1}\sum_i^{|H_q|}\sum_{l\neq j}^{|R_{LCU}|-1}(\delta_jc_i\delta_l)P_{jk}P_iP_{kl} = \sum_j^{|R_{LCU}|-1}\sum_i^{|H_q|}\sum_{l>j}^{|R_{LCU}|-1}(\delta_jc_i\delta_l)\Big(P_{jk}P_iP_{kl} + P_{lk}P_iP_{kj}\Big) \tag{S.53}$$

We can expand then expand this equation into the four cases for when:

1. $[P_{jk}, P_i] = 0$ and $[P_{lk}, P_i] = 0$

2. $[P_{jk}, P_i] = 0$ and $\{P_{lk}, P_i\} = 0$

3. $\{P_{jk}, P_i\} = 0$ and $[P_{lk}, P_i] = 0$

4. $\{P_{jk}, P_i\} = 0$ and $\{P_{lk}, P_i\} = 0$

For the first case and last case:

$$\begin{aligned}\sum_{j}^{|R_{LCU}|-1}\sum_{i}^{|H_q|}\sum_{l>j}^{|R_{LCU}|-1}(\delta_j c_i \delta_l)\Big(\underline{P_{jk}P_i}P_{kl} + \underline{P_{lk}P_i}P_{kj}\Big) &= \sum_{j}\sum_{i}^{|H_q|}\sum_{l>j}(\delta_j c_i \delta_l)\Big(\pm P_i\underline{P_{jk}P_{kl}} \pm P_i\underline{P_{lk}P_{kj}}\Big)\\ &= \sum_{j}\sum_{i}^{|H_q|}\sum_{l>j}(\delta_j c_i \delta_l)\Big(\pm P_iP_jP_l \pm P_iP_lP_j\Big)\\ &= \sum_{j}\sum_{i}^{|H_q|}\sum_{l>j}(\delta_j c_i \delta_l) \pm P_i\{P_j, P_l\}\\ &= 0\end{aligned} \tag{S.54}$$

Whereas, for the second and third cases:

$$\begin{aligned}\sum_{j}^{|R_{LCU}|-1}\sum_{i}^{|H_q|}\sum_{l>j}^{|R_{LCU}|-1}(\delta_j c_i \delta_l)\Big(\underline{P_{jk}P_i}P_{kl} + \underline{P_{lk}P_i}P_{kj}\Big) &= \sum_{j}\sum_{i}^{|H_q|}\sum_{l>j}(\delta_j c_i \delta_l)\Big(\pm P_i\underline{P_{jk}P_{kl}} \mp P_i\underline{P_{lk}P_{kj}}\Big)\\ &= \sum_{j}\sum_{i}^{|H_q|}\sum_{l>j}(\delta_j c_i \delta_l)\Big(\pm P_iP_jP_l \mp P_i\underline{P_lP_j}\Big)\\ &= \sum_{j}\sum_{i}^{|H_q|}\sum_{l>j}(\delta_j c_i \delta_l)\Big(\pm P_iP_jP_l \pm P_iP_jP_l\Big)\\ &= \sum_{j}\sum_{i}^{|H_q|}\sum_{l>j}(\delta_j c_i \delta_l) \pm 2P_iP_jP_l\end{aligned} \tag{S.55}$$

We can rewrite Equation S.51 using this result:

$$\begin{aligned}\sum_{j}^{|R_{LCU}|-1}\sum_{i}^{|H_q|}\sum_{l}^{|R_{LCU}|-1}\delta_j c_i \delta_l P_{jk}P_iP_{kl} = &\sum_{j}\sum_{i}^{|H_q|}\sum_{\substack{l=j\\[P_{jk},P_i]=0}}(c_i\delta_j\delta_j^*)P_i + \sum_{j}\sum_{i}^{|H_q|}\sum_{\substack{l=j\\\{P_{jk},P_i\}=0}}(-c_i\delta_j\delta_j^*)P_i +\\ &\sum_{j}\sum_{i}^{|H_q|}\sum_{\substack{l>j\\\forall[P_{jk},P_i]=0\\\{P_{lk},P_i\}=0}}(\delta_j c_i \delta_l)2P_iP_jP_l - \sum_{j}\sum_{i}^{|H_q|}\sum_{\substack{l>j\\\forall\{P_{jk},P_i\}=0\\[P_{lk},P_i]=0}}(\delta_j c_i \delta_l)2P_iP_jP_l\\ = &\sum_{i}^{|H_q|}\nu_iP_i + \sum_{j}^{|R_{LCU}|-1}\sum_{i}^{|H_q|}\sum_{\substack{l>j\\\forall\{P_i,P_jP_l\}=0}}^{|R_{LCU}|-1}\nu_{ijl}P_iP_jP_l\end{aligned} \tag{S.56}$$

where we have combined the second and third conditions into a single condition of $\{P_a, P_{jk}P_{kl}\} = \{P_a, P_jP_l\} = 0$ and combined the new coefficients into one coefficient denoted ν.

Next consider the S.50d term of equation S.50. One can use the fact that j and l run over the same indices:

$$\underbrace{\sum_{l}^{|R_{LCU}|-1}\sum_{i}^{|H_q|}\delta_{\mathcal{I}}c_i\delta_l P_i P_{kl}}_{\text{re-write using } l=j}+\sum_{j}^{|R_{LCU}|-1}\sum_{i}^{|H_q|}\delta_{\mathcal{I}}\delta_j c_i P_{jk}P_i = \sum_{j}^{|R_{LCU}|-1}\sum_{i}^{|H_q|}\delta_{\mathcal{I}}c_i\delta_j P_i P_{kj}+\sum_{j}^{|R_{LCU}|-1}\sum_{i}^{|H_q|}\delta_{\mathcal{I}}\delta_j c_i P_{jk}P_i$$

$$\begin{aligned}
&= \sum_{j}^{|R_{LCU}|-1}\sum_{i}^{|H_q|} -\delta_{\mathcal{I}}c_i\delta_j P_i P_{jk}+\sum_{j}^{|R_{LCU}|-1}\sum_{i}^{|H_q|}\delta_{\mathcal{I}}\delta_j c_i P_{jk}P_i \\
&= \sum_{j}^{|R_{LCU}|-1}\sum_{i}^{|H_q|}\delta_{\mathcal{I}}c_i\delta_j\big(P_{jk}P_i - P_i P_{jk}\big) \\
&= \sum_{j}^{|R_{LCU}|-1}\sum_{i}^{|H_q|}\delta_{\mathcal{I}}c_i\delta_j[P_{jk},P_i] \\
&= \sum_{j}^{|R_{LCU}|-1}\sum_{\substack{i \\ \forall\{P_{jk},P_i\}=0}}^{|H_q|} 2\delta_{\mathcal{I}}c_i\delta_j P_{jk}P_i
\end{aligned} \tag{S.57}$$

Overall we can re-write equation S.50 using these results, yielding:

$$\begin{aligned}
R_{LCU}H_qR_{LCU}^\dagger = &\underbrace{\delta_{\mathcal{I}}^2\sum_{i}^{|H_q|}c_iP_i}_{S.50c}+\underbrace{\sum_{j}^{|R_{LCU}|-1}\sum_{\substack{i \\ \forall\{P_{jk},P_i\}=0}}^{|H_q|}2\delta_{\mathcal{I}}c_i\delta_j P_{jk}P_i}_{S.50d \text{ using } S.57}+ \\
&\underbrace{\sum_{i}^{|H_q|}\nu_iP_i+\sum_{j}^{|R_{LCU}|-1}\sum_{i}^{|H_q|}\sum_{\substack{l>j \\ \forall\{P_i,P_jP_l\}=0}}^{|R_{LCU}|-1}\nu_{ijl}P_iP_jP_l}_{S.50e \text{ using } S.56} \\
= &\sum_{i}^{|H_q|}(\delta_{\mathcal{I}}^2c_i+\nu_i)P_i+\sum_{j}^{|R_{LCU}|-1}\sum_{\substack{i \\ \forall\{P_{jk},P_i\}=0}}^{|H_q|}2\delta_{\mathcal{I}}c_i\delta_jP_{jk}P_i+ \\
&\sum_{j}^{|R_{LCU}|-1}\sum_{i}^{|H_q|}\sum_{\substack{l>j \\ \forall\{P_i,P_jP_l\}=0}}^{|R_{LCU}|-1}\nu_{ijl}P_iP_jP_l
\end{aligned} \tag{S.58}$$

We observe that the number of terms in $R_{LCU}H_qR_{LCU}^\dagger$ at worst scales as $|H_q|+|H_q|\cdot(|R_{LCU}|-1)+|H_q|\big(\frac{(|R_{LCU}|-1)(|R_{LCU}|-2)}{2}\big)$ or $\mathcal{O}\big(\ |H_q|\cdot|\mathcal{A}|^2\ \big)$. The total number of qubits n bounds the size of $|\mathcal{A}|\leq 2n+1$ [**?**], and thus the number of terms in H_q will increase quadratically with the size of $\mathcal{A}$ or number of qubits n when R is defined by a linear combination of unitaries.

3. Mapping Pauli operators to single-qubit Pauli Z operators

In Appendix A of [**?**] a proof is given on how to map a completely commuting set of Pauli operators to a single qubit Pauli Z operator. We summarise the operation required and omit the proof. We denote a given Pauli operator on n qubits as: $P=\bigotimes_{i=0}^{n-1}\sigma_i^P$, where σ_i are a single qubit Pauli operators. There are two cases we need to consider (diagonal and non-diagonal), with the goal to reduce the operators in $\mathcal{R}^{'}\equiv\{P_0^{(k)}\}\cup\mathcal{G}$ (Equation **??**) to single-qubit Z Pauli operators.

For a non-diagonal Pauli operators $P_a\in\mathcal{R}'$, there must be at least one single qubit Pauli operator indexed by qubit k such that: $\sigma_k^{P_a}\in\{X,Y\}$. We can use this to define operator P_b that must anticommute with P_a:

$$\begin{aligned} P_a &= \left(\bigotimes_{i=0}^{k-1} \sigma_i^{P_a}\right) \otimes \sigma_k^{P_a} \otimes \left(\bigotimes_{i=k+1}^{n-1} \sigma_i^{P_a}\right) \\ P_b &= \left(\bigotimes_{i=0}^{k-1} \sigma_i^{P_a}\right) \otimes \sigma_k' \otimes \left(\bigotimes_{i=k+1}^{n-1} \sigma_i^{P_a}\right) \end{aligned} \quad \text{where } \{P_a, P_b\} = 0 \Leftrightarrow \sigma_k' = \begin{cases} X, & \text{if } \sigma_k^{P_a} = Y \\ Y, & \text{if } \sigma_k^{P_a} = X \end{cases} \tag{S.59}$$

These two Pauli operators differ by exactly one Pauli operator on qubit index k. We can define the rotation:

$$B = \exp\left(i\frac{\pi}{4}P_b\right) \tag{S.60}$$

Conjugating P_a with this operator results in:

$$BP_aB^\dagger = \pm 1\left(\bigotimes_{i=0}^{k-1} I_i\right) \otimes Z_k \otimes \left(\bigotimes_{i=k+1}^{n-1} I_i\right) = P_a', \tag{S.61}$$

and P_a has been mapped to a single qubit Pauli Z operator.

For diagonal operators $P_c \in \mathcal{R}'$, all the n-fold tensor products of single qubit Pauli operators must be either Z or I: $P_c = \bigotimes_{i=0}^{n-1} \sigma_i^{P_c}$ where $\sigma_i^{P_c} \in \{I, Z\}\ \forall i$. Since $\mathcal{R}'$ is an independent set, for all the rotated P_a' there must be at least one index l such that $\sigma_l^{P_a'} = I$ and $\sigma_l^{P_c} = Z$. We denote this operator P_c. We also define a new operator P_d from this, which only acts non-trivially on the l-th qubit with a single qubit Y. To summarise:

$$\begin{aligned} P_c &= \left(\bigotimes_{i=0}^{l-1} \sigma_i^{P_c}\right) \otimes Z_l \otimes \left(\bigotimes_{l=k+1}^{n-1} \sigma_i^{P_c}\right) \text{ where } \sigma_i^{P_c} \in \{I, Z\}\ \forall i \\ P_d &= \left(\bigotimes_{i=0}^{l-1} I_i\right) \otimes Y_l \otimes \left(\bigotimes_{i=l+1}^{n-1} I_i\right) \\ P_a' &= \left(\bigotimes_{i=0}^{l-1} \sigma_i^{P_a'}\right) \otimes I_l \otimes \left(\bigotimes_{i=l+1}^{n-1} \sigma_i^{P_a'}\right) \text{ where } [P_d, P_a'] = 0 \text{ and } \sigma_i^{P_a'} \in \{I, Z\} \forall\ i \end{aligned} \tag{S.62}$$

We can define the rotation:

$$D = \exp\left(i\frac{\pi}{4}P_d\right) \tag{S.63}$$

Conjugating P_c with this operator results in:

$$DP_cD^\dagger = \pm 1\left(\bigotimes_{i=0}^{l-1} \sigma_i^{P_c}\right) \otimes X_l \otimes \left(\bigotimes_{i=l+1}^{n-1} \sigma_i^{P_c}\right) = P_c'. \tag{S.64}$$

P_c' is now a non-diagonal Pauli operator (contains a single qubit X acting on qubit l). This operator P_c' can now be mapped to a single qubit Z operator using a further $\frac{\pi}{2}$-rotation following the previously given procedure for non-diagonal Pauli operators.

The operators V_i in the main text (equation **??**) are defined by these $\frac{\pi}{2}$-rotations, such that each q_iG_i and $P_0^{(k)}$ is mapped to a single qubit Pauli Z term. At worst, two $\frac{\pi}{2}$-rotations are needed for every operator in $\mathcal{R}'$ (Equation **??**), which occurs when all operators in $\mathcal{R}'$ are diagonal.

II. UNITARY PARTITIONING MEASUREMENT REDUCTION

In unitary partitioning, the Hamiltonian is partitioned into groups of operators that's linear combination are unitary Hermitian operators. This is done by forming normalized groups of Pauli operators that pairwise anticommute. We can write this as:

$$\begin{aligned} H &= \sum_i c_i P_i \\ &= \sum_j \gamma_j C_j \\ &= \sum_j^{N_C} \gamma_j \Bigg(\sum_{\substack{k \\ \{P_a, P_b\}=0 \\ \forall P_a, P_b \in C_j \\ a \neq b}}^{|C_j|} \frac{c_k}{\gamma_j} P_k \Bigg), \end{aligned} \tag{S.65}$$

where $\gamma_j = \left(\sum_k^{C_j} c_k^2 \right)^{0.5}$. The complete approach is provided in [**?** **?** **?**]. We follow the analysis of Crawford *et al.* to determine the measurement cost to determine $\langle H \rangle$ to a certain precision [**?**]. The measurement requirement for measuring the Hamiltonian in terms of grouped terms to precision ϵ is [**?**]:

$$M_g = \frac{1}{\epsilon^2_{\langle H \rangle}} \left(\sum_j^{N_C} \sqrt{Var[C_j]} \right)^2, \tag{S.66}$$

We can use this to determine the number of measurements when no partitioning has being done [**?**]:

$$M_u = \frac{1}{\epsilon^2_{\langle H \rangle}} \left(\sum_j^{N_C} \left[\sum_{k=0}^{|C_j|-1} |c_k^{(j)}| \sqrt{Var[P_k^{(j)}]} \right] \right)^2. \tag{S.67}$$

This can be thought of as each clique is of size one. The subscript u is to denote no grouping. A natural metric to evaluate the the measurement cost of a particular grouping of Pauli operators is therefore given by the ratio R of these two terms:

$$R = \frac{M_u}{M_g} = \left(\frac{\sum_j^{N_C} \left[\sum_{k=0}^{|C_j|-1} |c_k^{(j)}| \sqrt{Var[P_k^{(j)}]} \right]}{\sum_j^{N_C} \sqrt{Var[C_j]}} \right)^2 \tag{S.68}$$

where the greater the value of R, the better the measurement saving is by assembling these operators into a particular group.

Next, our analysis diverges from Crawford *et al.*, where we consider groups of anticommuting operators (rather than commuting operators)[**?**]. First we consider the covariance of two anticommuting Pauli operators.

The amount two random variables vary together (co-vary) is measured by their covariance. Consider the results of random variables x and y, one can obtain a set of M paired measurements:

$$\begin{aligned} \{&(x_0, y_0), \\ &(x_1, y_1), \\ &\ldots, \\ &(x_{M-1}, y_{M-1})\}. \end{aligned} \tag{S.69}$$

A positive covariance indicates that higher than average values of one variable tend to be paired with higher than average values of the other variable. A negative covariance indicates that a higher than average value of one variable tend to be paired with lower than average values of the other. If two random variables are independent, then their

covariance will be zero. However, a covariance of zero does not mean two random variables are independent, as nonlinear relationships can result in a covariance of zero.

In the context of measuring a quantum state in the Pauli basis on a quantum computer this would be a set of paired single shot samples $\{s_i^a, s_i^b | i = 0, 1, \ldots, N-1\}$, where $s_i^a, s_i^b \in \{-1, +1\}$. Experimentally, each pair is the (single shot) measurement outcome for P_a followed by the (single shot) measurement outcome for P_b. Taking simultaneous projective measurements, without re-preparing the quantum state is a meaningful operation if the operators share a common eigenbasis. The order of measurement does not effect measurement outcomes, but the paired samples will be statistically correlated and have a certain covariance. However, for anticommuting Pauli operators this is not the case, as these operators do not share a common eigenbasis. Projective measurement means the expectation value of these operators cannot be known simultaneously. We consider the covariance in this scenario.

Consider the the spectral decomposition of two anticommuting Pauli operators $\{P_a, P_b\}$:

$$P_a = +1 \left|\kappa_0\right\rangle \left\langle\kappa_0\right| - 1 \left|\kappa_1\right\rangle \left\langle\kappa_1\right|, \tag{S.70}$$

and

$$P_b = +1 \left|\Omega_0\right\rangle \left\langle\Omega_0\right| - 1 \left|\Omega_1\right\rangle \left\langle\Omega_1\right|, \tag{S.71}$$

where for Pauli operators:

$$\left\langle\kappa_0 \middle| \kappa_0\right\rangle = \left\langle\kappa_1 \middle| \kappa_1\right\rangle = \left\langle\Omega_0 \middle| \Omega_0\right\rangle = \left\langle\Omega_1 \middle| \Omega_1\right\rangle = 1, \tag{S.72a}$$

$$\left\langle\kappa_0 \middle| \kappa_1\right\rangle = \left\langle\Omega_0 \middle| \Omega_1\right\rangle = 0, \tag{S.72b}$$

$$\left|\left\langle\kappa_0 \middle| \Omega_0\right\rangle\right|^2 = \left|\left\langle\kappa_0 \middle| \Omega_1\right\rangle\right|^2 = \left|\left\langle\kappa_1 \middle| \Omega_0\right\rangle\right|^2 = \left|\left\langle\kappa_1 \middle| \Omega_1\right\rangle\right|^2 = 0.5. \tag{S.72c}$$

Without loss of generality, assume P_a is measured first on a general normalized quantum state $|\psi\rangle = \gamma |\kappa_0\rangle + \delta |\kappa_1\rangle$. The only possible post measurement outcomes are $|\kappa_0\rangle$ or $|\kappa_1\rangle$, with probabilities $|\gamma|^2$ or $|\delta|^2$ respectively. Consider the result of subsequently measuring P_b. The expectation value in each scenario will be:

$$\begin{aligned}
\left\langle\kappa_0\right| P_b \left|\kappa_0\right\rangle &= \left\langle\kappa_0\right| \big(\left|\Omega_0\right\rangle \left\langle\Omega_0\right| - \left|\Omega_1\right\rangle \left\langle\Omega_1\right| \big) \left|\kappa_0\right\rangle \\
&= \left\langle\kappa_0 \middle| \Omega_0\right\rangle \left\langle\Omega_0 \middle| \kappa_0\right\rangle - \left\langle\kappa_0 \middle| \Omega_1\right\rangle \left\langle\Omega_1 \middle| \kappa_0\right\rangle \\
&= \left|\left\langle\kappa_0 \middle| \Omega_0\right\rangle\right|^2 - \left|\left\langle\kappa_0 \middle| \Omega_1\right\rangle\right|^2 \\
&= \underbrace{0.5}_{\mathbb{P}(\Omega_0|\kappa_0)} - \underbrace{0.5}_{\mathbb{P}(\Omega_1|\kappa_0)} = 0
\end{aligned} \tag{S.73a}$$

$$\begin{aligned}
\left\langle\kappa_1\right| P_b \left|\kappa_1\right\rangle &= \left\langle\kappa_1\right| \big(\left|\Omega_0\right\rangle \left\langle\Omega_0\right| - \left|\Omega_1\right\rangle \left\langle\Omega_1\right| \big) \left|\kappa_1\right\rangle \\
&= \left\langle\kappa_1 \middle| \Omega_0\right\rangle \left\langle\Omega_0 \middle| \kappa_1\right\rangle - \left\langle\kappa_1 \middle| \Omega_1\right\rangle \left\langle\Omega_1 \middle| \kappa_1\right\rangle \\
&= \left|\left\langle\kappa_1 \middle| \Omega_0\right\rangle\right|^2 - \left|\left\langle\kappa_1 \middle| \Omega_1\right\rangle\right|^2 \\
&= \underbrace{0.5}_{\mathbb{P}(\Omega_0|\kappa_1)} - \underbrace{0.5}_{\mathbb{P}(\Omega_1|\kappa_1)} = 0
\end{aligned} \tag{S.73b}$$

Overall, we find the probabilities of all possible combinations of measurement outcomes to be:

$$\begin{aligned}
\mathbb{P}\big(P_b = |\Omega_0\rangle \,|P_a = |\kappa_0\rangle\big) = \mathbb{P}\big(P_b = |\Omega_1\rangle \,|P_a = |\kappa_0\rangle\big) = 0.5 \\
\mathbb{P}\big(P_b = |\Omega_0\rangle \,|P_a = |\kappa_1\rangle\big) = \mathbb{P}\big(P_b = |\Omega_1\rangle \,|P_a = |\kappa_1\rangle\big) = 0.5
\end{aligned} \tag{S.74}$$

This result shows that the probability of obtaining $|\Omega_0\rangle$ or $|\Omega_1\rangle$ is not affected by the probability of obtaining $|\kappa_0\rangle$ or $|\kappa_1\rangle$ in the first measurement. The variables are therefore statistically independent [1]. We find the covariance of P_a and P_b, where $\{P_a, P_b\} = 0$, to be:

---

[1] This analysis is strictly for the case of subsequent measurement of anticommuting Pauli operators.

$$
\begin{aligned}
Cov[P_a, P_b] &= \mathbb{E}\left[\Big(p_a - \langle P_a\rangle\Big)\Big(p_b - \langle P_b\rangle\Big)\right] \\
&= \mathbb{E}\left[\Big(p_a p_b - p_a\langle P_b\rangle - \langle P_a\rangle p_b + \langle P_a\rangle\langle P_b\rangle\Big)\right] \\
&= \Big(\mathbb{E}[p_a p_b] - \mathbb{E}[p_a\langle P_b\rangle] - \mathbb{E}[\langle P_a\rangle p_b] + \mathbb{E}[\langle P_a\rangle\langle P_b\rangle]\Big) \\
&= \langle P_a P_b\rangle - \langle P_a\rangle\langle P_b\rangle - \langle P_a\rangle\langle P_b\rangle + \langle P_a\rangle\langle P_b\rangle \\
&= \langle P_a P_b\rangle - \langle P_a\rangle\langle P_b\rangle \\
&= \langle P_a\rangle\langle P_b\rangle - \langle P_a\rangle\langle P_b\rangle = 0
\end{aligned}
\tag{S.75}
$$

where under independence: $\langle P_a P_b\rangle = \langle P_a\rangle\langle P_b\rangle$. Intuitively, this result makes sense. The projective measurement of the first Pauli operator maximally randomizes the expectation value of the other Pauli operator and thus the covariance will be zero. Interestingly, the projective measurement causes the underlying distribution of the quantum state to change and so subsequent measurements generating paired samples are not well defined in this setting (for anticommuting operators). This phenomenon is not present in classical experiments. However, the same statistical analysis can be done if we just take pairs of subsequent measurements and only do a statistical analysis on these random variables. We note that our analysis did not have to account for $\langle P_a P_b\rangle$ not being a valid observable, as for anticommuting Pauli operators this operator is not Hermitian.

Given the covariance of two anticommuting Pauli operators is zero, we find the variance of a normalized anticommuting clique $\gamma_j C_j$ to be:

$$
\begin{aligned}
Var[\gamma_j C_j] = \gamma_j^2 Var[C_j] = \gamma_j^2 Var[\sum_i^{|C_j|}\frac{c_i}{\gamma_j}P_i] &= \gamma_j^2\sum_i^{|C_j|}\sum_k^{|C_j|} Cov[\frac{c_i}{\gamma_j}P_i, \frac{c_k}{\gamma_j}P_k] \\
&= \gamma_j^2\sum_i^{|C_j|}\frac{c_i^2}{\gamma_j^2}Var[P_i] + \gamma_j^2\sum_i^{|C_j|}\sum_{\substack{k\\ \forall k\neq i}}^{|C_j|}\frac{c_i}{\gamma_j}\frac{c_k}{\gamma_j}\underbrace{Cov[P_i,P_k]}_{=0} \\
&= \sum_i^{|C_j|} c_i^2 Var[P_i]
\end{aligned}
\tag{S.76}
$$

We use this to obtain the following R ratio (equation S.68):

$$
\begin{aligned}
R = \frac{M_u}{M_g} &= \left(\frac{\sum_j^{N_C}\left[\sum_{k=0}^{|C_j|-1}\sqrt{Var[c_k^{(j)}P_k^{(j)}]}\right]}{\sum_j^{N_C}\sqrt{Var[\gamma_j C_j]}}\right)^2 \\
&= \left(\frac{\sum_j^{N_C}\left[\sum_{k=0}^{|C_j|-1}|c_k^{(j)}|\sqrt{Var[P_k^{(j)}]}\right]}{\sum_j^{N_C}\sqrt{\sum_{k=0}^{|C_j|-1}|c_k^{(j)}|^2 Var[P_k^{(j)}]}}\right)^2 \\
&= \left(\frac{\sum_j^{N_C}\left[\sum_{k=0}^{|C_j|-1}|x_k^{(j)}|\right]}{\sum_j^{N_C}\sqrt{\sum_{k=0}^{|C_j|-1}|x_k^{(j)}|^2}}\right)^2 \\
&= \left(\frac{\sum_j^{N_C}\|\vec{x}_j\|_1}{\sum_j^{N_C}\|\vec{x}_j\|_2}\right)^2
\end{aligned}
\tag{S.77}
$$

where $x_k^{(j)} = |c_k^{(j)}|\sqrt{Var[P_k^{(j)}]}$ and $\vec{x}_j = (x_0^{(j)}, x_1^{(j)}, \ldots, x_{|C_j|-1}^{(j)})$. Minkowski inequality ensures $\|\vec{x}_j\|_2 \leq \|\vec{x}_j\|_1$. At worst unitary partitioning will achieve the same number of measurements as no grouping and will more often achieve an improvement. However, we can actually bound the improvement in general as:

$$\|u\|_1 = \sum_i^n |u_i| = \sum_i^n |u_i| \cdot 1 \leq \left(\sum_i^n |u_i|^2 \right)^{0.5} \cdot \left(\sum_i^n 1^2 \right)^{0.5} = \sqrt{n}\|u\|_2 \tag{S.78}$$

where the Cauchy-Schwarz inequality has been utilized. Overall, we find $\|u\|_2 \leq \|u\|_1 \leq \sqrt{n}\|u\|_2$ and thus:

$$1 \leq R = \frac{M_u}{M_g} = \left(\frac{\sum_j^{N_C} \|\vec{x}_j\|_1}{\sum_j^{N_C} \|\vec{x}_j\|_2} \right)^2 \leq \left(\frac{\sum_j^{N_C} \sqrt{|C_j|} \cdot \|\vec{x}_j\|_2}{\sum_j^{N_C} \|\vec{x}_j\|_2} \right)^2. \tag{S.79}$$

III. NUMERICAL DETAILS OF THE TOY EXAMPLE

This section provides all the details for the Toy problem described in Section **??**. The full noncontextual ground state is:

$$(\underbrace{-1, +1, -1}_{\vec{q}_0}, \underbrace{0.25318483, -0.65828059, -0.70891756}_{\vec{r}_0}). \tag{S.80}$$

This defines the $A(\vec{r}_0)$:

$$A(\vec{r}_0) = 0.25318483\, YXYI - 0.65828059\, XYXI - 0.70891756\, XZXI. \tag{S.81}$$

The operators to map $A(\vec{r}_0)$ to a single Pauli operator are:

$$R_S = \; e^{+1i \cdot -0.7879622757719398 \cdot ZYZI} \cdot e^{+1i \cdot 1.2036225088338255 \cdot ZZZI}, \tag{S.82}$$

and

$$R_{LCU} = \; 0.79157591\, IIII + 0.41580383i\, ZZZI - 0.44778874i\, ZYZI. \tag{S.83}$$

Their action results in: $R_S A(\vec{r}_0) R_S^\dagger = R_{LCU} A(\vec{r}_0) R_{LCU}^\dagger = YXYI$.

We then defined U depending on which generators we wish to fix. We found the optimal ordering of stabilizers (supplied in Equation **??**) to fix via a brute force search over all $\sum_{i=1}^{|\mathcal{W}_{all}|} \binom{|\mathcal{W}_{all}|}{i} = 2^4 - 1 = 15$ possibilities for $\mathcal{W}$. The following optimal ordering was obtained:

1. $\{-1\, IIIZ\}$
2. $\{+1\, IXYI, -1\, IIIZ\}$
3. $\{+1\, IXYI, -1\, IIIZ, +1\, \mathcal{A}(\vec{r}_0)\}$
4. $\{-1\, YIYI, +1\, IXYI, -1\, IIIZ, +1\, \mathcal{A}(\vec{r}_0)\}$.

This defines all the information required to implement CS-VQE. Table S.1 summarises the stabilizers fixed, the rotation $U_{\mathcal{W}}$, required projection $Q_{\mathcal{W}}$ and final projected Hamiltonian $Q_{\mathcal{W}}^\dagger U_{\mathcal{W}}^\dagger H U_{\mathcal{W}} Q_{\mathcal{W}}$ for this ordering.

The old approach of applying $U_{\mathcal{W}_{all}}^\dagger H U_{\mathcal{W}_{all}}$ and then fixing certain stabilizer eigenvalues are summarised in Table S.2. It can be seen from these results, that always implementing the unitary partitioning rotation R can unnecessarily increase the number of terms in the Hamiltonian and thus should only be applied if the eigenvalue for $\langle A(\vec{r}) \rangle$ is fixed.

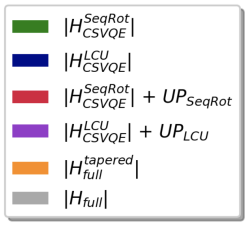
$\mathcal{W}$	$U_{\mathcal{W}}^{\dagger}$	$\mathcal{W}^Z = U_{\mathcal{W}}^{\dagger}\mathcal{W}U_{\mathcal{W}}$	$Q_{\mathcal{W}}$	$Q_{\mathcal{W}}^{\dagger}U_{\mathcal{W}}^{\dagger}HU_{\mathcal{W}}Q_{\mathcal{W}}$
-1 YIYI +1 IXYI -1 IIIZ $\mathcal{A}(\vec{r}_0)$	$e^{1i\frac{\pi}{4}XIYI}e^{1i\frac{\pi}{4}IYYI}R_{S/LCU}$	- ZIII + IZII - IIIZ + IIZI	$\|1\rangle\langle 1\| \otimes \|0\rangle\langle 0\| \otimes \|1\rangle\langle 1\| \otimes \|0\rangle\langle 0\|$	-2.475+0.000j
+1 IXYI -1 IIIZ $\mathcal{A}(\vec{r}_0)$	$e^{1i\frac{\pi}{4}IYYI}R_{S/LCU}$	+ IZII - IIIZ + IIZI	$I \otimes \|0\rangle\langle 0\| \otimes \|0\rangle\langle 0\| \otimes \|1\rangle\langle 1\|$	SeqRot: -1.827+0.000j I + -0.198+0.000j X + -0.467+0.000j Z + 0.648+0.000j Y LCU: -1.827+0.000j I + -0.414+0.000j X + -0.292+0.000j Z + 0.648+0.000j Y
+1 IXYI -1 IIIZ	$e^{1i\frac{\pi}{4}IYYI}$	+ IZII - IIIZ	$I \otimes \|0\rangle\langle 0\| \otimes I \otimes \|1\rangle\langle 1\|$	-0.500+0.000j II + 0.500+0.000j XI + 0.700+0.000j XX + 0.100+0.000j YI + -0.100+0.000j YX + 1.300+0.000j XZ + 0.600+0.000j IY + 0.700+0.000j ZZ
-1 IIIZ	$IIII$	-IIIZ	$I \otimes I \otimes I \otimes \|1\rangle\langle 1\|$	-0.500+0.000j III + 0.100+0.000j XXX + 0.200+0.000j YXX + 0.700+0.000j XZX + 0.700+0.000j XYX + 0.100+0.000j YZX + 0.200+0.000j XXZ + 0.600+0.000j IIY + 0.500+0.000j XXY + 0.100+0.000j YXY + 0.600+0.000j XZZ + 0.700+0.000j ZZZ + 0.200+0.000j YYZ + 0.100+0.000j ZYY

TABLE S.1: Different contextual subspace Hamiltonians defined from H (Equation **??**). R_S and R_{LCU} are defined in Equations S.82 and S.83.

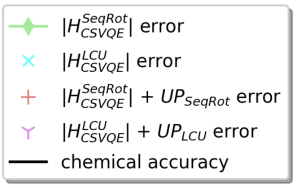
$H_{SeqRot} = U^{\dagger,SeqRot}_{\mathcal{W}_{all}} H U^{SeqRot}_{\mathcal{W}_{all}}$	$H_{LCU} = U^{\dagger,LCU}_{\mathcal{W}_{all}} H U^{LCU}_{\mathcal{W}_{all}}$	$\mathcal{W}^Z$	$Q_{\mathcal{W}}$	$Q^\dagger_{\mathcal{W}} H_{SeqRot} Q_{\mathcal{W}}$	$Q^\dagger_{\mathcal{W}} H_{LCU} Q_{\mathcal{W}}$
0.932-0.000j ZIII + -0.056+0.000j YIII + -0.025+0.000j ZXII + -0.025+0.000j YXII + 0.057-0.000j ZIXI + -0.197+0.000j YIXI + -0.051+0.000j ZXXI + 0.051+0.000j YXXI + 0.560-0.000j XZII + 0.395+0.000j ZZII + 0.397-0.000j YZII + 0.141-0.000j ZZXI + 0.142-0.000j YZXI + 0.345-0.000j XIZI + 0.093-0.000j XXZI + 0.467-0.000j IIYI + -0.187+0.000j IXYI + -0.496+0.000j ZIZI + 0.494-0.000j YIZI + 0.215+0.000j XZZI + -0.200+0.000j IYZI + -0.152+0.000j ZZZI + -0.153+0.000j YZZI + 0.071+0.000j ZYYI + 0.071-0.000j YYYI + -0.500+0.000j IIIZ	0.261-0.000j XIII + 0.932-0.000j ZIII + -0.230+0.000j YIII + -0.025+0.000j ZXII + -0.071+0.000j YXII + 0.295-0.000j ZIXI + -0.197+0.000j YIXI + -0.142+0.000j ZXXI + 0.051+0.000j YXXI + 0.395-0.000j XZII + 0.037-0.000j IYXI + 0.395-0.000j ZZII + 0.223-0.000j YZII + 0.120-0.000j ZZXI + 0.142-0.000j YZXI + 0.263-0.000j XIZI + 0.066-0.000j XXZI + 0.366-0.000j IIYI + -0.132+0.000j IXYI + -0.496+0.000j ZIZI + 0.419-0.000j YIZI + 0.393+0.000j XZZI + -0.200+0.000j IYZI + -0.074+0.000j IZYI + -0.152+0.000j ZZZI + -0.425+0.000j YZZI + 0.060+0.000j ZYYI + 0.071-0.000j YYYI + -0.500+0.000j IIIZ	- ZIII + IZII - IIIZ + IIZI	$\|1\rangle\langle 1\| \otimes \|0\rangle\langle 0\| \otimes \|1\rangle\langle 1\| \otimes \|0\rangle\langle 0\|$	-2.475+0.000j	-2.475+0.000j
		+ IZII - IIIZ + IIZI	$I \otimes \|0\rangle\langle 0\| \otimes \|0\rangle\langle 0\| \otimes \|1\rangle\langle 1\|$	-1.827+0.000j I + -0.198+0.000j X + 0.648+0.000j Z + 0.467+0.000j Y	-1.827+0.000j I + -0.414+0.000j X + 0.648+0.000j Z + 0.292+0.000j Y
		+ IZII - IIIZ	$I \otimes \|0\rangle\langle 0\| \otimes I \otimes \|1\rangle\langle 1\|$	-0.500+0.000j II + 0.560+0.000j XI + 1.327+0.000j ZI + 0.341+0.000j YI + 0.198+0.000j ZX + -0.056+0.000j YX + 0.560+0.000j XZ + 0.467+0.000j IY + -0.648+0.000j ZZ + 0.341+0.000j YZ	-0.500+0.000j II + 0.656+0.000j XI + 1.327+0.000j ZI + -0.006+0.000j YI + 0.414+0.000j ZX + -0.056+0.000j YX + 0.656+0.000j XZ + 0.292+0.000j IY + -0.648+0.000j ZZ + -0.006+0.000j YZ
		-IIIZ	$I \otimes I \otimes I \otimes \|1\rangle\langle 1\|$	-0.500+0.000j III + 0.932+0.000j ZII + -0.056+0.000j YII + -0.025+0.000j ZXI + -0.025+0.000j YXI + 0.057+0.000j ZIX + -0.197+0.000j YIX + -0.051+0.000j ZXX + 0.051+0.000j YXX + 0.560+0.000j XZI + 0.395+0.000j ZZI + 0.397+0.000j YZI + 0.141+0.000j ZZX + 0.142+0.000j YZX + 0.345+0.000j XIZ + 0.093+0.000j XXZ + 0.467+0.000j IIY + -0.187+0.000j IXY + -0.496+0.000j ZIZ + 0.494+0.000j YIZ + 0.215+0.000j XZZ + -0.200+0.000j IYZ + -0.152+0.000j ZZZ + -0.153+0.000j YZZ + 0.071+0.000j ZYY + 0.071+0.000j YYY	-0.500+0.000j III + 0.261+0.000j XII + 0.932+0.000j ZII + -0.230+0.000j YII + -0.025+0.000j ZXI + -0.071+0.000j YXI + 0.295+0.000j ZIX + -0.197+0.000j YIX + -0.142+0.000j ZXX + 0.051+0.000j YXX + 0.395+0.000j XZI + 0.037+0.000j IYX + 0.395+0.000j ZZI + 0.223+0.000j YZI + 0.120+0.000j ZZX + 0.142+0.000j YZX + 0.263+0.000j XIZ + 0.066+0.000j XXZ + 0.366+0.000j IIY + -0.132+0.000j IXY + -0.496+0.000j ZIZ + 0.419+0.000j YIZ + 0.393+0.000j XZZ + -0.200+0.000j IYZ + -0.074+0.000j IZY + -0.152+0.000j ZZZ + -0.425+0.000j YZZ + 0.060+0.000j ZYY + 0.071+0.000j YYY

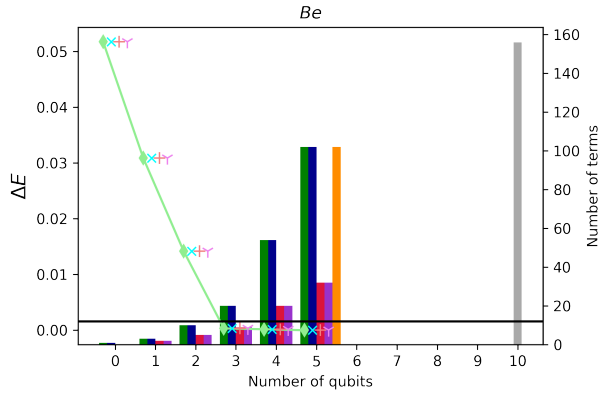
TABLE S.2: Different contextual subspace Hamiltonians defined from H (Equation **??**). Here $\mathcal{W}$ has been set to $\mathcal{W}_{all}$, which defines $U^\dagger_{\mathcal{W}_{all}} = e^{1i\frac{\pi}{4}XIYI} e^{1i\frac{\pi}{4}IYYI} R_{S/LCU}$. R_S and R_{LCU} are defined in Equations S.82 and S.83. The two left columns (H_{SeqRot} and H_{LCU}) give H rotated by $U_{\mathcal{W}}$. Each projected Hamiltonian is generated from these, where the eigenvalue of certain stabilizers are fixed according to the projector $Q_{\mathcal{W}}$. For the last two rows, the eigenvalue of $\mathcal{A}(\vec{r}_0)$ has not been fixed, but the non-Clifford operator $R_{S/LCU}$ is still included within $U^\dagger_{\mathcal{W}_{all}}$. This leads to an unnecessary increase in the number of Pauli operators for these two cases, as these transformed operators are isospectral with associated Hamiltonians in Table S.1.

IV. GRAPHICAL RESULTS FOR CS-VQE SIMULATION OF EACH MOLECULAR HAMILTONIAN

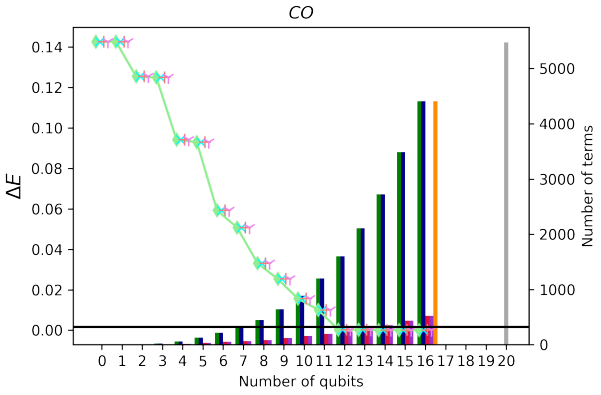


(a)

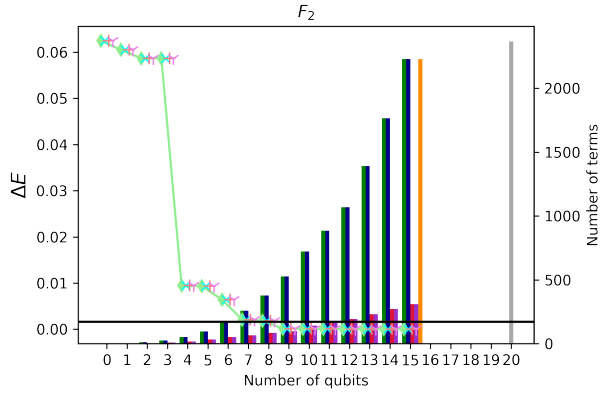




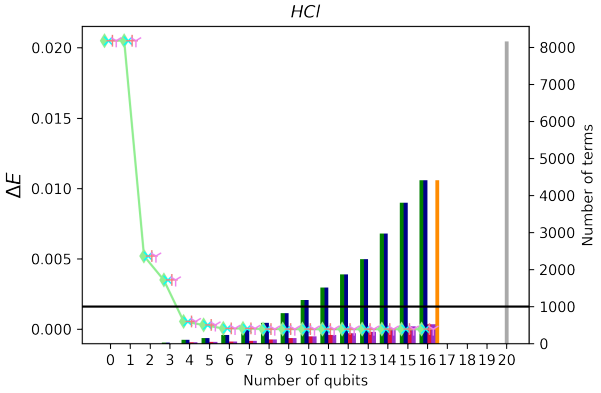
(b)



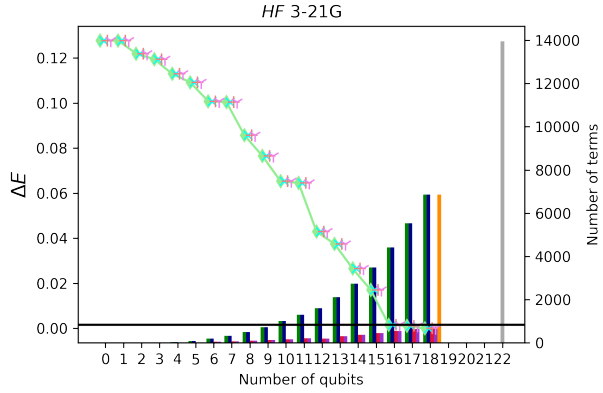
(c)



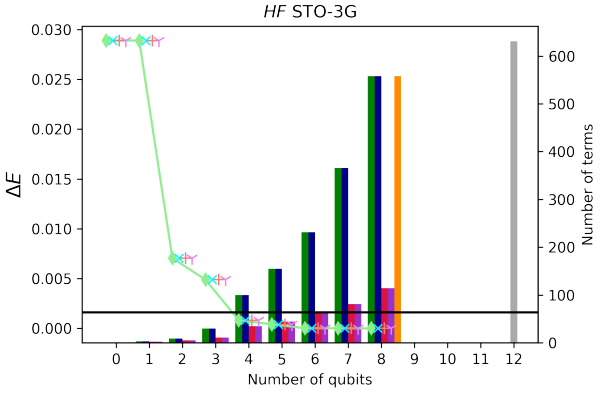
(d)



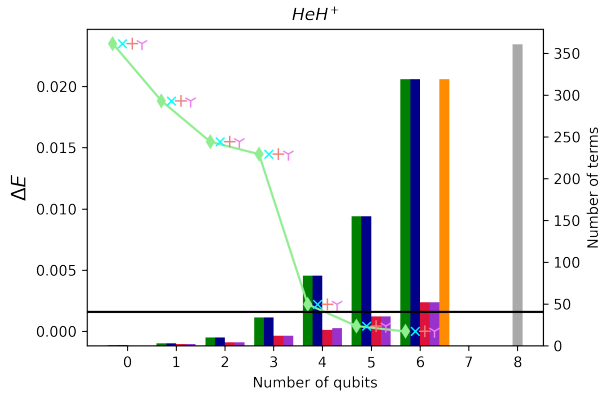
(e)



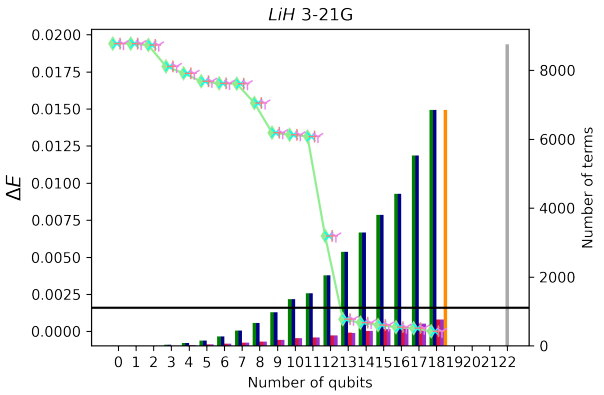
(f)



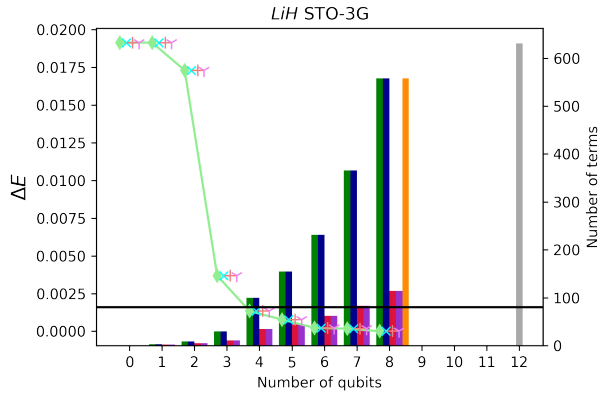
(g)


HeH+
ΔE
Number of terms
Number of qubits

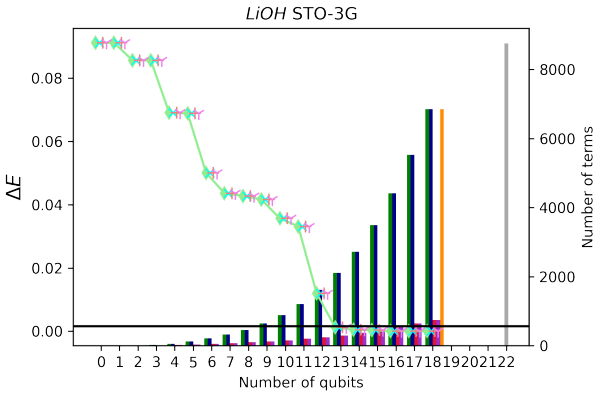
(h)


LiH 3-21G
ΔE
Number of terms
Number of qubits

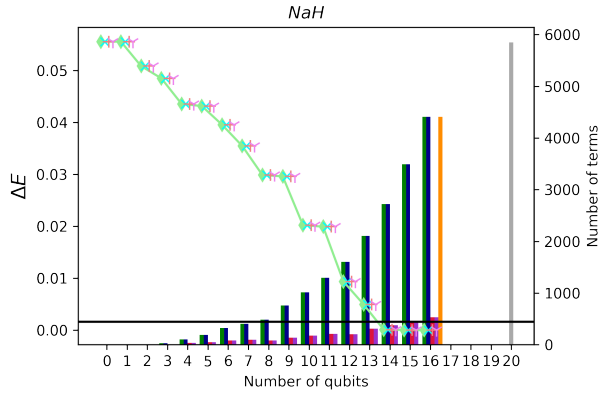
(i)


LiH STO-3G
ΔE
Number of terms
Number of qubits

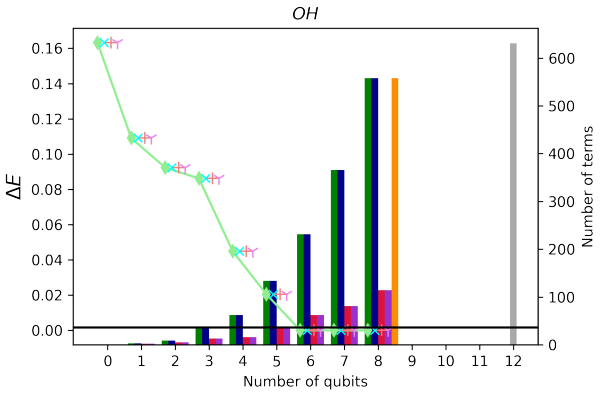
(j)


LiOH STO-3G
ΔE
Number of terms
Number of qubits

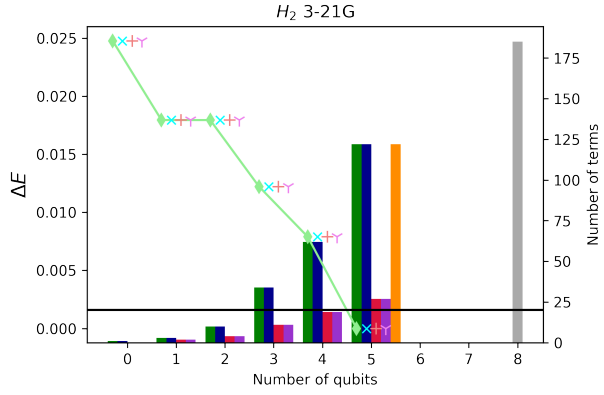
(k)


NaH
ΔE
Number of terms
Number of qubits

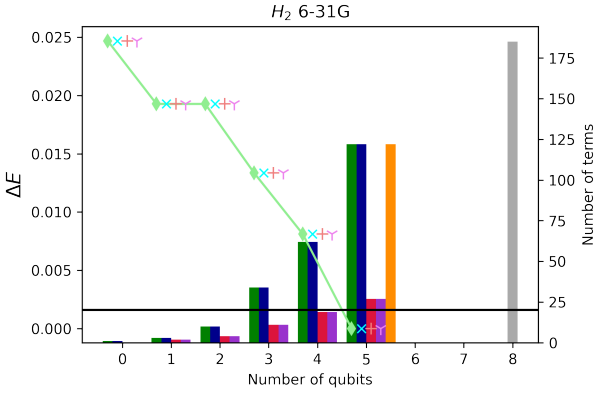
(l)


OH
ΔE
Number of terms
Number of qubits

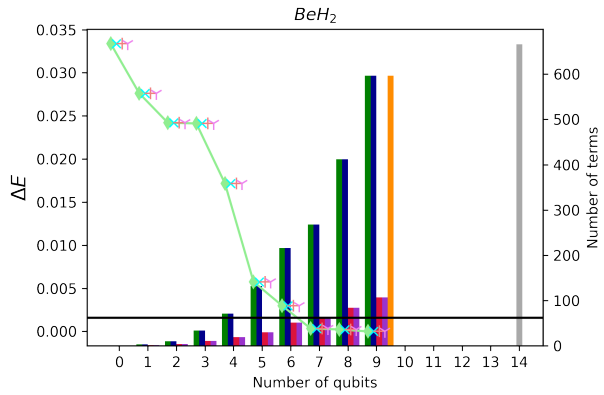
(m)


H2 3-21G
ΔE
Number of terms
Number of qubits

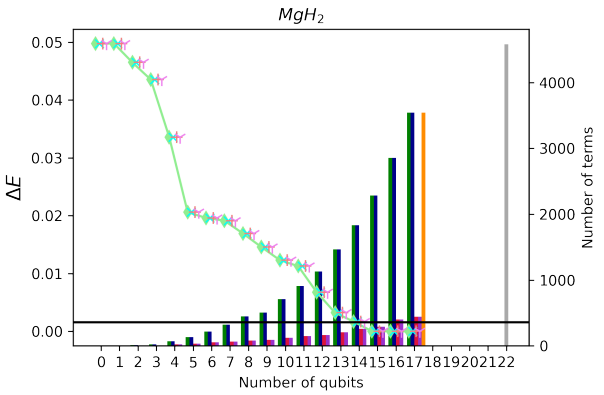
(n)


H2 6-31G
ΔE
Number of terms
Number of qubits

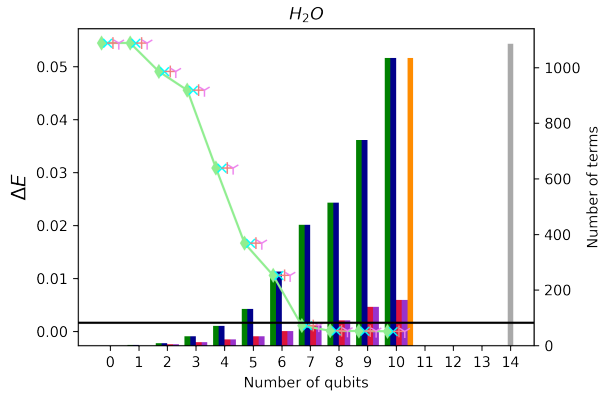
(o)


BeH_2
ΔE
Number of terms
Number of qubits

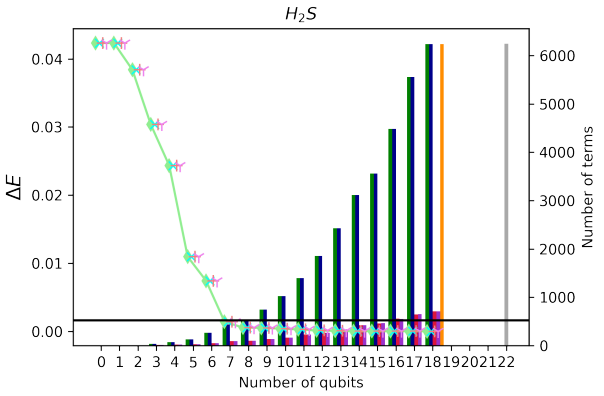
(p)


MgH_2
ΔE
Number of terms
Number of qubits

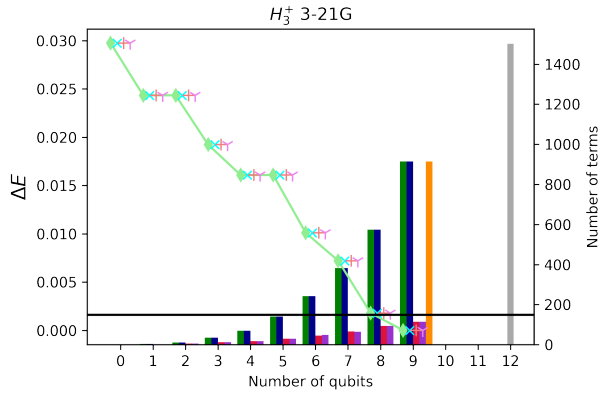
(q)


H_2O
ΔE
Number of terms
Number of qubits

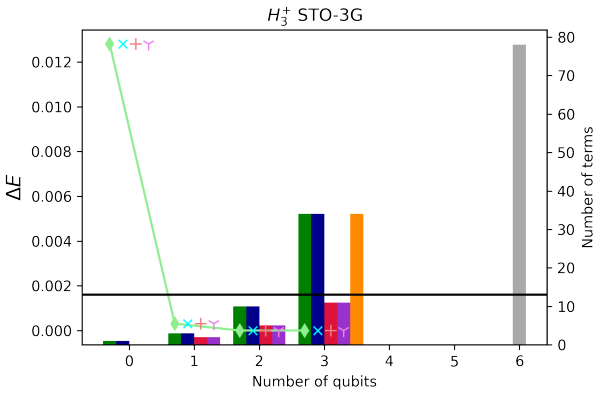
(r)


H_2S
ΔE
Number of terms
Number of qubits

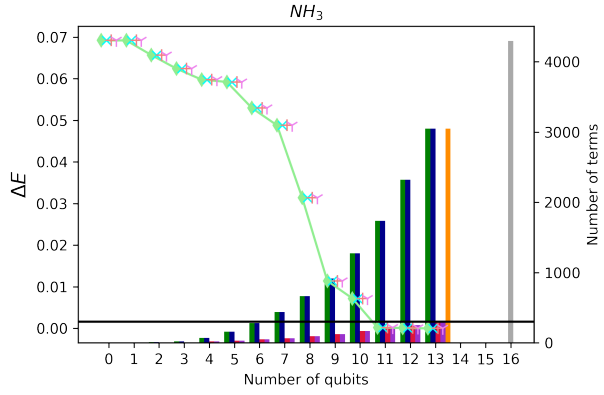
(s)


H_3^+ 3-21G
ΔE
Number of terms
Number of qubits

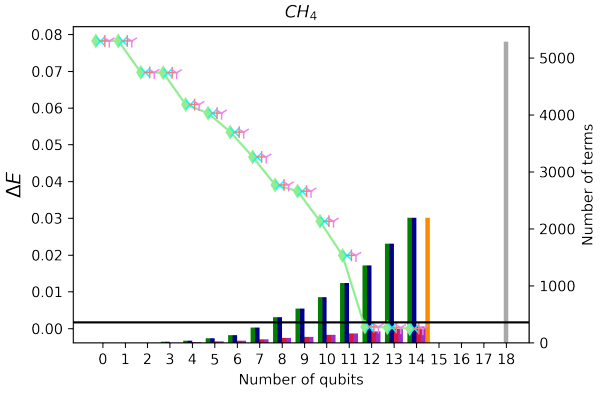
(t)


H_3^+ STO-3G
ΔE
Number of terms
Number of qubits

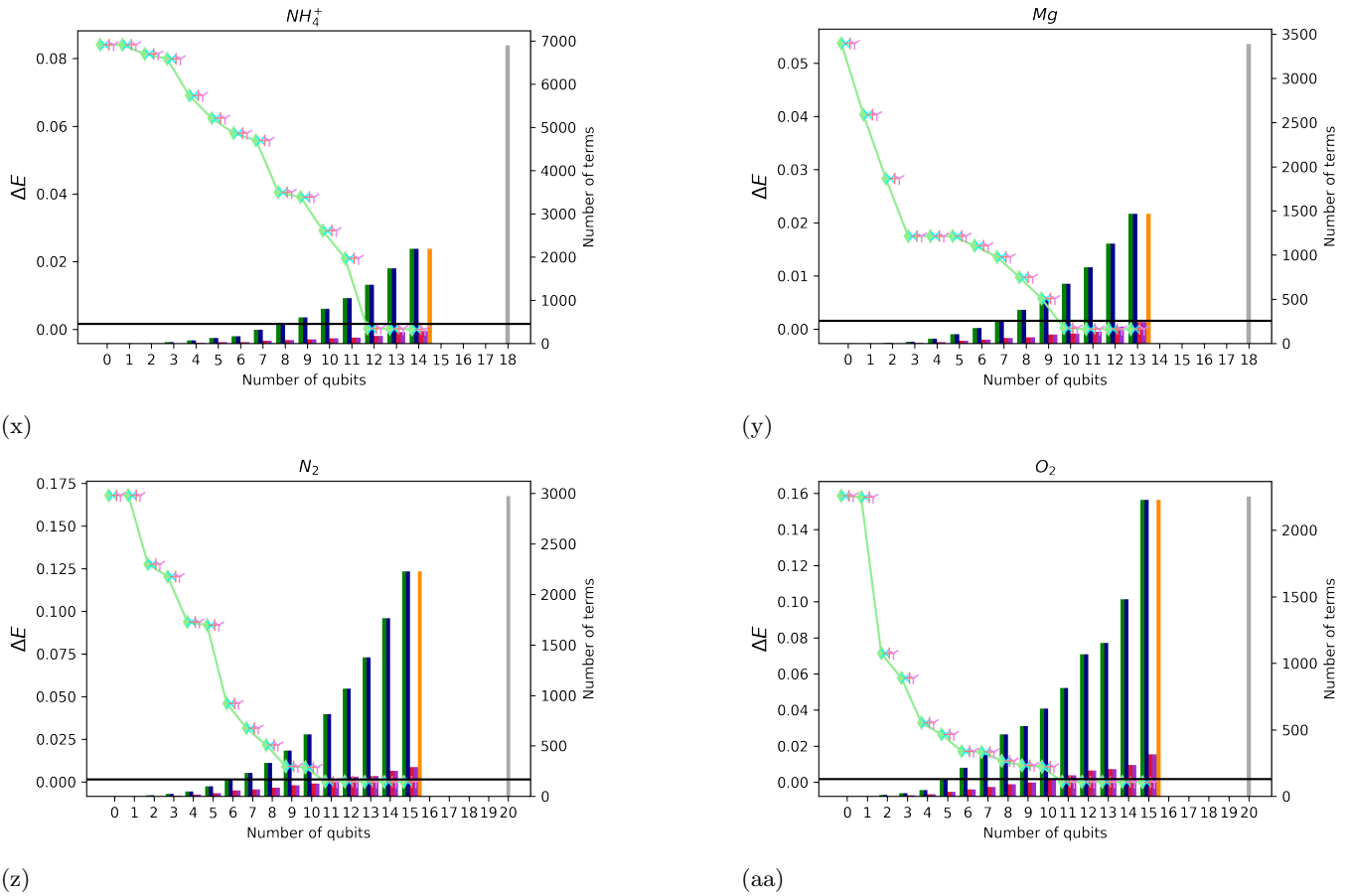
(u)


NH_3
ΔE
Number of terms
Number of qubits

(v)


CH_4
ΔE
Number of terms
Number of qubits

(w)



(x) (y)

(z) (aa)

FIG. S.1: CS-VQE approximation errors ΔE versus number of qubits used on the quantum computer (scatter plot). The horizontal solid black lines indicate chemical accuracy. The number of terms in each Hamiltonian is given by the bar chart.

All the subplots in Figure S.1 give the simulation results of each molecular Hamiltonian at different levels of noncontextual approximations. This is equivalent to how many contextual stabilizers $\mathcal{W}$ eigenvalues are fixed. In each plot, the leftmost data represents the case when all the noncontextual stabilizer eigenvalues are fixed and is the case for the full noncontextual approximation to a given problem [**?**]. Moving right, we remove a single stabilizer from $\mathcal{W}$ and thus don't fix the eigenvalue of that stabilizer. This reintroduces a qubits worth degree of freedom into the problem. At the limit that no stabilizer eigenvalues are fixed ($\mathcal{W} = \{\}$) we return to standard VQE over the full problem and no noncontextual approximation is made. In each plot this scenario is represented by the far right data point (excluding the data for the full non tapered Hamiltonian that is supplied for reference only). The raw data for these results is supplied in the Supplemental Material (see the zipped file). We include data beyond Hamiltonians achieving chemical accuracy, to show the different possible approximations, rather than stopping once chemical accuracy was achieved.

V. TABULATED RESULTS OF SIMULATION

Table S.3 summarises the numerical results of Figures **??** and **??**.

molecule	basis	$H_{\text{CS-VQE}}$	$H_{\text{CS-VQE}} + UP^{(LCU)}$	$H_{\text{CS-VQE}} + UP^{(SeqRot)}$	H_{tapered}	$RH_{tapered}R^{\dagger}$	H_{full}
BeH_2	STO-3G	(7, 268)	(7, 61)	(7, 61)	(9, 596)	(9, 614)	(14, 666)
Mg	STO-3G	(10, 675)	(10, 114)	(10, 114)	(13, 1465)	(13, 1465)	(18, 3388)
$H_3{}^+$	3-21G	(9, 914)	(9, 115)	(9, 115)	(9, 914)	(9, 786)	(12, 1501)
O_2	STO-3G	(11, 815)	(11, 157)	(11, 157)	(15, 2229)	(15, 2374)	(20, 2255)
OH	STO-3G	(6, 231)	(6, 62)	(6, 62)	(8, 558)	(8, 558)	(12, 631)
CH_4	STO-3G	(12, 1359)	(12, 203)	(12, 203)	(14, 2194)	(14, 2194)	(18, 5288)
Be	STO-3G	(3, 20)	(3, 9)	(3, 9)	(5, 102)	(5, 108)	(10, 156)
NH_3	STO-3G	(11, 1733)	(11, 200)	(11, 200)	(13, 3048)	(13, 2738)	(16, 4293)
H_2S	STO-3G	(7, 435)	(7, 92)	(7, 92)	(18, 6237)	(18, 6237)	(22, 6246)
H_2	3-21G	(5, 122)	(5, 27)	(5, 27)	(5, 122)	(5, 124)	(8, 185)
HF	3-21G	(17, 5530)	(17, 648)	(17, 648)	(18, 6852)	(18, 6852)	(22, 13958)
F_2	STO-3G	(9, 527)	(9, 99)	(9, 99)	(15, 2229)	(15, 2229)	(20, 2367)
HCl	STO-3G	(4, 100)	(4, 35)	(4, 35)	(16, 4409)	(16, 4409)	(20, 8159)
HeH^+	3-21G	(5, 155)	(5, 35)	(5, 35)	(6, 319)	(6, 319)	(8, 361)
MgH_2	STO-3G	(15, 2285)	(15, 289)	(15, 289)	(17, 3540)	(17, 3540)	(22, 4582)
CO	STO-3G	(12, 1599)	(12, 241)	(12, 241)	(16, 4409)	(16, 4409)	(20, 5475)
LiH	STO-3G	(4, 100)	(4, 35)	(4, 35)	(8, 558)	(8, 586)	(12, 631)
N_2	STO-3G	(11, 815)	(11, 153)	(11, 153)	(15, 2229)	(15, 2229)	(20, 2975)
NaH	STO-3G	(14, 2722)	(14, 375)	(14, 375)	(16, 4409)	(16, 4409)	(20, 5851)
H_2O	STO-3G	(7, 435)	(7, 73)	(7, 73)	(10, 1035)	(10, 1035)	(14, 1086)
$H_3{}^+$	STO-3G	(1, 3)	(1, 2)	(1, 2)	(3, 34)	(3, 35)	(6, 78)
LiOH	STO-3G	(13, 2104)	(13, 296)	(13, 296)	(18, 6852)	(18, 6852)	(22, 8758)
LiH	3-21G	(13, 2732)	(13, 375)	(13, 383)	(18, 6852)	(18, 6852)	(22, 8758)
H_2	6-31G	(5, 122)	(5, 27)	(5, 27)	(5, 122)	(5, 124)	(8, 185)
$NH_4{}^+$	STO-3G	(12, 1359)	(12, 176)	(12, 176)	(14, 2194)	(14, 2194)	(18, 6892)
HF	STO-3G	(4, 100)	(4, 35)	(4, 35)	(8, 558)	(8, 558)	(12, 631)

TABLE S.3: Different resource requirements to study different electronic structure Hamiltonians required to achieve chemical accuracy. Each round bracket tuple reports $(n, |H|)$ and gives the number of qubits and terms for each Hamiltonian considered. $RH_{tapered}R^{\dagger}$ describes the effect of the CS-VQE unitary partitioning rotation on the problem Hamiltonian and $H_{\text{CS-VQE}} = Q_{\mathcal{W}}U_{\mathcal{W}}^{\dagger}H_{\text{full}}U_{\mathcal{W}}Q_{\mathcal{W}}^{\dagger}$. The square tuple gives the upper bound of single qubit gates (SQG) and CNOT gates $[SQG, CNOT]$ required to perform R as a sequence of rotations in the unitary partitioning measurement reduction step, based on the largest anticommuting clique - representing the largest possible circuit for R_S. The size of the Hamiltonian for LiH (3-21G singlet) with measurement reduction applied is different for the sequence of rotations and LCU unitary partitioning methods. This is an artifact of the graph colour heuristic finding different anticommuting cliques in the CS-VQE Hamiltonian.